
Doctoral Dissertations

Student Theses and Dissertations

Spring 2023

Effects of Downwash when Measuring Gas Concentration with UAV-Mounted Gas Sensors

Jacob Lane Brinkman
Missouri University of Science and Technology

Follow this and additional works at: https://scholarsmine.mst.edu/doctoral_dissertations



Part of the [Explosives Engineering Commons](#)

Department: Mining Engineering

Recommended Citation

Brinkman, Jacob Lane, "Effects of Downwash when Measuring Gas Concentration with UAV-Mounted Gas Sensors" (2023). *Doctoral Dissertations*. 3254.

https://scholarsmine.mst.edu/doctoral_dissertations/3254

This thesis is brought to you by Scholars' Mine, a service of the Missouri S&T Library and Learning Resources. This work is protected by U. S. Copyright Law. Unauthorized use including reproduction for redistribution requires the permission of the copyright holder. For more information, please contact scholarsmine@mst.edu.

EFFECTS OF DOWNWASH WHEN MEASURING GAS CONCENTRATIONS WITH
UAV-MOUNTED GAS SENSORS

by

JACOB LANE BRINKMAN

A DISSERTATION

Presented to the Graduate Faculty of the
MISSOURI UNIVERSITY OF SCIENCE AND TECHNOLOGY

In Partial Fulfillment of the Requirements for the Degree

DOCTOR OF PHILOSOPHY

in

EXPLOSIVES ENGINEERING

2023

Approved by:

Catherine E. Johnson, Advisor
Joel G. Burken
William A. Harrison
Kyle A. Perry
Paul N. Worsey

© 2023

Jacob Lane Brinkman

All Rights Reserved

ABSTRACT

This research concludes that the downwash region of a rotary-wing unmanned aerial vehicle (UAV) does not produce pressure variations substantial enough to cause significant changes in density-based gas concentration measurements. US regulations evaluate gas concentration as a function of gas density, and accurate concentration measurements are critical for protecting health and safety, which means evaluation of actual downwash effects on measured gas concentration is essential.

During experimentation, the UAV was fixed to a stand in a sealed chamber filled with NO_x (NO and NO₂) of constant concentration. The UAV rotors ran at hovering speeds, and gas concentrations were measured at various locations around the UAV. NO_x was chosen due to intended US regulations on surface mine blasting NO_x emissions, though the results should be applicable to most emissions of interest that are monitored by a UAV system. All variables other than the presence of downwash were held constant or accounted for, so the only source of concentration variation would have been caused by pressure changes in the downwash region. No significant variations were observed, providing evidence that downwash pressure variations are not substantial enough to alter density-based gas concentration measurements.

Numerous researchers have suggested that downwash may affect gas concentration measurements, though no researcher has previously isolated and defined the effect. This dissertation's findings allow researchers to safely assume this source of previously undefined error is statistically negligible, provided the UAV and gas sampling point are located entirely within the gas cloud and the downwash region has stabilized.

ACKNOWLEDGMENTS

This dissertation would not be possible without the encouragement I received from my wife, my PhD advisor, my parents, my friends, my fellow graduate students, and my colleagues at Pantex. I especially want to thank my advisor, Dr. Catherine Johnson, for her unfailing friendship and support. I probably tested her patience to its very limits, but she never ceased to be a constant pillar of support. Her friendship, trust, support, knowledge, and dedicated work ethic are unparalleled sources of inspiration, and I would not have completed this dissertation without her as my advisor. I truly believe she improves the lives of everyone who has the pleasure of knowing her as she has done and continues to do for me.

Thank you to the Society for Mining, Metallurgy, and Exploration for providing the Faculty Career Award out of which this experiment was funded. Thank you to my advisory committee for providing the foundation needed to develop this project and dissertation. I also thank research technicians Jeff Heniff and Fred Eickelmann for designing and building the UAV stand. Thank you to Dean Keith for allowing me to use your facilities for testing. Thank you to all of the students who helped directly and indirectly with my research and studies; the camaraderie we shared made even our toughest challenges as enjoyable and memorable as our greatest victories.

Most importantly, thank you to my wife, Jackie, and my two children, Sawyer and Magnolia. You are each the inspiration driving everything I do.

TABLE OF CONTENTS

	Page
ABSTRACT.....	iii
ACKNOWLEDGMENTS	iv
LIST OF ILLUSTRATIONS.....	viii
LIST OF TABLES.....	x
NOMENCLATURE	xii
 SECTION	
1. INTRODUCTION.....	1
1.1. PROBLEM STATEMENT.....	1
1.2. UAV-BASED MEASUREMENT SYSTEMS.....	3
1.3. RESEARCH APPROACH.....	5
1.4. CONTRIBUTION TO SCIENCE	6
2. LITERATURE REVIEW.....	8
2.1. BLASTING EMISSION GASES	8
2.2. BLASTING EMISSION REGULATIONS.....	11
2.2.1. Regulations Regarding NO _x Exposure.	11
2.2.2. Potential for NO _x Incidents at Surface Mines.....	12
2.2.3. Existing Regulations on NO _x Produced by Blasting.	14
2.2.4. Upcoming Regulations on NO _x Produced by Blasting.....	16
2.3. FIELD MEASUREMENTS OF BLASTING EMISSIONS	18
2.3.1. Field Measurements of Surface Mine NO _x Production.	19

2.3.2. Fixed Location Gas Sensors.....	19
2.3.3. Spectrometry.....	22
2.3.4. Unmanned Aerial Vehicles.....	23
2.4. UAV-MOUNTED GAS MONITOR SYSTEMS.....	24
2.4.1. Downwash Modeling.....	26
2.4.2. Field Sample Collection.....	29
2.4.3. Downwash Effects on Field Measurement Accuracy.....	32
2.4.4. Downwash Effects on Air Pressure.....	36
2.5. SUMMARY.....	36
3. POST-MOVEMENT STABILIZATION TIME FOR THE DOWNWASH REGION OF A 6-ROTOR UAV.....	38
3.1. METHOD.....	38
3.1.1. Equipment.....	38
3.1.2. Test Procedure.....	40
3.2. RESULTS.....	42
3.2.1. Hovering Stationary.....	43
3.2.2. Rotor Speed Results.....	47
3.2.3. Wind Velocity Results.....	49
3.2.4. Vertical Movement Upward.....	50
3.2.5. Rotational Movement.....	53
3.2.6. Horizontal Movement.....	55
3.2.7. Rotor Speed Stability when Subjected to Outside Wind.....	56
3.2.8. Applicability of Results to Other UAVs.....	57
3.3. DISCUSSION.....	58

3.4. SUMMARY	60
4. EFFECTS OF DOWNWASH FROM A 6-ROTOR UAV ON GAS CONCENTRATIONS	62
4.1. EQUIPMENT	62
4.2. METHOD	67
4.2.1. Test Setup.	68
4.2.2. Data Processing.	71
4.2.3. Variables.	72
4.3. RESULTS	74
4.3.1. Measured Concentration Results.	77
4.3.2. Accounting for Uncontrolled Variables.	81
4.3.3. Effects of Downwash Presence.	83
4.3.4. Effects of Varying Measuring Point Location.	87
4.3.5. Relation to Turbulence.	91
4.3.6. Applicability of Results to Other UAVs.	97
4.4. DISCUSSION.....	98
4.5. SUMMARY	99
5. CONCLUSIONS	101
5.1. DOWNWASH REGION STABILIZATION TIME	102
5.2. EFFECTS OF DOWNWASH ON GAS CONCENTRATIONS	103
6. FUTURE WORK	105
BIBLIOGRAPHY.....	107
VITA.....	119

LIST OF ILLUSTRATIONS

	Page
Figure 2.1. Simulation of UAV Downwash, where the White Areas below the UAV Represent Locations with Pressures that Vary from Ambient Pressure [119]	25
Figure 2.2. Profile of Downwash Effects on (a) Air Velocity, values in m/s, and (b) Pressure, values in Pa [49]	27
Figure 2.3. UAVs with a Tube Extension Attached to a Pump on the Gas Monitor, shown extending (a) upwards [77] and (b) downwards [39]	32
Figure 3.1. 6-rotor DJI Matrice 600 Pro	39
Figure 3.2. Final Setup with UAV, Stand, and Anemometers.....	41
Figure 3.3. Flight 4b UAV Rotor Speed over Time	48
Figure 3.4. Flight 4b UAV Rotor Speed, Offset to Make Individual Rotor Results More Prominent	49
Figure 3.5. Test 3 Air Speed Measurements over Time	50
Figure 3.6. Results for Vertical Motion Stabilization Time after Returning to Hovering Rotor Speeds	52
Figure 3.7. Results for Rotational Motion Stabilization Time after Returning to Hovering Rotor Speeds	55
Figure 4.1. Gas Sensor Schematic	63
Figure 4.2. Gas Sensor (Gas Hood, Gas Sensors, and Circuit Board) Connected to the Data Logger.....	64
Figure 4.3. Gas Monitor (Gas Sensor Connected to the Laptop and Fan Pumps).....	64
Figure 4.4. Test Setup with UAV, Stand, and Gas Monitor; Measuring Points Extended Vertically.....	67
Figure 4.5. Test Configurations	69
Figure 4.6. Results for Percent Difference between “UAV On” and “UAV Off”, with Relation to Vertical Distance beneath the UAV	83

Figure 4.7. Results for Percent Difference between “UAV On” and “UAV Off”, with Relation to Horizontal Distance beside the UAV, Series Horizontal 1 and Horizontal 2.....	84
Figure 4.8. Results for Percent Difference between “UAV On” and “UAV Off”, with Relation to Horizontal Distance beside the UAV, Series Horizontal 3 and Horizontal 4.....	85
Figure 4.9. Results for Percent Difference between Sensor A and Sensor B, with Relation to Vertical Distance beneath the UAV	88
Figure 4.10. Results for Percent Difference between Sensor A and Sensor B, with Relation to Horizontal Distance beside the UAV, Series Horizontal 1 and Horizontal 2	89
Figure 4.11. Results for Percent Difference between Sensor A and Sensor B, with Relation to Horizontal Distance beside the UAV, Series Horizontal 3 and Horizontal 4	90
Figure 4.12. Standard Deviation in Excess of Inherent Error, with Relation to Vertical Distance beneath the UAV.....	92
Figure 4.13. Standard Deviation in Excess of Inherent Error, with Relation to Horizontal Distance beside the UAV, Series Horizontal 1 and Horizontal 2.....	93
Figure 4.14. Standard Deviation in Excess of Inherent Error, with Relation to Horizontal Distance beside the UAV, Series Horizontal 3 and Horizontal 4.....	94
Figure 4.15. Comparison of Turbulence (red) to Standard Deviation in Excess of Inherent Error.....	97

LIST OF TABLES

	Page
Table 2.1. Summary of Laboratory Results Regarding Factors that Increase NO _x Production during Explosive Detonation	10
Table 2.2. Air Quality Index and Expected Health Risk from NO ₂ Exposure over a 1-hour TWA.....	12
Table 2.3. Australian Guidelines for Assessing NO _x Production from Surface Mine Blasts [103].....	15
Table 3.1. Anemometer Locations during Test Flights	43
Table 3.2. Average “Hovering” Rotor Speeds.....	44
Table 3.3. Average “Hovering” Wind Velocities	46
Table 3.4. Results after Simulating Vertically Upward UAV Movement, Flight 4b	51
Table 3.5. Results after Simulating Rotational UAV Movement, Flight 1 & Flight 5	53
Table 3.6. Outside Wind Effects on UAV Rotor Speed	56
Table 4.1. Test Series Information.....	70
Table 4.2. Sensor Calibration Constants.....	72
Table 4.3. Measured Concentration Results, Average of All Tests.....	75
Table 4.4. Number of Tests and Samples Collected in Each Test Series	76
Table 4.5. Measured Concentration Results, Average of Vertical 1 Tests.....	77
Table 4.6. Measured Concentration Results, Average of Vertical 2 Tests	77
Table 4.7. Measured Concentration Results, Average of Horizontal 1 Tests.....	78
Table 4.8. Measured Concentration Results, Average of Horizontal 2 Tests.....	79
Table 4.9. Measured Concentration Results, Average of Horizontal 3 Tests.....	79
Table 4.10. Measured Concentration Results, Average of Horizontal 4 Tests.....	80
Table 4.11. Measured Concentration Results, Average of Top Tests	81

Table 4.12. Averages of the Linear Slopes Used to Adjust for Undefined Error	82
Table 4.13. Results for Percent Difference between “UAV On” and “UAV Off”, with Comparison of Measurements on Top of the UAV to Vertical Distance beneath the UAV and Horizontal Distance beside the UAV	86
Table 4.14. Results for Percent Difference between Sensor A and Sensor B, with Comparison of Measurements on Top of the UAV to Vertical Distance beneath the UAV and Horizontal Distance beside the UAV	91
Table 4.15. Standard Deviation in Excess of Inherent Error, with Comparison of Measurements on Top of the UAV to Vertical Distance beneath the UAV and Horizontal Distance beside the UAV	95
Table 4.16. p-values when Comparing Standard Deviation between Measurements Taken with the UAV On and Off	96

NOMENCLATURE

Symbol	Description
UAV	Unmanned aerial vehicle
NO _x	NO and NO ₂
UAS	Unmanned aerial system
NO ₂	Nitrogen dioxide
NO	Nitric oxide
CO	Carbon monoxide
ANFO	Ammonium nitrate and fuel oil
N ₂	Nitrogen
CO ₂	Carbon dioxide
H ₂ O	Water
CH ₂	Methylene (fuel oil)
VOD	Velocity of detonation
EPA	Environmental Protection Agency
NAAQS	National Ambient Air Quality Standards
TWA	Time-weighted average
AQI	Air Quality Index
AEISG	Australian Explosives Industry Safety Group
WEG	WildEarth Guardians
OSMRE	Office of Surface Mining Reclamation and Enforcement
Downwash	All airflow that is affected by the downward thrust of multi-rotor UAV propellers
OSHA	Occupational Safety and Health Administration

CFD	Computational flow dynamic
t_I	Adjusted time
t_0	Measured time
l	Tube length
D	Tube inner diameter
Q	Air pump flow rate
C	Concentration
S	Calibrated sensor sensitivity
n_T	Temperature correction for the NO ₂ sensor used
k'_T	Temperature correction for the NO sensor used
WE_e	Calibrated constant offset voltage due to natural electronic interference for the working electrode
AE_e	Calibrated constant offset voltage due to natural electronic interference for the auxiliary electrode
WE_0	Calibrated zero voltage for the working electrode
AE_0	Calibrated zero voltage for the auxiliary electrode
WE_u	Raw voltage measured by the working electrode
AE_u	Raw voltage measured by the auxiliary electrode
C_n	Adjusted instantaneous concentration
C_0	Original instantaneous concentration
t_n	Time at which C_0 was measured
t_{mid}	The midpoint time for a specific test
s	The slope of the linear trendline for all results of a specific test
t_a	The midpoint time of the adjustment period relevant to t_n

s_{on}	The slope of the linear trendline for all results of a specific test collected while the UAV rotors were turned on and the downwash region was stabilized
s_{off}	The slope of the linear trendline for all results of a specific test collected while the UAV rotors were turned off and ambient airflow was stabilized

1. INTRODUCTION

The subsections within this section give an overview of the problem statement (Section 1.1), how a gas monitor mounted on a rotary-wing unmanned aerial vehicle (UAV) could provide a solution (Section 1.2), the research approach for evaluating a previously undefined potential source of error for a UAV-based solution (Section 1.3), and the research results (Section 1.4). The overall hypothesis of this dissertation is:

For the purposes of measuring gas concentration in an open-air cloud using a gas monitor mounted on an unmanned aerial vehicle (UAV), the concentration measurement error created by UAV rotor downwash can be quantified. Once quantified, the error can be mitigated by either applying a correction factor to measured concentrations or by determining the error to be statistically negligible.

1.1. PROBLEM STATEMENT

Surface mining operations use explosives to fragment rock so it can be easily moved, though blasting can potentially produce noxious gases [1,2,3,4,5,6] that are toxic and possibly deadly if inhaled [7,8,9,10,11,12,13,14,15,16] [17,18,19]. Mining operations currently use previous laboratory research to estimate emission quantities [20,21], yet research has shown significant variation in the possible quantities produced [22,23,24,25,26,27,28,29]. Even if the quantities are accurately predicted, toxic gas exposure health risk is evaluated according to a time-weighted average of gas concentrations, which cannot be determined by solely observing the quantity of gas produced. Since 2006, exposure to blasting-produced NO_x (NO and NO₂) has caused 1

fatality and at least 27 hospitalizations over 6 six incidents worldwide [30,31,32,33], and state regulations in the US have begun implementing more stringent requirements on blasting fumes [34,35,36,37]. Although these regulations have historically only been enforced as a reactionary measure [38], a quantitative method of evaluating actual health risk from surface mine blasting emissions would serve to both protect human health and protect the surface mines from unwarranted disciplinary action and/or defamation. However, a method for quantifying emissions that is both cost-effective and has well-defined measurement error is yet to be determined.

Gas monitors mounted on unmanned aerial vehicles (UAV) are being explored by numerous researchers as a potential method for monitoring gas emissions from various sources. While this dissertation was inspired by the potential use in surface mine blasting, UAVs are being evaluated by researchers as potential gas emissions monitoring solutions for many industries, including surface mine emissions [39,40], military explosives [41], oil and gas leak monitoring [42,43,44,45,46,47], city pollution monitoring [48,49,50,51,52,53,54,55,56,57] [58,59,60,61], transportation pollution (highway [62,63], train [64,65], and boat [66,67]), agricultural air quality and chemical sprays [68,69,70,71,72,73], emergency response to accidental gas releases [74,75,76], and miscellaneous environmental concerns [45,77,78,79,80].

Despite the growing popularity of UAV-mounted gas monitors, this method still has numerous undefined variables that must be evaluated prior to acceptance of these systems as a viable solution. The primary undefined source of measurement error underlying all measurements collected by rotary-wing UAV systems is the potential effects of UAV downwash, which is the airflow on all sides of the UAV that is made

turbulent by rotor thrust [81]. Air in the downwash region will have areas of artificially high and low pressure, which will unnaturally alter the gas density measured inside the downwash region. Because US regulators quantify gas exposure according to density-based concentration rather than unitless concentration [82,83], measured gas quantities can potentially be artificially altered by turbulent pressures created by UAV downwash. It is expected that empirical data collected during this project will either (a) prove the concentration measurement errors due to downwash are statistically negligible or (b) allow the creation of a correction factor that can be used to adjust the measured concentration results based on the thrust and the measuring point location relative to the UAV location. Either result will enable quantification of the previously undefined error that underlies all UAV-based gas measurements.

1.2. UAV-BASED MEASUREMENT SYSTEMS

A UAV-mounted gas monitor is a potentially viable option for recording gas concentrations within a blast cloud. Collecting air samples at a surface mine blasting site presents a variety of problems that are resolved by using a UAV for data collection. The most apparent concern with collecting air samples is the danger of the explosion itself and the resulting rock movement. For human safety, it is required that all people remain at least 300-600 m away from the blast site, depending on the size of the blast [84]. One potential measurement method is to install stationary gas sensors near the blast that can read this data, though this creates three new problems: the sensor may be destroyed by the shockwave or moving rock, sudden changes in the weather may cause the post-blast gas cloud to travel so that no part of the cloud contacts the sensor, and the cloud may

move above the sensor so the concentration values at ground level will be more dispersed and measurements will have greater percent error than measurements taken within the cloud [84,85,86]. An unmanned aerial system (UAS) consisting of a gas monitor attached to a rotary-wing UAV is capable of overcoming each of these concerns. It can theoretically monitor within the cloud at any height, adjust rapidly to changing wind directions, maintain a safe distance from the shot while approaching the blast site quickly for initial measurements, and determine the measuring point location.

When evaluating human health risk from gas emissions based on measured concentration within the cloud, the total mass released must also be known. Cloud dispersion equations can be used to calculate the total mass released from a measured concentration if the measurement point location and weather conditions are also known [87,88,89,90,91,92]. Using a UAV with a gas monitor is capable of measuring both concentration and point location, thereby allowing calculation of the total mass emitted. An alternative method is to quantify concentration using a spectrometer, and then calculating mass based on the observed concentration and cloud volume. However, determining cloud volume in open air has undefined potential sources of error that are more difficult to define than the errors associated with the UAS. Additionally, a UAS costs considerably less than alternative options for open air gas concentration measurement [93,94,95]. Therefore, the UAS with a gas monitor is desirable as a more cost-effective method that can theoretically produce the information required to calculate the mass of gas emitted by a surface mine blast, provided the undefined errors associated with this method can be accounted for, including the effects of downwash on gas measurements.

1.3. RESEARCH APPROACH

The intent of this research was to define and understand the effect that UAV downwash could have on gas concentration measurements. Experiments were conducted by measuring gas concentration within a controlled environment that contained constant concentration. Three objectives were defined and completed through this research.

Objective 1: Establish the time required for the downwash region to stabilize after UAV rotor thrust variations cease. Any alterations to vertical, horizontal, or rotational movement of the UAV will change the rotor thrust and thereby the downwash region pressures. In an attempt to minimize variables during testing for Objective 2, gas concentration samples were only collected during times when the UAV was not altering its motion and the downwash region was stabilized. Therefore, the first experiment conducted was to determine how much time was required for the downwash region to stabilize once the UAV stopped applying thrust and returned to an unvarying thrust configuration. The experimental methodology and results pertaining to this objective are discussed in Section 3.

Objective 2: Quantify the effects of downwash on gas concentration measurements. The primary objective of this dissertation research is to evaluate and understand the effects that rotary-wing UAV downwash can have on measured gas concentrations. Numerous publications have expressed concern that this ever-present factor may be affecting concentration measurements, yet to the author's knowledge, this potential source of error was previously undefined. Understanding downwash mechanisms on gas concentration measurements and quantifying its effects will provide an essential advancement towards validating UAS as a means of gas sample collection.

The experimental methodology and results pertaining to this objective are discussed in Section 4.

Objective 3: Develop a system for correcting measured concentration according to location within the downwash region. If the concentration measurements were significantly affected by downwash pressures, then an equation could be developed to account for the error and correct the measured gas concentration. However, results from Objective 2 provided substantial evidence that a stabilized downwash region does not create statistical differences in measured concentration, and developing a correction factor was not necessary. This conclusion applied to all test scenarios irrespective of measurement location within the downwash region. The experimental methodology and results pertaining to this objective are discussed in Section 4.3.

1.4. CONTRIBUTION TO SCIENCE

This research provides evidence to support that the downwash region of a rotary-wing UAV does not produce pressure variations substantial enough to cause significant changes in density-based gas concentration measurements. Many researchers have described the need to define or mitigate this potential source of measurement error [39,40,41,44,45,47,50,56,58,60] [66,68,72,76,77,78,79,80,83,96]. To the author's knowledge, no such study has been performed to isolate, quantify, and evaluate the significance of downwash pressure as a source of gas sampling error. Accurate concentration measurements are critical for protecting health and safety, which means evaluation of actual downwash effects on measured concentration is essential. This potential source of error was previously undefined, and it was the only source of

undefined error that was ever present in all rotary-wing UAS studies. This dissertation's findings allow researchers to safely assume this source of previously undefined error is statistically negligible, provided the UAV and gas sampling point are located entirely within the gas cloud and the downwash region has stabilized.

Empirical evidence from 40 tests that collected 2,900 downwash air speed samples shows the maximum downwash region stabilization time is approximately 6 seconds after the UAV has ceased altering motion and returned to an unvarying thrust configuration.

Empirical evidence from 78 tests that collected over 363,000 gas concentration samples shows that downwash effects on gas concentration measurements are negligible with 95% statistical confidence. Additionally, the standard deviation in measured concentration showed no relation to turbulence gradients found during air speed studies, further implying that downwash turbulence has negligible effect on gas samples. These conclusions are valid for:

- distances 0.1-3.5 m vertically below the UAV,
- distances 0.1-0.8 m horizontally from the UAV propeller tip,
- distances 0.0 m on top of the UAV body,
- situations in which both the UAV and the measuring point are located entirely within the gas cloud, and
- samples collected after the UAV has ceased altering motion and the downwash region is allowed to stabilize.

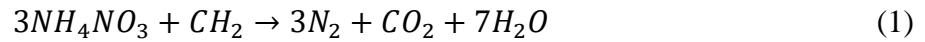
2. LITERATURE REVIEW

The primary goal of this dissertation was to determine whether or not UAV downwash pressures are great enough to cause statistical differences in measured gas concentration values so that observed concentrations can be reported accurately in industries where emissions are historically difficult to measure, such as surface mine blasting. If downwash pressure did cause a significant difference, this dissertation also aimed to define the extent of this source of error. To understand the driving factors of this research, background information from published literature is presented on gas emissions from surface mine blasting (Section 2.1), existing and potential regulations for such emissions (Section 2.2), and potential methods for monitoring blasting emissions (Section 2.3). Of these potential methods, UAS is the most desirable solution, but several undefined potential sources of error must be evaluated before a UAS can be accepted as a viable means of data collection. Numerous researchers have expressed concern that downwash may be negatively affecting concentration measurements (Section 2.4), but to the author's knowledge, no prior study has attempted to isolate, quantify, and account for this potential source of error.

2.1. BLASTING EMISSION GASES

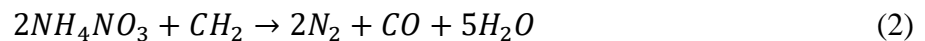
Detonation of explosives used in surface mining can potentially create toxic gases, yet the chemical reaction for ideal detonation does not show production of toxic fumes. Toxic gas byproducts include nitrogen dioxide (NO₂), nitric oxide (NO), and carbon monoxide (CO). However, explosive materials are not intended to produce these

gases [1]. The most common explosives used in surface mining are emulsions, ammonium nitrate and fuel oil (ANFO), and ANFO/emulsion blends [97]. As an example, Equation (1) shows the chemical reaction for the detonation of ANFO, using methylene as the fuel oil for this example [2].

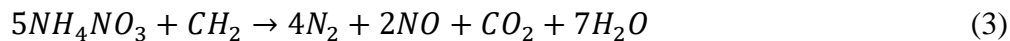


As shown, the reaction is intended to produce nitrogen (N₂), carbon dioxide (CO₂), and water vapor (H₂O). The toxic gases NO_x (NO and NO₂) and CO are formed when the oxygen is over- or under-fueled, which means the explosive is oxygen deprived or has excessive oxygen, respectively [1].

Over- or under-fueled ANFO exists when the ammonium nitrate and fuel oil components are mixed in improper ratios or not mixed properly. Additionally, the ammonium nitrate component can separate into nitrate and ammonia when dissolved in a solution, so exposure to a foreign solution such as water prior to detonation can break down ammonium nitrate, creating an excess of fuel oil. Equation (2) shows the ANFO detonation reaction when it is over-fueled. The fuel oil component (CH₂) has less ammonium nitrate to react with, and this oxygen deprivation results in fewer N₂ and H₂O molecules and produces CO instead of CO₂ [2].



Equation (3) shows the ANFO detonation reaction when it is under-fueled. This process has excessive oxygen, which results in additional N₂ and H₂O as well as NO. NO is relatively unstable, so it usually reacts quickly with oxygen in the atmosphere to produce NO₂, shown in Equation (4) [2].



The explosive property correlated with over- or under-fueling is velocity of detonation (VOD), which is the rate at which a detonation shock front travels through a particular explosive material. However, VOD is not itself a primary source of NOx because changes in VOD are a result of other factors. VOD can be improved by using a more sensitive explosive or increasing the explosive density. The primary causes of VOD reduction are excessive water content, lack of confinement, rock fragment contamination, improper explosive mixing, and detonation charges approaching the critical diameter [3,4]. Several laboratory tests have been performed to evaluate the effects on NOx production when each of these factors is varied. The results and references are summarized in Table 2.1. Note that each of the factors affecting NOx production are highly specific to local geology at each mine site, different locations within a mine, and even between individual blast holes [5,6]. Therefore, accurate gas emission reporting requires frequent measurement of post-blast gas concentrations.

Table 2.1. Summary of Laboratory Results Regarding Factors that Increase NOx Production during Explosive Detonation

Factor	Percentage Increase of NOx Production (%)			Citation
	ANFO	Emulsion	50/50 Blend of ANFO/Emulsion	
Increased Water Content	295	13	3	[22,23,24,25]
Increased Time Exposed to Water	N/A	313	86	[23,24]
Decreased Confinement	1,770	306	369	[22,23,26]
Increased Rock Dust Contamination	95	235	N/A	[22,26]
Non-Ideal Fuel Oil Mixture	4,638	100	N/A	[22,26,27,28,29]

2.2. BLASTING EMISSION REGULATIONS

Recently, NO_x has become of particular interest for regulators regarding surface mine blasting emissions. NO_x is potentially hazardous to human health if respired in high concentrations for extended periods of time or in extremely high concentrations for brief periods of time, causing a range of conditions from brief discomfort up to permanent and potentially fatal lung damage [7,8,9,10,11,12,13,14,15,16] [17,18,19]. In an effort to mitigate harmful effects, many government organizations set limits and/or time-weighted averages for human exposure to hazardous gases, including NO_x. Specific regulations on NO_x emissions from blasting have only been implemented in Australia so far, but US regulatory agencies have recently considered and implemented more stringent regulations on blasting emissions.

2.2.1. Regulations Regarding NO_x Exposure. The Environmental Protection Agency (EPA) is the primary US organization that regulates air toxin emissions from mining operations. The EPA has created the National Ambient Air Quality Standards (NAAQS), which are a set of regulations governing human exposure to air toxins according to a time-weighted average (TWA). Exposure limits for NO_x are set in the NAAQS to 100 ppb over a 1-hour TWA, or 53 ppb over an annual TWA [98]. Additionally, regulations also limit maximum exposure concentrations for any period of time, which has a ceiling limit of 2,000 ppb, or 1,000 ppb in California [82,99,100].

In addition to the NAAQS, health risks are reported to the EPA according to Air Quality Index (AQI). The AQI for an operation is a guideline calculated using formulas specific for each gas type, and the AQI value relates exposure to the expected level of health risk. Table 2.2 relates 1-hour NO₂ concentration to health risk, according to the

AQI [101]. The upper limits for categories above “Moderate” may be based on generalizations from other EPA studies, though available data is scarce for very high exposure concentrations [9]. According to the AQI, the annual average according to the NAAQS should remain “Good” and the 1-hour average should not exceed “Moderate”.

Table 2.2. Air Quality Index and Expected Health Risk from NO₂ Exposure over a 1-hour TWA

Category	Air Quality Index	NO ₂ (ppb per 1-hour TWA)
Good	0-50	0-53
Moderate	51-100	54-100
Unhealthy for Sensitive Groups	101-150	101-360
Unhealthy	151-200	361-649
Very Unhealthy	201-300	650-1249
Hazardous	301-400	1250-1649
Very Hazardous	401-500	1650-2049

On average, the atmosphere in the US is expected to have between 0.02-1.0 ppb of NO_x at any given moment, and therefore values exceeding 53 ppb can be considered abnormal. However, urban locations such as those in Southern California have been shown to exceed NAAQS standard, likely due to traffic after the end of the typical work day [9].

2.2.2. Potential for NO_x Incidents at Surface Mines. Multiple incidents resulting in injury or fatality are confirmed to have been caused by blast cloud fumes.

- In 2006, a blaster in the Philippines fell into a cavity during a post-blast inspection. He was treated for physical injuries but was not treated for

respiratory disease. It is believed the cavity was filled with blast fumes, because he contracted pulmonary edema and died on the following day [30].

- In 2009, three different Australian mines created blast clouds that did not dissipate and remained at presumably high NO_x concentrations for an exceptionally long duration. The first cloud resulted in hospitalization for 3 miners, the second cloud traveled 3.8 km and caused hospitalization or first response treatment for 14 miners, and the third resulted in first response treatment for 1 miner [30].
- On March 6, 2011, a similar incident occurred that affected two more Australian mines. The cloud traveled 4.2 km from one mine to the other [31]. 24 miners, a total from both mines, received precautionary hospitalization to assess any respiratory effects [33].
- On April 2, 2011, a second incident occurred at the same mines as the March 6, 2011 incident. A blast cloud was created that traveled over 10 km before dissipating; it did not affect any miners from the originating mine, but multiple miners were hospitalized from the second mine. An exact number of miners affected by this incident was not released to the public [32].






These six incidents prove NO_x exposure to be a potential hazard for blasting operations, though substantial research must be performed to provide a method for evaluating the health risk posed by this hazard.

2.2.3. Existing Regulations on NO_x Produced by Blasting. There are presently no nations that regulate exact NO_x emission levels from surface mine blasting. The US does require blasting to be conducted in a manner that prevents human injury [102], but enforcement has historically only been reactionary rather than preventative [38]. The US also requires surface mines to report an estimation of NO_x produced by blasting, however an approximation is acceptable using an assumed value of 17 lb of NO_x per ton of explosive (4.4 L of NO_x per kg of explosive) [20]. According to the test results in laboratory research (Table 2.1 in Section 2.1), the EPA's estimated value is lower than any lab tests with 50/50 blend (6.3 L/kg minimum) [23,24,26], and on the very low end of possible production from ANFO [22,26,27,28,29]. Each of the most commonly used explosive materials can be detonated in conditions that cause a mine's NO_x emissions to be significantly overestimated or underestimated, which emphasizes the need for each mine site to measure their own site specific emission levels for the purpose of NO_x emission reporting. Therefore, there is need to either re-evaluate the EPA estimated value or to develop a system for site-specific NO_x quantification.

Australia is the only nation that has regulations expressly considering the monitoring of blasting emission effects, though these laws do not specify a method of measuring emissions, allowable emission concentrations, or limits for exposure. In an effort to predict the effects of emissions, the Australian Explosives Industry Safety Group (AEISG) produced guidelines for blast emission supervision in 2011, and these guidelines only consider the presence of visible NO_x. Clouds of dust and gas created by blasting can have varying color, from yellow to dark red, depending on quantity and concentration of NO_x. The AEISG guidelines provide a method for ranking the severity

of visible NO_x based on cloud color and the percentage of blast holes that produced visible NO_x during the blast. These guidelines are outlined in Table 2.3, where “Localized” refers to “only a few blast holes”, “Medium” refers to “up to 50% of blast holes in the shot”, and “Extensive” refers to “extensive generation of NO_x gases across the whole blast” [103].

Table 2.3. Australian Guidelines for Assessing NO_x Production from Surface Mine Blasts [103]

Level	Typical Appearance
Level 0 No NO _x gas	
Level 1 Slight NO _x gas	
1A Localised	
1B Medium	
1C Extensive	
Level 2 Minor yellow/orange gas	
2A Localised	
2B Medium	
2C Extensive	
Level 3 Orange gas	
3A Localised	
3B Medium	
3C Extensive	
Level 4 Orange/red gas	
4A Localised	
4B Medium	
4C Extensive	
Level 5 Red/purple gas	
5A Localised	
5B Medium	
5C Extensive	

There are three items of note from the Australian guidelines:

1. The guidelines are based on a percentage of holes affected, not quantity of explosives used, which has the potential to treat one blast much more severely than another despite producing the same NO_x quantity and concentration as another blast.
2. The guidelines are based on the initial color of the blast cloud, despite any visible NO_x (minimum 2,500 ppb [104]) being well above both the NAAQS 1-hour TWA limit (100 ppb) [98] and the AQI “Very Unhealthy” range (1650-2049 ppb) [101].
3. Finally, the initial concentration does not equate to a TWA concentration exposure to humans. For example, the cloud may be visible (greater than 2,500 ppb) immediately after the blast, but then dissipates rapidly to levels below 100 ppb and/or moves rapidly over persons in the path of the cloud, resulting in a 1-hour average concentration that complies with the NAAQS. On the contrary, it is also possible that the cloud does not dissipate rapidly or that the wind is relatively stagnant, thereby increasing the likelihood of human exposure to health risks.

These three discrepancies reveal that the AEISG guidelines do not rank cloud severity on NO_x concentrations within the cloud or on actual generated health risk.

2.2.4. Upcoming Regulations on NO_x Produced by Blasting. US interest in regulation of NO_x produced by surface mine blasting is relatively recent. The NAAQS 1-hour NO₂ exposure limit was not implemented until 2012, and NO is currently unregulated as it is assumed all NO will rapidly react with the atmosphere to become

NO₂ [98]. In 2014, the environmentalist group WildEarth Guardians (WEG) petitioned the Office of Surface Mining Reclamation and Enforcement (OSMRE) for regulation regarding NO_x from surface mine blasting. After reviewing the petition and public comments, OSMRE approved the petition on Feb 20, 2015. Initially, OSMRE chose not to adopt the regulatory changes as outlined by WEG, electing instead to form a new rule [105]. However, on July 29, 2019, OSMRE withdrew their approval after determining that OSMRE does not have legal authority to regulate surface mine blasting emissions. OSMRE concludes that “incidents of persons or property being adversely affected by toxic blasting emissions are rare,” though the supporting data is extremely limited and is largely based on visual observance of NO_x discoloration within the blast cloud [38]. Because NO_x can be visible without being harmful and vice versa, quantitative studies regarding the safety and health risk posed by surface mine blasting emissions are needed rather than subjective observance of the blast cloud.

Public perception in the US has grown increasingly concerned that NO_x emissions from surface mine blasting may be negatively affecting health and safety or the environment [38,104]. Such concern has caused some US states to implement more stringent regulations on surface mine blasting emissions [34,35,36], and further regulatory restrictions are under consideration [37]. Despite the inaccuracy of enacting discipline based on visual appearance of the blast cloud, Wyoming has done so on at least three occurrences after significant outcry from concerned locals.

If surface mines were able to measure emissions produced and actual human exposure, they would have quantifiable evidence to determine whether the mine is adequately complying with regulations and protecting health and safety. If violating

incidences are as rare as OSMRE believes them to be [38], then a method of evaluating actual risk will provide surface mines with a verifiable defense against unjust regulatory discipline and public outcry. One potential method for evaluating health risk is to use cloud dispersion equations. Attalla [106] has used cloud dispersion modeling to determine peak NO₂ concentrations in blast clouds over time, though no attempt was made to relate the concentrations to human health risk [106]. Madden [33] also discusses a future need for studying cloud dispersion to evaluate health risk [33]. No studies have been found at this time that apply cloud dispersion to determine if emissions from surface mine blasting actually violate NAAQS or pose any health risks. However, such studies are not possible without first knowing the mass of gas produced during a blast event [87,88,89,90,91,92].

2.3. FIELD MEASUREMENTS OF BLASTING EMISSIONS

Several attempts have been made to evaluate NO_x emission quantities from blasting. Table 2.1 in Section 2.1 discusses laboratory tests, which are good for estimation. However, field blasts are much more complex with each of the laboratory test variables interacting in complex ways. Estimations produce a wide range of possible emission quantities for each blast event, and any specific emissions quantity per unit of explosives chosen within that range may prove paradoxical [20,21]; health and safety may not be protected if the assumed emissions are near the low end of the range, while blasting sites may receive unjust punitive penalties if the assumed emissions are higher than actual. The need for clear and actionable regulation necessitates a more accurate system of collecting field measurements after each blast event. A few field emission

studies have been performed, although none of these have attempted to relate the measured quantities and concentrations to health risk, and many of them lacked in-depth analysis of the errors inherent to their tests.

2.3.1. Field Measurements of Surface Mine NO_x Production. Measuring blasting gas emissions at surface mines presents several difficulties. Blasting produces large shock forces and moving debris that would probably damage or destroy any gas sampling devices that have very close proximity to the blast. However, sensors placed at ground level that are too far from the blast site will encounter a gas cloud so dispersed that the percent error in measurement readings will be relatively high. Furthermore, the weather can be difficult to predict and may carry the cloud away from sampling locations or far above them. People or vehicles carrying gas sensors may be able to correct for unpredicted wind changes, though a rapid approach to the blast site is not possible, and it is not ideal for people to physically take samples within a cloud that may potentially contain hazardous gases [106,107].

After extensive literary review, few reports have been found discussing attempts to quantify NO_x emissions from full-scale surface mine blasts. The results of these reports are discussed in the following sections.

2.3.2. Fixed Location Gas Sensors. The earliest identified field measurement attempt used sensors placed strategically around a blast site that detonated an ANFO/emulsion blend containing between 50-60% ANFO. The experiment made three attempts to measure blasting emissions by placing gas capture devices at ground level near the blast holes. Most of the sensors were destroyed by the blast, but the measured results contained 10-64 ppm of NO_x [85], which is very low compared with laboratory

results, implying the surviving sensors were too close to the ground and/or too far from the blast site to have direct contact with the gas cloud.

English [84] studied NO_x production using ground-level sensors downwind from the blast location. The study did not attempt to measure the quantity of NO_x produced, only the concentration at ground level away from the blast site. The experiment measured concentrations for 10 blast events at 3 different mine sites. For each event, 1 station was placed directly downwind from the blast site, 1 other station was placed further downwind from the first station, and 3 additional stations were placed at approximately the same distance as the first station but at 10-45° from the wind direction. The stations were moved prior to each event in an effort to predict wind direction, and the sensor distances from the blast site were not constant between events, resulting in sensors placed at various distances approximately 60-600 m from the blast site. All stations were placed 1.5 m above ground level in an attempt to measure human exposure concentrations at that distance. For stations 60-150 m from the blast site, peak NO₂ concentrations ranged from 0 to 4,200 ppb with an average of 1,340 ppb. For stations 150-300 m from the blast site, peak NO₂ concentrations ranged from 0 to 800 ppb with an average of 170 ppb. For stations 300-600 m from the blast site, peak NO₂ concentrations ranged from 0 to 3,600 ppb with an average of 540 ppb. Of the data that could be collected, none of the sensors were directly in line with each other downwind, so it was not possible to track individual cloud progression. The study attempted to relate powder factor, explosive weight, and humidity to NO₂ production, although no trends could be found, and other potential factors such as geology and water content were not recorded [84].

The study by English [84] presented several areas for improvement. English [84] believes that wind direction was not predicted accurately for some of the events, causing some stations to miss recording useful data. No consistent trends can be found in the measured data, which provides a further example of NO_x production variation between blast events, and even between successive events at the same mine site. The difficulties in wind direction estimation and downwind trend measurements provide evidence that an improved measurement method should be employed for future NO_x studies at surface mining blast sites. Additionally, the sensors used measured NO_x in increments of 100 ppb despite 100 ppb being the maximum value for 1-hour exposure according to the NAAQS.

Battelle [86] performed a similar study by placing gas sensors at points of interest within a community nearby a surface mine. The study found no correlation to measured NO_x peaks and mine blasting. However, the study had many limitations that made it unlikely to collect data from mine blasting, including a short testing duration in which there were only 37 blast events, weather and topography factors that made it unlikely for air from the mine to be transported to the measuring points, and measuring points that were 1-8 km away from the blast site. The study found it impossible to differentiate NO_x produced by the surface mine from NO_x produced by sources within the community, such as automobiles [86].

In summary, using fixed sensors for human exposure evaluation requires a vast number of sensors located at each place where people may be present in the possible path of a gas cloud, and the cost of purchasing, installing, and moving sensors is not ideal. While this method is a feasible system of measurement for determining total human

exposure, it is still incapable of distinguishing the level of exposure caused by specific sources, thereby making it impossible for regulatory agencies to determine the source(s) of exposure violations. Feasible regulation will require site-specific emissions monitoring, which is unlikely to be accomplished by fixed location sensors.

2.3.3. Spectrometry. Attala [106] used differential optical absorption spectrometry to measure multiple gas concentrations after full-scale blasts at 2 surface mine sites. This type of spectrometry can measure multiple gas concentrations simultaneously at considerable distances. While it was not possible for the spectrometer to relate the measured concentration to an exact measuring location, the overall cloud concentration could potentially be combined with the cloud volume at the time of measurement to determine the total mass emitted [106]. Once the mass is known, cloud dispersion equations can be used to estimate human exposure at any location downwind from the blast site [87,88,89,90,91,92].

The most limiting factor for using spectrometers is the cost. Commercially available spectrometers cost approximately \$230,000 [93]. Custom systems can be developed for considerably less cost, approximately \$17,000, but they require extensive research and labor to develop [93,108,109,110,111]. For comparison, a UAV-mounted gas monitor as discussed in Section 2.4 has an approximate maximum cost of \$8,000 [94,95].

Spectrometry is also a feasible method of quantifying blasting emissions, though the largest limiting factor is capital costs as spectrometers are extremely costly compared with the other methods described in this literature review. Additionally, further research is required to accurately determine the volume of gas in the cloud at the time of

concentration measurement, which is crucial information for calculating the mass emitted. Comparisons of Attala's [106] calculated mass with the measured masses of prior laboratory tests [22,23,24,26,27,28,29] implies that Attala's method may have drastically overestimated the volume of gas in the cloud.

2.3.4. Unmanned Aerial Vehicles. The primary configurations of UAVs are balloon, fixed-wing (similar to an airplane), and rotary-wing (similar to a helicopter) UAVs. Balloon UAVs have little to no control over their movement, and will therefore encounter similar problems as fixed location gas sensors [112]. Fixed-wing UAVs have high battery life, but they require precise timing. The high flight speeds and inability to hover only allow for a small number of samples to be collected with each pass, and adjusting flight patterns to make a subsequent pass can take a significant amount of time. Therefore, fixed-wing UAVs are more suitable for collecting data across a vast flight path rather than relatively localized gas releases such as those from surface mine blasting [112]. Rotary-wing UAVs are much more adaptable to changing cloud paths, and they are able to hover within the cloud to obtain a large number of data samples. Due to the short duration of blasting events, rotary-wing UAVs are ideal for ensuring data can be collected directly within the blast cloud while maximizing the number of samples that can be collected before the cloud disperses, thus a short flight time due to short battery life is less likely to be a concern [76]. For the remainder of this dissertation, "UAV" and "UAS" will refer to rotary-wing UAVs and systems unless otherwise specified.

McCray [39] used a gas monitor mounted on a UAV to evaluate NO_x emissions from full-scale surface mine blasts. The project was not extensive; only three tests were performed to measure the immediate post-blast data. The first two attempted to measure

concentration in the cloud immediately after the event, taking measurements as quickly and closely to the origin as possible, but only one of these produced concentration data. The third test measured NO_x within the cloud 450 m downwind from the blast site [39].

McCray [39] attempted to calculate the “worst case” mass of NO_x produced. The study estimated the volume of the gas cloud at the time of measurement, and then assumed the peak concentration measured was present throughout the entire cloud. The resulting mass was within the expected range of NO_x values according to the laboratory results [22,23,24,26,27,28,29], which appears to show that UAV observation is viable for obtaining emission data from full-scale blasts [39]. However, a more accurate method might be found in using cloud dispersion equations to back-calculate the total emitted mass [87,88,89,90,91,92,113,114,115,116] [117,118].

Using a UAV to quantify blasting emissions is another viable option, and it is significantly more cost effective than fixed location sensors and spectrometers. However, it requires additional work before it can be fully implemented. The first step in that process is quantifying the errors associated with UAV measurements, such as the effects of UAV rotor airflow on measured concentrations.

2.4. UAV-MOUNTED GAS MONITOR SYSTEMS

Although UAV gas monitoring systems appear to be the most cost effective solution for measuring emissions from blasting events, there are a significant number of undefined factors that must be evaluated before the accuracy of such a system can be established. Many of these factors are related to downwash, which is airflow that is disrupted by any amount from the downward thrust of the UAV rotors. Downwash is

named such because the majority of the air is flowing in a downward direction, but the downwash region actually refers to the air on all sides of the UAV that experiences turbulence caused by the UAV's rotor thrust [81]. Downwash can disrupt the natural cloud airflow or dilute it with ambient air [39,40,41,44,45,47,50,56,58,60] [66,68,72,76,77,78,79,80,83,96]. Figure 2.1 is taken from a simulation of UAV rotor downwash, in which the white areas below the UAV show areas of varying pressure affected by the UAV thrust [119].



Figure 2.1. Simulation of UAV Downwash, where the White Areas below the UAV Represent Locations with Pressures that Vary from Ambient Pressure [119]

Before the accuracy of a UAV-mounted gas monitoring system can be established, each of the factors must be defined that can cause potential measurement errors. Of these, the most basic factor that is ever present is the change in air pressure within the downwash region. Although concentration is typically measured in volume-to-volume or mass-to-mass ratios, the standard set by the Occupational Safety and Health Administration (OSHA) is to measure concentration as mass-to-volume at a standard

temperature and pressure [83], and this standard is adopted by many US regulatory organizations including the EPA. Therefore, pressure changes have the potential to alter concentrations that are measured according to regulatory standards.

2.4.1. Downwash Modeling. The earliest found study on UAV rotor downwash was performed in 2014 by Haas [49]. The project evaluated a 6-rotor UAV downwash using computational flow dynamic (CFD) analysis and empirical data collected in a controlled wind tunnel. The paper attempts to analyze the downwash effects on air velocity and pressure, though it does not attempt to relate these findings to gas concentrations measured within the downwash region. Both the CFD and wind tunnel results were statistically similar, and the CFD results are shown in Figure 2.2. The results showed changes in air pressure and velocity up to 2 m above the UAV and down to 8 m below the UAV. It is possible the affected region extends beyond these values, but these distances were the extents evaluated by this study [49]. The results show that the downwash region is relatively localized around the UAV. The greatest distance from the UAV that is affected extends below the UAV, while the area to the sides and above the UAV are affected to a relatively short distance. Additionally, the downwash beneath the UAV does not spread horizontally, but rather joins together making a conical shape beneath the UAV. Therefore, the results of this study imply that the concentration is not likely to be greatly affected outside of the immediate downwash region. The decreased air velocity and pressure immediately beneath the UAV body shows an area that is not as influenced by the rotor flow due to the UAV body buffer and distance from the rotors. The airflow beneath the UAV is also focused by the angle of the rotors, implying the downwash region may be conical in shape. The results also appear to show significant

decreases in air pressure changes at further distances beneath the UAV despite being inside the region where air speed is increased greater than 5 m/s. This implies that concentration measurements taken within the downwash region may potentially be negligibly affected by downwash, provided the measuring point location is still some distance from the UAV.

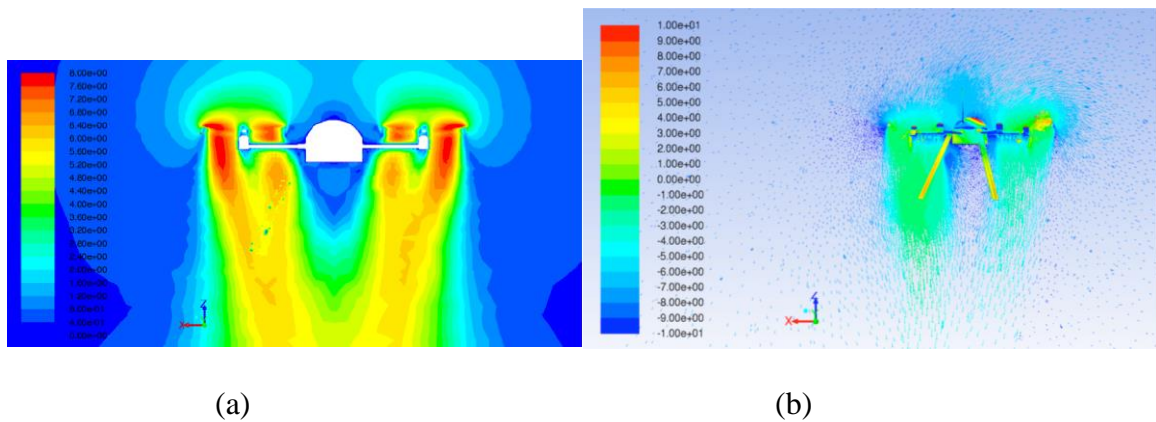


Figure 2.2. Profile of Downwash Effects on (a) Air Velocity, values in m/s, and (b) Pressure, values in Pa [49]

Several models and measurements have produced results that verify findings presented by Haas [49]. Li [60] modeled and measured the airflow of a 6-rotor UAV hovering 7 m above ground level. Yang [70] modeled the airflow of a 6-rotor UAV hovering 3.55 m above ground level. Yeo [120] measured air velocity at a distance of 7 rotor diameters from a 4-rotor UAV. Ni [121] modeled the airflow of a 4-rotor UAV hovering 1.3 m above ground level. The results from these tests agree with Haas' [49] findings that the velocity profile below the UAV remains relatively localized around the UAV, extending horizontally by a maximum of one half of the UAV diameter. Additionally, Li [60], Yang [70], and Ni's [121] results verify the same conically shaped

downwash region with the low velocity region immediately beneath the UAV body [60,70,121]. Another study by Yang [71] uses the same model with varying UAV payload weights. The results show increasing air velocities produced by the greater thrust required for increasing payload weights [71]. Zheng [72] modeled airflow of a 6-rotor UAV hovering 2, 3, and 5 m above ground level, Tang [69] modeled and measured airflow of particulate matter dispersed beneath an 8-rotor UAV hovering 2 m above ground level at various rotor speeds, and Shi [122] modeled and measured airflow of particulate matter dispersed beneath a 4-rotor UAV hovering 0.3-0.9 m above ground level. All of the results show very wide regions of airflow circulation as the air is reflected off the ground. The recirculation regions extend horizontally by approximately two times the UAV diameter. Substantial recirculation is still seen at 5 m above ground level, which implies the downwash region extends at least 5 m below a 6-rotor UAV [69,72,122].

Villa [50] measured air velocity around a 6-rotor UAV in greater depth than Yeo's [120] experiment. Vertical airflow was measured above, below, and horizontally from the UAV at 0.1 m increments up to 1.4 m vertically from the UAV center (above and below) and up to 2.0 m horizontally from the propeller tip. Horizontal airflow was also measured at 0.2 m increments at distances from 0.1 to 1.9 m from the propeller tip. In summary, Villa's [50] results show multiple findings: (1) air speed is highest beneath the UAV, (2) air speed is lowest horizontally from the UAV, (3) airflow beneath the center of the UAV does not experience high speed until a distance at which the individual rotor contributions begin to interact, (4) horizontal airflow and vertical airflow horizontally from the UAV potentially decays at a faster rate than airflow directly above

and below the UAV [50]. Each of these findings are presented in previously mentioned papers [49,70,120,121], though Villa's [50] study provides substantial empirical evidence to validate the findings.

2.4.2. Field Sample Collection. In 2013, Smidl [74] published the earliest found report mentioning the use of rotary-wing UAVs specifically for collecting physical samples from open air gas releases. The paper modeled a theoretical gas release, and it also modeled theoretical measurements that would be taken from stationary gas monitors and UAV-mounted gas monitors. The objective of the simulation was to compare mapping of approximate concentration regions within the cloud. The results showed high mapping similarities between a series of strategically located stationary gas monitors and the use of two UAV units along a strategic flight plan, although the UAV system had a greater range of error that did not include the possibility of downwash interference [74]. This theoretical paper was followed shortly by Neumann's [48] empirical study, which measured multiple gases using a 4-rotor UAV. The tests were able to collect data. Downwash was visually observed to disturb the cloud, and it was believed that the disturbance could affect the concentration measurements, but measurement accuracy with and without downwash was not compared [48].

Since those initial studies, papers have been published with increasing frequency. Several papers have been published on the theoretical application of UAV-mounted gas monitors without actually performing data collection. Nash [42] discusses the potential applications, but does not mention downwash or measurement accuracy [42]. Alvear [51,54], Facinelli [75], and Tosato [123] discuss and simulate automatic flight plans for swarms of UAVs to measure over a large area simultaneously [51,54,75,123]. Alvear's

[51] paper mentions that wind can have great effect on sensor readings, but none of the four papers consider downwash [51]. Bolla [55] also discusses swarms of UAV-mounted gas monitors, as well as briefly discussing downwash and the potential need to extend the measuring point outside of the downwash region [55]. Ahlawat [59] develops a lightweight sensor for use on a UAV, but does not actually test with a UAV or mention potential errors associated with UAV testing [59].

In addition to theoretical papers, several papers have also discussed measurement attempts using UAV-mounted gas monitors, though most of these do not consider downwash effects on accuracy of the collected data. Chang [64,65] used an 8-rotor UAV system to collect gas samples after gases were released from an exhaust vent. Rather than using real-time gas sensors, a volume of air was taken to be tested later in a laboratory setting. The paper compared the measured results to those upwind from the gas release, but did not compare with results gathered without UAV downwash [64,65]. Ali [52] and Aboubakr [53] used a 4-rotor UAV system to measure greenhouse gases in an urban environment, though they did not discuss accuracy of their measurements [52,53]. Kersnovski [96] and Golston [46] used a UAV-mounted gas detecting infrared camera rather than a gas sensor as seen in most other papers. The former study was performed indoors to avoid wind-induced error and the latter was performed outdoors, but neither considered error due to downwash [96,46]. Liu [57], Pochwala [61], and Mawrence [63] used a similar 4-rotor system to measure particulate matter in urban environments. The papers discussed error due to weather and topographical effects, but did not discuss downwash [57,61,63]. Barchyn [124] used a 4-rotor UAV along gas pipelines to discover leaks. However, the study was only concerned with finding methane spikes that may

relate to a leak rather than the actual quantity released, and therefore was not concerned with measurement accuracy [124]. Similarly, Liu [43] measured potential methane leaks. While Liu [43] did measure actual concentration values, the study did not mention downwash or make any attempt to quantify UAV-associated errors [43]. Zhou [67] measures gas emissions from a freight ship and mentions error sources such as wind, but does not quantify errors or mention downwash [67]. Bao [125] measured concentrations in a building and mentions downwash as a potential error source, but the study assumes downwash error is negligible and does not attempt to quantify it [125].

Some papers discuss using UAV-mounted gas monitors while considering downwash, though not directly attempting to quantify the downwash effect on measurement accuracy. Brady [77] used a gas monitor mounted on a 4-rotor UAV to measure aerosol particles released by ocean waves. In an attempt to overcome downwash interference, a pump was attached to the gas monitor and a rigid tube extended from the pump to a distance above the UAV that was theoretically beyond the range of downwash interference, though no testing was performed to verify that downwash was sufficiently negligible at that distance. The measuring point was 0.25 m above the rotor height and located above the front edge of the UAV body, as shown in Figure 2.3 (a) [77]. McCray [39] separately developed a similar concept by extending a tube below a UAV that was used to evaluate NO_x emissions from surface mine blasts. To avoid landing interference, a flexible tube was used with a bag of weights attached to keep the tube as vertical as possible, shown in Figure 2.3 (b) [39]. In the time since these studies were published, the idea of extending the measuring point beyond the downwash region has grown in popularity. Several UAS have been developed with the measurement point extended

below [44,45,58,76,79], above [45,60,80], and to the side of the UAV [47]. Despite attempting to alleviate downwash error, none of these studies attempted to evaluate measurements for accuracy, and no published testing was performed to verify that the tube extensions were of sufficient length to consider downwash effects to be negligible [39,44,45,47,58,60,76,79,80].

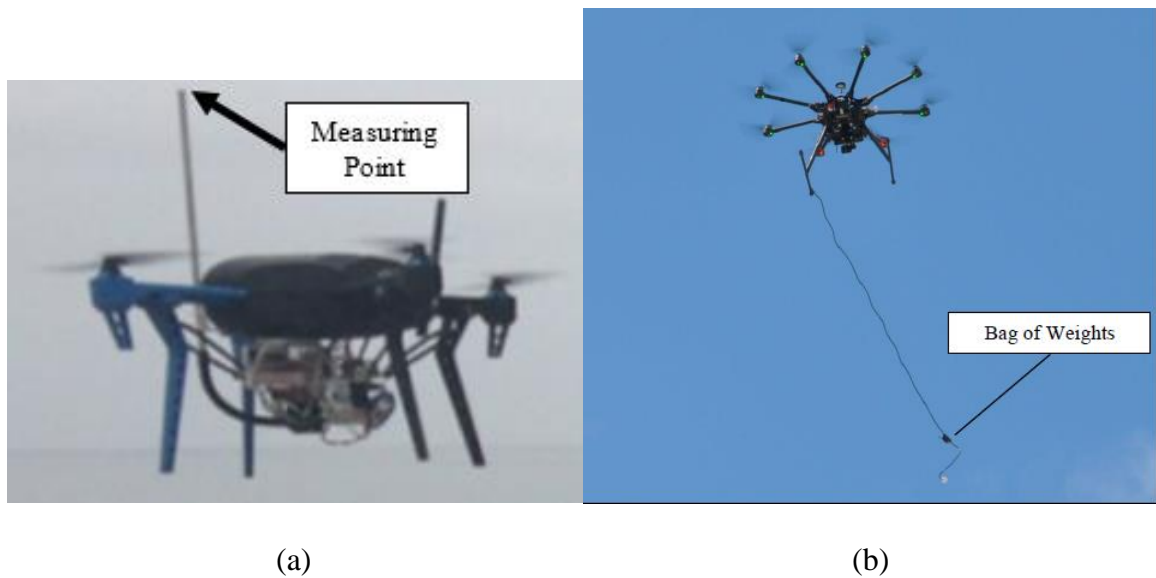


Figure 2.3. UAVs with a Tube Extension Attached to a Pump on the Gas Monitor, shown extending (a) upwards [77] and (b) downwards [39]

2.4.3. Downwash Effects on Field Measurement Accuracy. Few papers have been found that discuss tests to determine accuracy of data collected by a UAV-mounted gas monitor. The earliest found published field measurement using a UAV system, as well as the first direct discussion of downwash interference with gas monitoring results, was presented by Roldan [68]. The study used a gas monitor on a 4-rotor UAV to measure CO₂ concentrations. Air velocity was evaluated using CFD and by measuring

directly above and below the UAV on a 24-point grid to determine the point where the air speed was lowest, and therefore potentially having the lowest downwash interference. The study found that the top center of the UAV experienced the lowest air velocities, and this is where the gas monitor was placed. The study measured the difference between results measured with and without the UAV rotors running on two separate CO₂ releases of identical size. The measuring point was at the same height for both experiments, and 6 samples were collected for each test at 1 m horizontal increments from the gas release point. The results showed an average of 3.84% error, although the readings have approximately 13% error at 0 m, 9% error at 1 m, and near 0% error for all samples measured between 2-5 m. The paper did not address potential causes for the apparent effect that distance from the gas source has on the percent error, and downwash error was not evaluated further [68].

Villa [50] measured concentrations of CO, CO₂, NO, and NO₂ produced by an idling diesel vehicle. The gas was directed from the vehicle's exhaust pipe through a tube so that the gas release point was a constant 0.7 m horizontal distance from the gas sensor measuring point at a constant height of 2.5 m. The measuring point was variable, extending 0.7 m and 1.1 m away from the UAV center, repeated three times to measure at both distances above, below, and horizontally from the UAV. One test was also performed with the UAV rotors off, though the sensor location is not defined in the paper. Comparison of results with the propellers on and off did show a significant decrease in concentration. However, the gas release was likely not enough to fill the test area, so it is not possible to determine how much of the concentration change was caused by changing pressures in the downwash region or by downwash airflow causing mixture

with ambient air. Comparison of UAV location relative to the cloud reveals that measured concentration is significantly higher when the UAV is located within the cloud rather than above or below it, further implying the need for a gas cloud large enough to envelop the UAV prior to determining concentration changes due to varying pressure in the downwash region [50]. Based on the results of this vehicle study, Villa [62,66] performed two studies to measure gases and particulate matter produced by vehicles on a highway and by an ocean ship. However, the two tests do not discuss downwash accuracy in more depth [62,66]. The second test was also performed while the UAV was in constant motion, and the complexities of the downwash region changes during motion likely produced greater errors [66].

Alvarado [40] measured airborne particulate matter by using a leaf blower to expel a fixed quantity of dust at a height of 5 m. A 4-rotor UAV was used, and testing was performed to determine the extent of downwash above, below, and beside the UAV. Only the results above the UAV are discussed in the text, and it was found that airflow above the UAV became isokinetic, having a constant and non-turbulent speed, on a plane at a distance of 0.40-0.45 m above the UAV. Therefore, the inlet measuring point for the gas monitor was placed 0.475 m directly above the UAV. However, comparison with results measured without downwash showed the UAV-measured results had an average of 50% error. Measurements for all but one of the particulate matter bins was much lower when measured by the UAV, and it is possible that the downwash caused mixture with ambient air while pushing the particulate matter down away from the sensor [40].

Aurell [41] measured airborne particulate matter emissions from burning military ordnance in open air. Data was collected using a 6-rotor UAV-mounted system, and the

results were compared with historical data measured by systems mounted on stationary balloons and airplanes. The measuring point was located approximately 0.2 m below the height of the UAV rotors and 0.3 m horizontally from the UAV center. The results, measured over 84 different burn plumes, showed 4.0 g of particulate matter less than 2.5 μm (± 1.2 std. dev.) and a total quantity of 4.8 g (± 2.8 std. dev.), while previous research from the airplane and balloon systems showed 6.9 g and 5.7 g of particulate matter less than 10 μm , respectively. Aurell claims the results are statistically similar, additionally claiming that varying factors between the tests, including downwash interference, are negligible. However, it is unclear how the UAV-measured values were related to measurements from the airplane and balloon systems [41].

Zhou [78] measured CO, CO₂, and particulate matter produced by detonating explosives. Prior to explosives testing, downwash effects on concentration were also tested using a single fan that had the same dimensions and rotational speed as the UAV rotors. Measurement locations were placed 2 m above the fan and 0.5 m downwind from the fan, and a fixed quantity of particulate matter was released upwind by burning cardboard. Three tests were performed with the fan on and off. The measured results with the fan on varied by a maximum of 4% from the results with the fan off. It was then assumed that downwash did not significantly affect the results during detonation testing [78].

Gu [56] measured NO₂ near buildings and roadways. The paper discusses the need to evaluate downwash effects on concentration measurements, but the study's primary source of error came from the decision to power the gas monitor using the UAV batteries. As the UAV altered thrust, the power input to the gas monitor also surged and

waned. The gas monitor's output was not shielded from input interference, so the output voltages and readings were altered so greatly that no coherent pattern could be found in any measurements. Therefore, the paper recommends using a separate power source and using gas monitors with isolated outputs [56].

2.4.4. Downwash Effects on Air Pressure. Density-based gas concentration measurements are potentially subject to alterations caused by air pressure. Previous studies have simulated air pressures for a variety of UAV models with widely varying propeller shapes, number of rotors, and rotor configurations. Air pressure changes due to downwash were relatively similar across all studies [49,70,72]. By calculating the change in pressure with relation to ambient pressure, the results imply that density-based gas concentrations would only be altered by a maximum of $\pm 0.10\%$. Based on these findings, the author hypothesizes that a wide variety of UAVs will experience similar results and are not capable of producing downwash pressures substantial enough to alter gas concentration measurements.

2.5. SUMMARY

Based on the literature review the proposed project has the potential for industry-wide application in the monitoring of NO_x gas emissions produced by surface mine blasting. Previous laboratory experiments show a wide variance in potential NO_x production from explosive detonation depending on site specific conditions that can result in non-ideal detonation. Despite EPA regulations on NO₂ exposure, NO_x produced by surface mine blasting remains unmonitored. As state regulators in the US implement more stringent restrictions and public opinion grows more concerned about surface mine

blasting emissions, this project seeks to establish the first step towards determining the level of risk that is present in current surface mine blasting operations.

Regardless of the likelihood for specific mine sites to produce NO_x clouds, mines may still desire NO_x monitoring to evaluate the health risk at each specific site and as a method for proving safe conditions at the mine site. Frequent measurement at numerous locations requires a cost effective system and easily repeatable method for measurement and evaluation of these emissions. A potential solution is to use a UAV-mounted gas monitor to measure post-blast gas concentrations, and then use the measured data with established cloud dispersion equations in an attempt to quantify human health risk. However, several factors must be evaluated and defined to establish the errors and feasibility of using UAVs to measure gas concentrations.

This dissertation project will evaluate and define the undefined potential source of error that is present in all rotary-wing UAS samples, which is the potential for downwash pressures to affect concentration measurements. Many published studies have described downwash as a potential source of measurement error, and several attempted to mitigate the error by distancing the measuring point from the UAV body. However, all of the found previous studies have either assumed the error to be negligible or they assumed their mitigation techniques were sufficient despite lacking evidence to support these assumptions. After extensive literature review, the author has found no evidence that downwash error has been isolated, quantified, and evaluated for direct effect on measurements prior to this dissertation. Experimentation for this dissertation has successfully isolated and measured downwash error, and the experimental method, results, and conclusions are discussed in greater detail in the following sections.

3. POST-MOVEMENT STABILIZATION TIME FOR THE DOWNWASH REGION OF A 6-ROTOR UAV

While a constant thrust is being applied to a UAV's rotors, the air velocities in the downwash region are relatively constant. In contrast, the individual rotor thrusts are changing when the UAV is altering its motion, which in turn will alter the downwash air velocities. Changes in air velocity will create changes in air pressure, which has the potential to alter the density-based gas concentrations in the downwash region. Accounting for every possible combination of rotor thrust is not currently feasible, but error evaluation can be simplified by only considering measurements taken when the downwash region is relatively stable. In addition to the time that the aircraft is in motion, more time may be required for the downwash region to stabilize after UAV motion has ceased. The objective of this section is to determine the time required after UAV movement for wind speeds in the downwash region to stabilize. The author has published the results of this section in the peer-reviewed journal *Heliyon* [126].

3.1. METHOD

The goal for the testing in this section is to determine the time for the air velocity under the craft to return to a constant rate after the craft has ceased maneuvering. The experimental design monitored changes to the downwash region after completing vertical motion upward and downward, horizontal motion, and rotational motion.

3.1.1. Equipment. The UAV studied for this project was a 6-rotor DJI Matrice 600 Pro. The UAV is shown in Figure 3.1, though the camera was removed for this experiment. This UAV was selected due to commercial availability, while also

considering the carrying capacity, flight time, and flight speed. The UAV used TB47S batteries, which allow a flight time of 16-35 minutes, depending on payload weight and wind conditions. With the TB47S batteries, the total UAV weight is 9.1 kg, and the payload capacity is 6 kg [127]. A gas monitor is expected to weigh less than 3.5 kg, so the UAV should be capable of achieving a relatively long flight time. The UAV is also capable of moving at speeds up to 65 km/h, which allows for rapid approach to the sampling location [127]. All of the UAV's capabilities theoretically allow the UAV-gas monitor system to maximize the sampling time.



Figure 3.1. 6-rotor DJI Matrice 600 Pro (Camera Removed Prior to Testing)

Holdpeak 866A anemometers were selected as an economical anemometer that is capable of recording results in real time. The anemometers take samples once per second, calculating a time weighted average of the wind speed measured over each second, which was also the fastest sampling anemometer that was available commercially to the authors'

knowledge. Each anemometer was connected to a laptop at the test site to record wind speed data.

A stand was built to elevate the UAV so the rotors are 4.66 m above the ground. The UAV was operated in a controlled building to prevent outside wind interference. The stand was required to maintain a constant position because the building structure interfered with the UAV's Global Navigation Satellite System positioning. The tallest height at which the stand can support the UAV's weight is 4.66 m, and this height is beyond the theoretical point at which ground interference produces significant airflow backwash for a 6-rotor UAV [72]. The final version of the stand, with the UAV and anemometers in place, can be seen in Figure 3.2. The stand grips onto the bottom chassis of the UAV. The original plan was to create a stand that reached over the UAV so that no parts would be beneath the UAV in attempt to minimize the stand's interference with the downwash. Unfortunately, the design was predicted to be too unstable, so the final stand design does extend directly below the UAV. This experiment did not evaluate the effects of the stand on the downwash region. Despite this, the stand was successful in preventing UAV motion for any thrust combination.

3.1.2. Test Procedure. On the stand, the UAV rotors were 4.66 m above the ground. Two anemometers were placed at ten distances from 0.52 m to 3.48 m beneath the UAV rotors. Of the eighteen found papers that use a UAV-mounted gas monitor, eight placed the measuring point above the UAV [40,45,60,68,77,78,79,80], four placed the measuring point horizontally from the UAV [47,50,62,66], and sixteen placed the

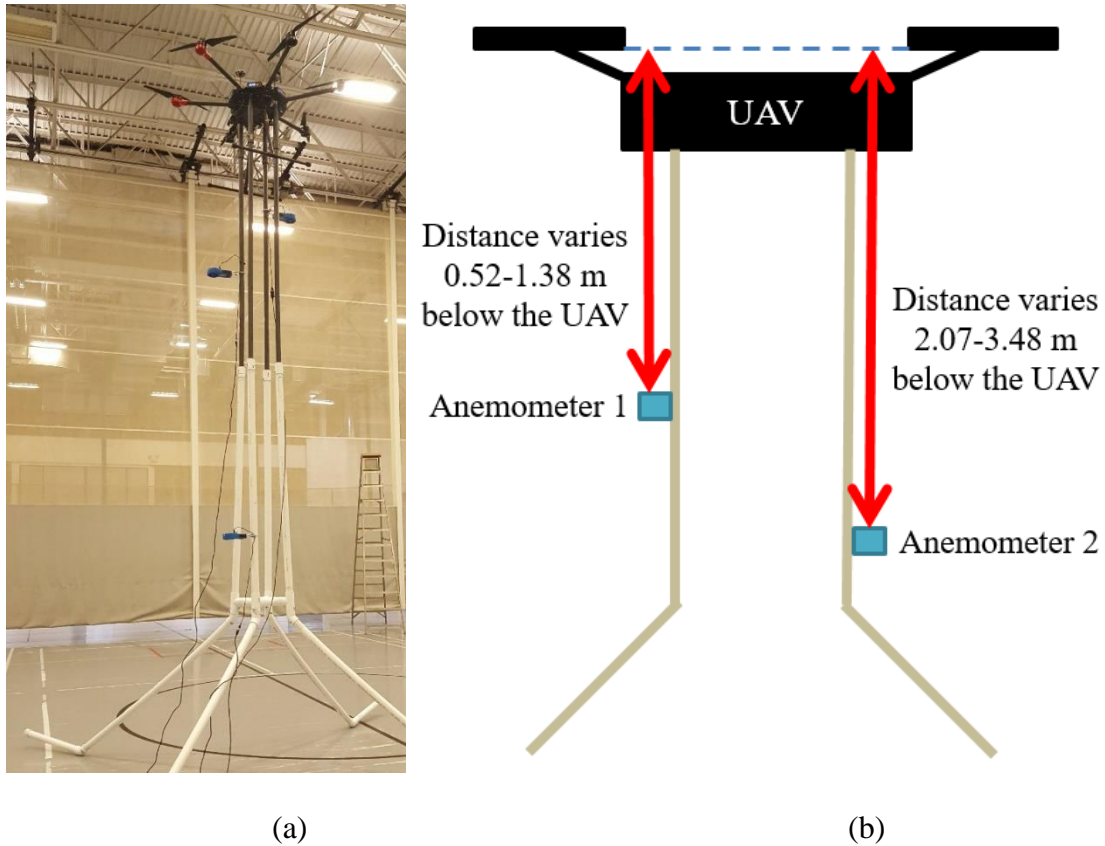


Figure 3.2. Final Setup with UAV, Stand, and Anemometers; (a) Actual Setup; (b) Schematic Showing Anemometer Distance (arrows) below the Bottom of the UAV rotors (dashed line)

measuring point beneath the UAV [39,41,45,48,52,53,56,57,58,61] [63,64,65,74,76,124]. Gas monitor placement beneath the UAV appears in 59% of found papers, which implies this as the most popular configuration. Of the five tests that attempted to evaluate accuracy for a UAV system, the tests with measuring points beside and above the UAV saw results similar to results measured with no downwash [50,41], while the tests with measuring points above the UAV measured error up to 50% [68,78,40]. This project focused on the downwash region beneath the UAV because of the popularity of this

configuration and the potential for greater inconsistency while measuring above the UAV.

At each anemometer distance beneath the UAV, at least four iterations were performed for vertical upward and rotational UAV movement. The UAV programming does not allow vertical downward or horizontal movement while the UAV is on the ground. While on the stand, the UAV recognizes that its height is not changing, so it believes it is on the ground, which means this experiment cannot study vertical downward or horizontal motion. For consistency, a timer was used to ensure that the operator applied the thrust for 5 s for each iteration. The timer was also used to allow at least 60 s for the downwash region to stabilize between each iteration. The anemometers were connected to the same stand as the UAV and oriented perpendicular to the stand to measure air velocity moving vertically downward. Clamps were used to extend the center of each anemometer 0.17 m from the stand post. Using multiple anemometers and distances allowed researchers to view how the air velocity behaved as the distance is increased from the UAV.

3.2. RESULTS

The data collection plan is shown in Table 3.1. Two anemometers were available for this test, so five separate “flights” were performed to study the ten anemometer distances. Flight 4 was interrupted by a loose anemometer clamp connection, which caused Anemometer 2 to turn perpendicular to the downwash flow direction. Data was still obtainable from readings taken prior to the clamp failure, but the test was repeated in

the field as a precaution, resulting in two iterations of Flight 4 that both produced useful data.

Table 3.1. Anemometer Locations during Test Flights

	Distance Below UAV (m)		Number of Thrust Variances	
	Anemometer 1	Anemometer 2	Vertical	Rotational
Flight 1	0.52	2.07	4	5
Flight 2	0.88	2.36	8 & 6**	5
Flight 3	1.13	2.65	5	5
Flight 4a	1.38	3.08	5 & 6**	0
Flight 4b	1.38	3.08	5	5
Flight 5	1.81*	3.48	0***	5

*Data lost

**An anemometer clamp came loose, so the two anemometers recorded a different number of samples.

***UAV battery died prior to collecting the data. Facility time restrictions did not allow recharging or getting new batteries.

3.2.1. Hovering Stationary. While mounted on the stand, the UAV's safety mechanisms only allowed this experimental setup to consistently replicate rotor behavior as if the UAV were hovering in a stationary position. Vertical and rotational thrust could be applied to the rotors, but not at the same level of precision as when "hovering" on the stand. Therefore, "hovering" was the only stable downwash region configuration tested for this dissertation, though prior research implies that any unvarying application of thrust should produce a stable downwash region [40,48,49,50,60,68,69,70,71,72] [73,120,121,122].

The average “hovering” rotor speed over all periods where the UAV is fully powered on and thrust is not applied was very consistent with a 1.0% or lower std. dev., shown in Table 3.2.

Table 3.2. Average “Hovering” Rotor Speeds

Flight Number	Anemometer Locations (m below the UAV)		Average Hover Rotor Speed (RPM)	Std. Dev.	Number of Samples
	Anemometer 1	Anemometer 2			
1	0.52	2.07	1532	0.8%	17,899
2	0.88	2.36	1487	1.0%	23,891
3	1.13	2.65	1457	0.6%	19,106
4a	1.38	3.08	1442	0.6%	10,349
4b	1.38	3.08	1428	0.7%	18,823
5	-	3.48	1415	0.5%	12,419

Though the average rotor speed decreased between each test, this effect was negligible during each test, and the effect should not occur during tests in which the UAV is actually airborne rather than affixed to the stand. The rotor speeds are probably lower than the actual hovering rotor speeds because the stand provided support rather than the rotor thrust providing sole support, which would be the case during unrestrained flight. Therefore, while it is on the stand, the UAV system’s calculations assume it is still resting on the ground where full hovering speeds are not required. Additionally, the resting speed decreases with each flight from 1532 RPM to 1415 RPM. As the battery levels decreased, the stationary speeds also decreased, which the authors believe to be a difference unique to placing the UAV on a stand. If the UAV were actually hovering, the same thrust would be required to maintain the hover position, so the thrust is relatively

constant regardless of the battery level. A test flight was performed to verify this, recording 3 min of data while “hovering” on the ground, 10 min of data while hovering in air, and then 3 more min while “hovering” on the ground. Weather conditions during the flight were 25°C, 5 mph wind speed, and 82% humidity. The rotor speeds experienced virtually no change while hovering in the air (0.0% change with 1.5% std. dev.), despite the battery levels decreasing 49% during the test. However, the post-flight period of “hovering” on the ground saw rotor speeds that were over 9% lower than the pre-flight period. The results confirm that battery level does affect “hovering” rotor speed while on the ground. This effect will not affect measurements taken during actual flight because the rotor speeds will not decrease during actual flight as they are required to maintain constant thrust to keep the UAV in position. This effect also does not affect the results of this study because the experimental results were valid as long as the rotor speed during each test was constant. The test time was relatively short, and most of the battery life was expended during the time between tests, so the rotor speed was statistically constant during each sample collection period.

Table 3.3 shows the average air velocity during a period of at least 4 minutes during which the UAV thrust is not changed.

The average wind speed increases with distance from the UAV until 1.13 m, after which it decreases with distance from the UAV. The trend is consistent despite the changing UAV rotor speeds as the battery level decreases. The initial period of increasing wind speed also has considerably higher standard deviations. Papers found during the literature review discussed a conical region immediately beneath the body of the UAV

Table 3.3. Average “Hovering” Wind Velocities (No UAV Movement)

Distance below UAV (m)	Average Hover Wind Speed (m/s)	Std. Dev.	Number of Samples
0.52	3.01	25.4%	249
0.88	4.11	11.6%	436
1.13	4.23	7.2%	263
1.38	4.09	6.6%	303
2.07	3.96	4.4%	284
2.36	3.92	4.4%	345
2.65	3.66	5.4%	266
3.08	3.48	5.3%	306
3.48	3.21	6.2%	447

that experiences relatively low air velocity and relatively high turbulence because the rotors push air vertically, not into the space immediately beneath the UAV body. The anemometers at 0.52 m and 0.88 m were likely inside that conical region, evidenced by the lower wind speeds and high standard deviations. Adding even more evidence, the researchers observed during preliminary setup that the anemometer vane rotation at 0.52 m below the UAV would periodically change directions, not shown in the results because the anemometer only records absolute values. The reverse direction phenomenon could not be replicated for video recording during subsequent testing, but the problems seen in this highly turbulent conical region make it unlikely to determine any meaningful information from the results at this distance. High turbulence means continual changes in velocity, which in turn will also change the air pressure and gas concentrations. For gas measurement, a consistent speed is more desirable in order to maintain relatively constant air pressure, which in turn relates to more reliable gas concentration measurements.

Therefore, even though the conical region has relatively low average wind speed, the greater inconsistencies seen during this test show that this region is not ideal for gas measurement. The exact end of the conical region was not defined in this test, but it likely ends between 0.88 m and 1.13 m beneath the UAV rotors.

The trend in the wind speed standard deviations shows an ideal distance for obtaining accurate results for this UAV and stand. The deviation decreases until 2.07 m, after which it stays the same at 2.36 m before increasing again until 3.48 m. It is possible that the initially increasing stability is caused by decreasing wind speeds to a point where turbulence is minimal. The final decreasing stability may be caused by interference with the ground as air impacting the ground may be backwashed into the downwash region, though further testing will be required to verify this. For testing with this stand, a distance of 2.07-2.36 m from the rotors has the most stable wind velocity.

3.2.2. Rotor Speed Results. The six individual UAV rotor speeds over the test durations were taken from the UAV's internal record system. Flight 4b results are shown in Figure 3.3 as an example. The initial spike at approximately 40 seconds is when the rotors were turned on. Each of the remaining peaks represents changes made in the UAV thrust. The first five peaks represent the simulation of upward movement. The operator increased the thrust as if the UAV were accelerating upward, and then released the throttle to allow the UAV to return to the hovering thrust. The following five series of peaks represents rotational movement.

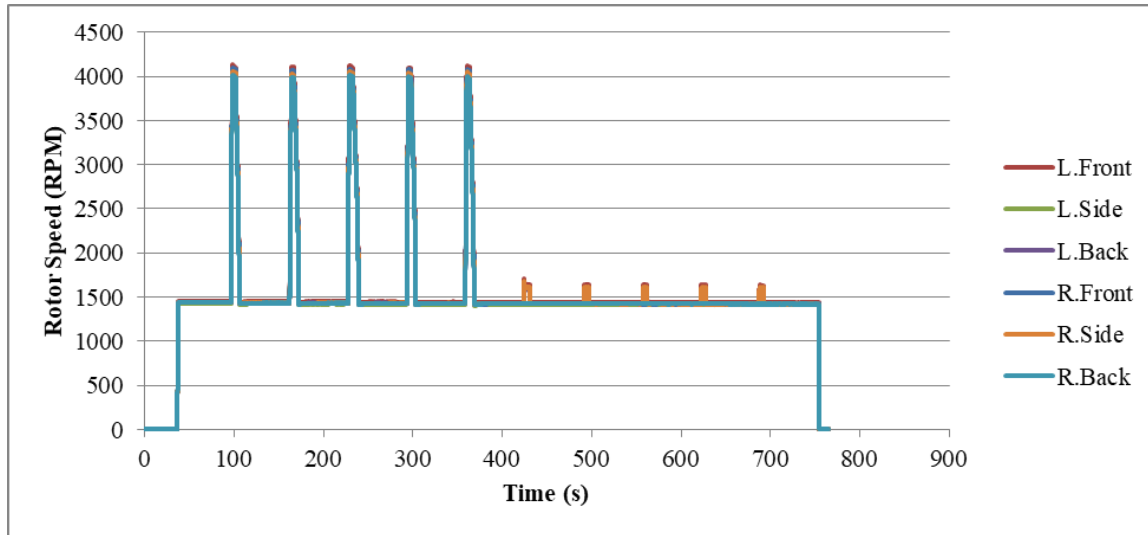


Figure 3.3. Flight 4b UAV Rotor Speed over Time

The graphical results for each of the six rotor speeds are visually very similar. In order to accentuate differences, Figure 3.4 has offset the results so each plot can be viewed individually. As shown, the results are still primarily very similar, aside from the final five peaks that pertain to rotational motion. Only the right side, left front, and left back rotors experience thrust, while the other three remain at the average hovering rotor speed. The UAV rotor arms alternate clockwise and counterclockwise rotation, and the three rotors that experience peaks are the three rotors that rotate clockwise. The operator only moved the UAV in the clockwise direction, which is why these three rotors experienced more thrust to counteract the counterclockwise rotors. Counterclockwise movement would simply have the opposite effect, so studying both directions would be redundant. These five peaks associated with rotational movement have significantly lower peak rotor speeds than observed in vertical movement. The difference in rotor speed is potentially caused by the greater kinetic energy required to change the UAV's

potential energy moving vertically, rather than the rotational movement that maintains the same potential energy.

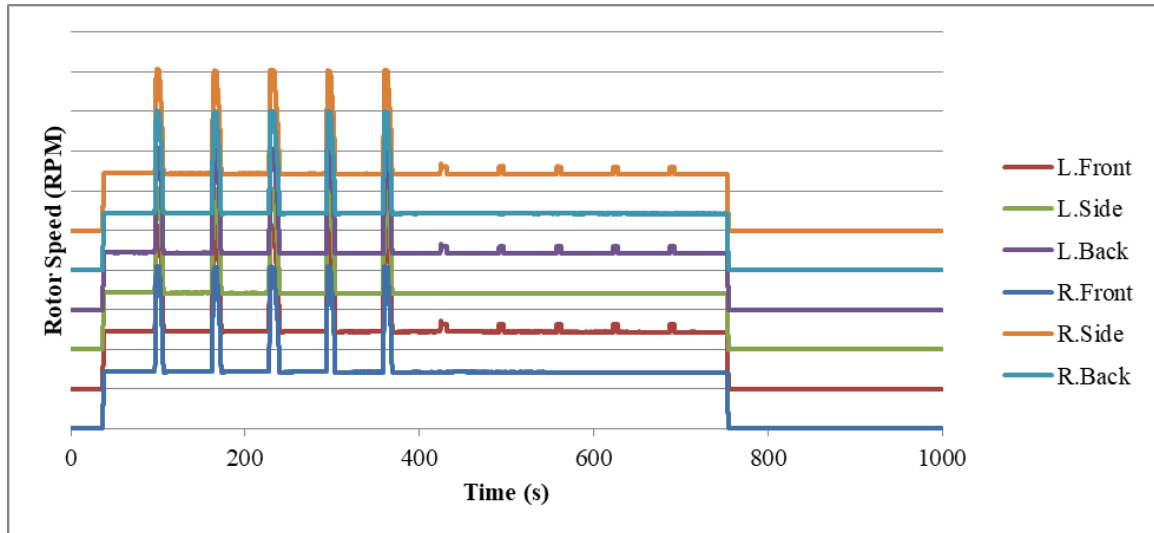


Figure 3.4. Flight 4b UAV Rotor Speed, Offset to Make Individual Rotor Results More Prominent

3.2.3. Wind Velocity Results. The air velocities measured by the anemometers are shown in Figure 3.5, where time 0 is the same as time 0 in Figure 3.3 and Figure 3.4. The data from both anemometers has peaks that appear to align with the vertical movement peaks in Figure 3.3. However, it is unclear what caused the spike at approximately 250 s for the anemometer at 1.38 m. The results from the anemometer located at the greatest distance beneath the UAV experiences lower wind speeds. For example, in Figure 3.5, the anemometer at 3.08 m has wind speeds lower than the anemometer at 1.38 m. This trend was seen in nearly all results as previously discussed in Table 3.3. Lastly, the data does not visually appear to have peaks associated with rotational movement, which is likely due to the lower changes in rotor speed.

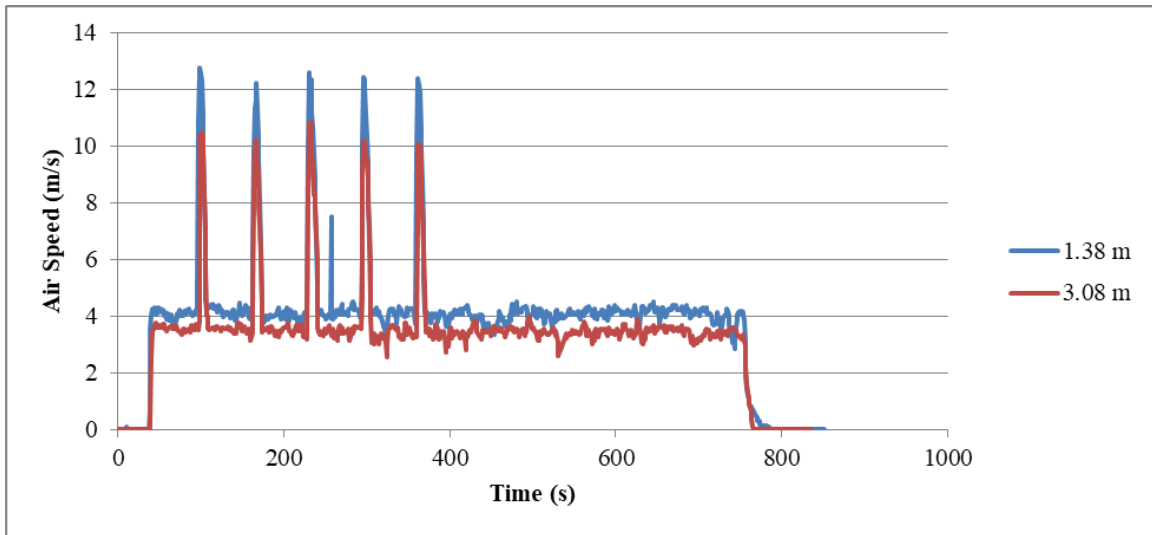


Figure 3.5. Test 3 Air Speed Measurements over Time

3.2.4. Vertical Movement Upward. For upward vertical movement, the operator engaged the throttle for 5 s, reaching peak rotor speeds up to 185.4% greater than the “hovering” rotor speed. The results for Flight 4b are shown in Table 3.4. If the air speed at any point in time had a deviation from the mean that was greater than two times the standard deviation for at least three consecutive 1-second periods, then the air speed at that time was assumed to be disturbed. For example, the air speed at the anemometer 1.38 m below the UAV had an average wind speed of 4.09 m/s with 6.6% standard deviation. Between 96 and 106 s, deviation from the mean ranged from 30.1% to 207%, coinciding with the time the UAV rotor speeds were above the mean rotor speed. Therefore, the air velocity was disturbed during that time, and the total time of disturbance is equal to the end time minus the beginning time. The stabilization time after releasing the throttle was calculated by subtracting the time that the throttle was released from the ending time of

downwash air speed disturbance. The stabilization time after the rotor speeds returned to hover was calculated likewise.

Table 3.4. Results after Simulating Vertically Upward UAV Movement, Flight 4b

Anemometer Location	No.	Event Times (s)		Time Downwash Air Speed Was Disturbed (s)			Stabilization Time (s)	
		Throttle Duration	Time to Return to Hover	Begin	End	Total	After Releasing Throttle	After Rotor Speed Returns to Hover
1.38 m below the UAV	1	5.078	4.602	96	106	10	4	0
	2	5.142	5.204	163	173	10	6	0
	3	5.647	6.323	229	241	12	8	1
	4	4.899	5.166	294	304	10	6	1
	5	4.968	5.069	360	370	10	6	1
3.08 m below the UAV	1	5.078	4.602	98	109	11	7	3
	2	5.142	5.204	163	174	11	7	1
	3	5.647	6.323	229	241	12	8	1
	4	4.899	5.166	294	309	15	11	6
	5	4.968	5.069	361	371	10	7	2

For all tests, including those not shown in Table 3.4, the time required for the UAV to return to hovering rotor speeds was approximately 5 seconds after the throttle was released. Overall, the stabilization times ranged from 4 to 11 s (avg. 6 s, std. dev. 1.5 s) after releasing the throttle and from 0 to 6 s (avg. 2 s, std. dev. 1.4 s) after the UAV rotor speeds have returned to hovering speeds. Removing the data from the 0.52 m and 0.88 m readings, which are believed to be in the extremely turbulent portion of the downwash region, does not change the average values, but it does improve the standard deviation to 1.4 s after releasing the throttle and 1.3 s after returning to hovering rotor speeds.

Figure 3.6 shows all results for the vertical UAV motion. As shown, there is an upward trend in stabilization time as the distance from the UAV increases, though the linear R^2 value is too low to consider the trend line to be statistically significant. All 53 instances of vertical movement produced significant changes in wind speed. During the period of simulated motion, the average deviations were 128% for the rotor speed and 129% for the wind speed. Note that some values actually returned to standard hovering wind speeds prior to the UAV fully reaching hovering speeds. These are the points that required 0 or fewer seconds for the wind speeds to stabilize. 10 out of 53 tests were stabilized by the time the rotor speeds returned to hovering speeds, so 19% of the observed movements did not cause significant downwash disturbance beyond the time that the UAV was in motion.

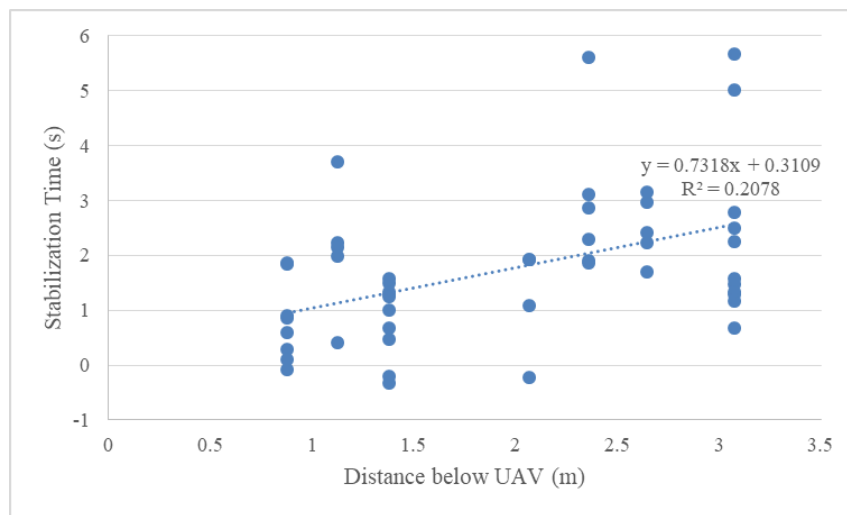


Figure 3.6. Results for Vertical Motion Stabilization Time after Returning to Hovering Rotor Speeds

3.2.5. Rotational Movement. For rotational movement, the operator engaged the throttle for 5 s, reaching peak rotor speeds up to 6.2% greater than the hovering rotor speed. The low changes in rotor speed produced lower changes in air speed, which made determination of the disturbance time less precise. The results for Flight 1, anemometer 2, and Flight 5, anemometer 2, are shown in Table 3.5, and the results were found using the same methods as with the results in Table 3.4. The two results in Table 3.5 were selected because they contain the greatest number of significant disturbances.

Table 3.5. Results after Simulating Rotational UAV Movement, Flight 1 & Flight 5

Anemometer Location	No.	Event Times (s)		Time Downwash Air Speed Was Disturbed (s)			Stabilization Time (s)	
		Throttle Duration	Time to Return to Hover	Begin	End	Total	After Releasing Throttle	After Rotor Speed Returns to Hover
2.07 m below the UAV	1	4.582	0.103	-	-	-	-	-
	2	4.684	0.034	434	439	5	0	0
	3	6.156	0.068	500	507	7	3	3
	4	5.088	0.066	570	573	3	3	3
	5	4.813	0.033	635	636	1	2	2
3.48 m below the UAV	1	4.582	0.135	-	-	-	-	-
	2	4.684	0.136	164	165	1	-3	-4
	3	6.156	0.138	231	232	1	-2	-3
	4	5.088	0.135	359	365	6	0	0
	5	4.813	0.102	425	428	3	-2	-2

For all tests, it took less than 0.25 seconds for the UAV to return to hovering rotor speeds after releasing the throttle, which is significantly faster than seen in the vertically upwards movement tests, likely due to the significantly slower rotor speeds. Since the anemometer only sampled once per second, the stabilization time was the same after

releasing the throttle and after returning to hovering rotor speeds. Another considerable difference with the rotational movement tests is that only 15 out of 45 tests were able to see a significant change in wind speeds, and those that did provide results showed even lower statistical significance than the vertical upward movement results. Overall, the stabilization times ranged from -4 to 6 s (avg. 2 s, std. dev. 2.5 s). Note that a negative stabilization time means the region had statistically stabilized prior to the time that the rotors returned to hovering speeds. Compared with the vertical movement results, the much wider range and greater standard deviation show the unreliability of the results, which is undesirable for predicting concentration changes for gas monitoring.

Despite the limitations in predicting exact stabilization time, rotational movement is actually better suited for gas monitoring than vertical movement due to the greater number of instances in which no stabilization time was recorded. Figure 3.7 shows all results for the rotational UAV motion. As shown, there appears to be a downward trend in stabilization time as the distance from the UAV increases. At 19.46%, the linear R^2 value is still too low to consider the trend line to be statistically significant, though it is very similar to the 20.78% linear R^2 value seen in the vertical upward movement results. The primary difference from the vertical movement results is that only 15 out of 45 rotational tests produced significant changes in wind speed. During the period of simulated movement, the average deviation from the mean rotor speed was 5.8%, and the average deviation for wind speed was 15.7%. Both of these values are significantly lower than seen in the vertical movement tests, and the lower rotor speeds are likely the primary reason why most of these tests did not produce significant results. Additionally, 7 of the measured results stopped showing downwash disturbance during UAV motion or

immediately when UAV motion ceased, which means only 8 out of 45 rotational tests produced significant changes in wind speed that lasted longer than UAV motion. For this experiment, stabilization time did not matter for 82% of tests, which implies that rotational movement causes a more desirable disturbance for gas monitoring than vertical movement.

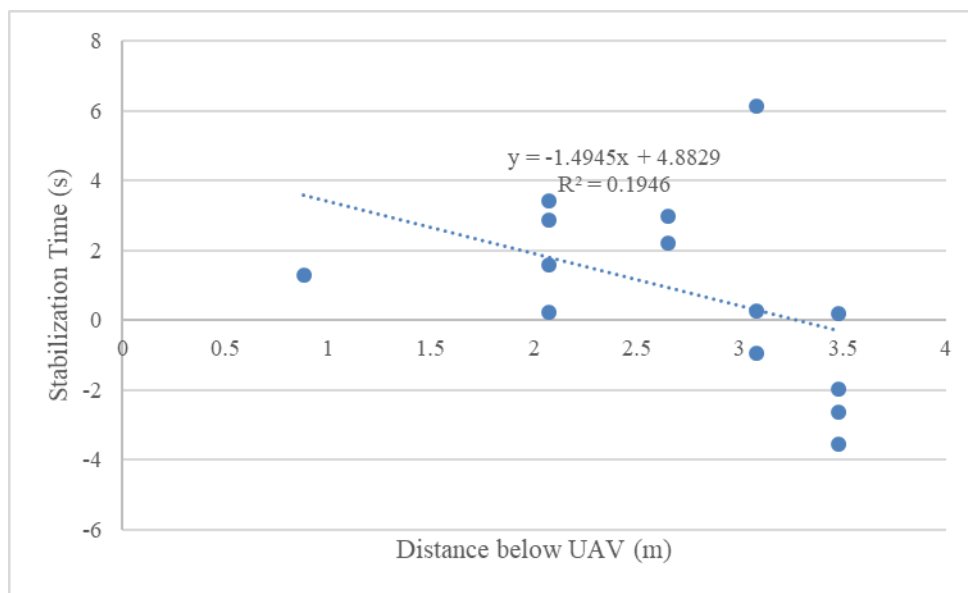


Figure 3.7. Results for Rotational Motion Stabilization Time after Returning to Hovering Rotor Speeds (Note: Negative times indicate the wind speed is stable before UAV motion has ceased)

3.2.6. Horizontal Movement. For aforementioned reasons, horizontal movement could not be simulated while attached to the stand. However, since horizontal and rotational motion do not change potential energy, low changes in rotor speed can be expected when altering horizontal movement, as was observed when altering rotational movement. A flight was performed outdoors to test this prediction, and the weather conditions at the time of the flight were 25°C, 5 mph wind speed, and 82% humidity. 6

min of data was recorded while the UAV was hovering to obtain the average hovering speed, which was 2842 RPM. Over periods of 3 min, the rotational movement produced a 8.7% average deviation in rotor speed from the hovering speed, while the horizontal movement produced 3.9% average deviation. Because the horizontal motion deviation is lower than rotational, it is predicted that horizontal motion will produce even less downwash disturbance time than rotational motion.

3.2.7. Rotor Speed Stability when Subjected to Outside Wind. As outside wind interacts with a UAV in flight, the UAV automatically adjusts its rotor speeds to maintain a constant hovering position or motion vector. Ideal conditions for flight are with minimal outside wind and dense air; air is dense when temperature is low and humidity is high. Additionally, the UAV manufacturer does not recommend flying the UAV in wind speeds greater than 35 mph [127].

Tests were performed in various weather conditions. The UAV was hovering stationary for approximately 10 minutes. For each test, the average rotor speed and the standard deviation were observed, and the results are presented in Table 3.6.

Table 3.6. Outside Wind Effects on UAV Rotor Speed

Flight	Temperature (°C)	Wind Speed (mph)	Humidity	Number of Samples	Avg. Rotor Speed (RPM)	Std. Dev.
1	14	14	33%	7,104	2,784	1.58%
2	13	10	33%	7,192	2,706	1.56%
3	32	23	53%	6,575	2,842	1.56%
4	25	5	82%	7,762	2,745	1.53%

Throughout each study, the standard deviation remained relatively minimal while the UAV was hovering, even in non-ideal flying conditions. Flight 3 had the least optimal weather conditions with above average humidity and the highest wind speed and humidity of the test series, but this test experienced similar rotor speed deviations to the other tests. Deviations observed while subject to outside wind were higher than the 0.5-1.0% deviations observed without wind (Table 3.2 in Section 3.2.1), but were considerably lower than deviations observed when altering vertical thrust (128%, Section 3.2.4), rotational thrust (5.8%, Section 3.2.5), or horizontal thrust (3.9%, Section 3.2.6). These results imply that the presence of wind has a minimal effect on hovering rotor speeds, and therefore downwash turbulence, compared to any alteration in the UAV's motion.

3.2.8. Applicability of Results to Other UAVs. This experimentation only collected results for a single UAV model. However, the rotor speed of the UAV varied drastically throughout this study with no significant difference on the maximum time required for the downwash region to stabilize. Therefore, the results are applicable to all rotor speeds and thrust variations for the UAV used. Previous studies have measured and simulated wind velocities and downwash region dimensions for a variety of UAV models with widely varying propeller shapes, number of rotors, and rotor configurations. While these studies show significant variation in downwash region dimensions, wind velocities were relatively similar across all studies [40,48,49,50,60,68,69,70,71,72] [73,120,121,122]. Therefore, the author hypothesizes that (a) if downwash affects concentration readings, then the downwash region dimensions should be evaluated for each UAV model, and (b) air velocity and turbulence response within the downwash

region is likely to remain similar for all UAV models, propeller shapes, and rotor configurations, though future work is needed to verify that stabilization times are similar across UAV models.

3.3. DISCUSSION

The objective of this section was accomplished by determining a maximum of 6 seconds is required after UAV movement for wind speeds in the downwash region to stabilize. Data was collected by mounting a 6-rotor UAV to a stand, placing the stand in a controlled indoor environment with no external sources of airflow, and placing anemometers at ten locations beneath the UAV. Wind speed results while the UAV was not altering thrust show a decrease in standard deviation until 2.07 m beneath the UAV rotors, which then remains constant at 2.36 m. Beyond 2.36 m, standard deviation begins increasing, though this is likely due to air backwash as the wind impacts the ground. Such backwash is not expected to be a problem for open air testing, but it may interfere with testing performed indoors or in underground mines and tunnels. Turbulence likely causes higher standard deviations, and low reliability in gas concentration measurements is linked to turbulence. Therefore, the ideal measuring point for this test's UAV stand is 2.07-2.36 m below the UAV rotors because this range of distances experienced the least turbulence. Without ground interference, the authors believe the turbulence will continue decreasing beyond 2.07 m below the UAV rotors, though this hypothesis remains untested. Additionally, wind speeds proved extremely turbulent at 0.52 m and 0.88 m, and turbulence decreased considerably starting at 1.13 m. Papers by other authors have discussed a conical region of low wind speed beneath the body of the UAV. This

experiment's results show that the conical region extends to a point 0.88-1.13 m beneath the rotors for the UAV used for this project. Samples taken within this region experienced considerably higher turbulence, which implies that gas samples should not be collected in the conical region of any UAV if turbulence is to be avoided. Future tests with this UAV should place the measuring point at least 1.13 m from the UAV rotors, or closer if the conical region is better defined.

The wind speed results with UAV movement found that stabilization times after vertical upward UAV motion ranged from 4 to 11 s (average of 6 s) after releasing the throttle, or 0 to 6 s (average of 2 s) after the rotor speeds returned to the average hovering speeds. The average values had a standard deviation of 1.4 s and 1.3 s, respectively, which are both lower than the 2.5 s standard deviation seen in stabilization times after rotational movement. Stabilization times after rotational UAV motion ranged from -4 to 6 s after the rotor speeds returned to the average hovering speeds. The significantly lower air speeds measured during rotational UAV movement likely caused the greater deviation. The low air speeds were a result of the significantly lower rotor speeds. The wind speed was so low that only 18% of tests produced significant wind disturbance that lasted longer than the period of UAV motion, whereas this value for vertical motion is 81%. Therefore, it can be concluded that altering rotational UAV movement during gas monitoring is more desirable than altering vertical movement because the rotational movement is much less likely to alter the downwash region significantly. However, altering either type of motion can still cause downwash disturbance up to 6 seconds after UAV motion has ceased, which means it is desirable to avoid altering motion during gas sampling. Changes in rotor speeds while off the testing stand suggest that altering

horizontal motion may be even less likely to produce downwash disturbance that lasts longer than the period of UAV motion, though this project was not able to collect wind speed data to verify this hypothesis. Changes in rotor speeds while outdoors and off the testing stand also suggest that the presence of outside wind may have less of an effect on rotor speeds, and therefore downwash disturbance, than any UAV motion alteration. Finally, prior research suggests that any unvarying application of thrust should produce a stable downwash region, regardless of whether the UAV is hovering stationary or in constant motion, and regardless of UAV model, propeller shape, or rotor configuration.

3.4. SUMMARY

Downwash region stabilization times were determined after applying movement thrust using a 6-rotor UAV. Data was collected by mounting the UAV to a stand, placing the stand in a controlled indoor environment with no external sources of airflow, and placing anemometers at ten locations beneath the UAV. Turbulence results were collected that were specific to the test setup for this research. Conclusions from this experimentation included:

- Turbulence stabilized up to 6 seconds after the UAV rotor speeds returned to an unvarying configuration. The 6-second maximum period was observed after alterations to both vertical and rotational movement, and preliminary evidence suggests that altering horizontal motion would yield similar results. Therefore, the author recommends all future research refrain from recording gas samples until at least 6 seconds after alterations to UAV thrust has ceased.

- Turbulence was greatest when vertical thrust was applied, and it was significantly less prevalent when altering rotational motion. Based on UAV rotor speeds, horizontal motion is likely to create similar or less turbulence than rotational motion.
- The presence of outside wind is unlikely to alter UAV rotor speeds significantly enough to cause greater downwash disturbance than any applied UAV motion.
- The author hypothesized that the locations with highest turbulence would provide the highest deviation in gas concentration measurements. This effect is evaluated further in Section 4.

4. EFFECTS OF DOWNWASH FROM A 6-ROTOR UAV ON GAS CONCENTRATIONS

Substantial changes in pressure are capable of affecting measured gas concentrations because regulatory concentration limits are based on gas density [82,83]. To the author's knowledge, no previous studies have successfully evaluated the direct effects of UAV downwash on measured gas concentration values. Understanding this effect, and accounting for it if needed, will allow researchers to utilize UAVs for a multitude of gas monitoring scenarios. Based on quantified downwash region turbulence for a 6-rotor UAV as defined in Section 3, the objectives of this section are to determine if the turbulence creates pressure differences substantial enough to affect measured concentrations and how to overcome differences in measured concentration caused by said pressure differences. The author has published the results of this section in the peer-reviewed journal, *Mining, Metallurgy, and Exploration* [128].

4.1. EQUIPMENT

The primary equipment used included a UAV, gas monitoring system, UAV stand, and gas chamber. The gas monitor was attached to the UAV, which was mounted on the UAV stand inside of the chamber. Each of these components is described in more detail in this section.

To determine gas concentration measurement variance using a UAV, a 6-rotor DJI Matrice 600 Pro was used, as previously discussed in Section 3.1.1. This UAV model was chosen according to commercial availability, flight time, carrying capacity, and flight speed. The testing did not require open-air sample collection, but the UAV was selected

to be representative of UAVs that may be used for open-air sampling in effort to ensure applicability of the results.

Alphasense NO-A4 and NO₂-A43F gas sensors were used to measure NO and NO₂, respectively, which were the only commercially available sensors found capable of measuring NO_x at the ppb scale. The sensors are accurate to ± 1 ppb for NO [129] and ± 0.5 ppb for NO₂ [130]. The general schematic is shown in Figure 4.1, gas sensor and data logger are shown in Figure 4.2, and the complete gas monitoring system is shown in Figure 4.3. Note that two separate systems of fan pump, gas hood, circuit board, NO sensor, and NO₂ sensor were attached to the data logger. In each test, one system was the test system and the second was the control.

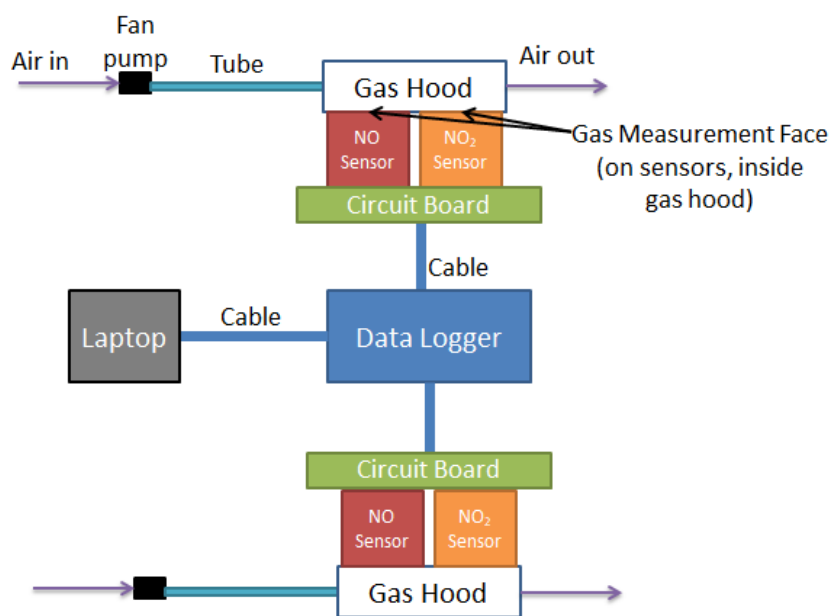


Figure 4.1. Gas Sensor Schematic

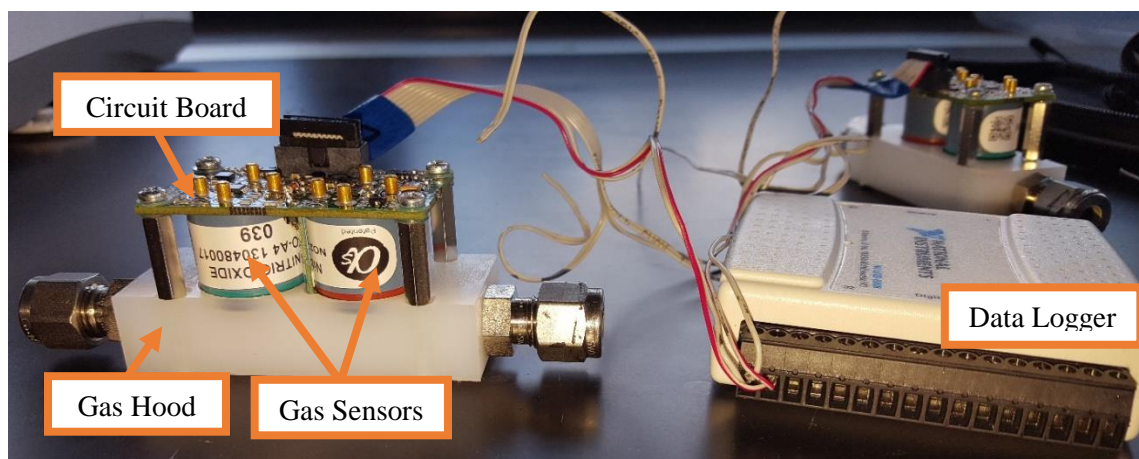


Figure 4.2. Gas Sensor (Gas Hood, Gas Sensors, and Circuit Board) Connected to the Data Logger

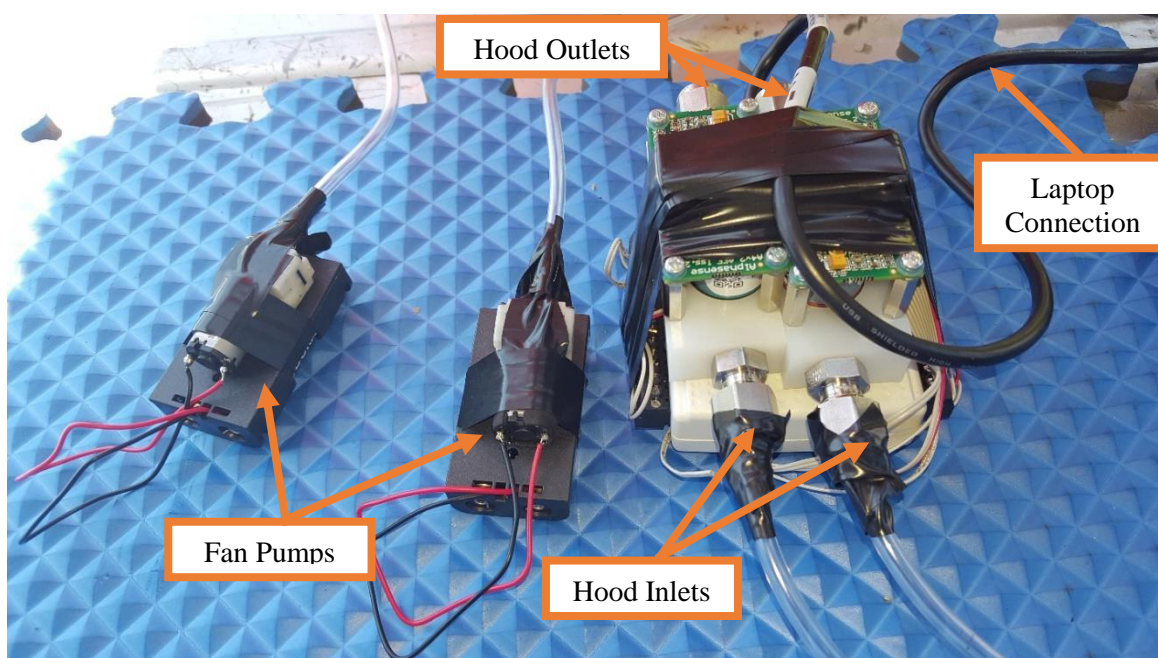


Figure 4.3. Gas Monitor (Gas Sensor Connected to the Laptop and Fan Pumps)

The NO and NO₂ gas sensors were attached to a gas hood to maintain constant airflow across the sensor. A tube was attached to one open end of the gas hood, and a one-way airflow filter was attached to the other opening. An air pump with flowrate of

0.6 L/min was attached to the tube to draw air to the sensor; the gas sensor manufacturer recommended a flowrate of 0.5 L/min [131], and the chosen fan pump was the closest fit that was both commercially available and compatible with the experimental setup. The tube connecting the sensor to the fan pump was not to exceed 10 m, beyond which the resistance within the tube would become great enough to cause inadequate airflow through the sensor inlet [132]. Data from the sensors was output as voltage, which was recorded by a National Instruments USB-6008 voltage data logger. The data logger was capable of sampling every 1.6 ± 0.04167 ms, which was transmitted to the data acquisition software installed on the connected laptop [133]. The NO and NO₂ sensors were both attached to a circuit board that had four output channels, two for each sensor [134]. The other end of the sensors was connected to a gas hood, which is the contained location in which the sensor is exposed to the gas. The gas hood has an inlet and outlet through which the gas can pass at a controlled rate. The data logger was capable of recording up to 8 channels (4 sensors) at a time [133]. Throughout this dissertation, all of the components shown in Figure 4.3 will be collectively referred to as the “gas monitor,” one combination of NO sensor, NO₂ sensor, circuit board, and gas hood will be referred to as a “sensor”, and the location of the fan pump inlet will be referred to as the “measuring point.”

The total weight of the gas monitor was well below the UAV’s maximum payload capacity of 6 kg. The fan pumps weighed 66.4 g each. One gas sensor set including a circuit board, two sensors, a gas hood, and an IDC cable together weighed 101.5 g. The data logger weighed 157.9 g, but note that the weight may vary greatly if a portable data

logger were used. Lastly, the tubing weighed 13.0 g at its maximum length. In total, the payload weight was 569.1 g.

The UAV was mounted on a stand so that the rotors were located 4.66 m above ground level, which was above the height at which this 6-rotor UAV will experience significant backwash from ground interaction as determined in Section 3. The stand and UAV were placed in a controlled chamber to maintain uniform air mixture and to eliminate outside wind interference. The structure interfered with the UAV's Global Navigation Satellite System positioning, so a stand was necessary for maintaining a constant position. The stand gripped onto the bottom chassis of the UAV. The stand leg sizes and protrusions were minimized to achieve minimal interference. The gas monitor was attached to the camera mount that extended 7 cm beneath the UAV body. The UAV, gas monitors, and stand placement in the controlled chamber can be seen in Figure 4.4. The building was cylindrical in shape to eliminate corner turbulence, with a total volume of 211 m³. The chamber's interior diameter was 7.9 m, the interior wall height was 4.9 m, and the roof angled up to a center height of 7.2 m. The chamber was sealed externally, minimizing the ability for gas to escape during testing.

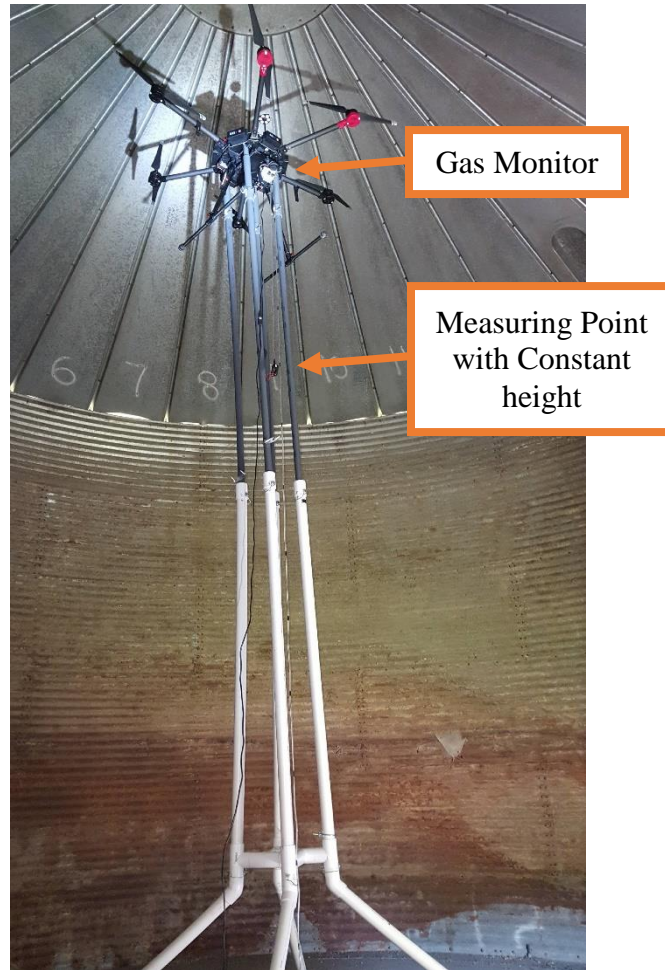


Figure 4.4. Test Setup with UAV, Stand, and Gas Monitor; Measuring Points Extended Vertically

4.2. METHOD

UAVs are an ideal remote method of measuring toxic gas emissions. The goal of the experiment was to determine if rotor downwash has any significant effect on gas concentration measurements. The test was performed in a controlled environment with measurements taken during stationary flight to eliminate sources of concentration variation that were present in experiments detailed in previous literature. The

environment contained a uniform mixture of the measured gas to avoid mixing with ambient air.

4.2.1. Test Setup. To eliminate the effects of backwash, the UAV was placed on a stand so that the height of the rotors was 4.66 m above the ground; the height to the bottom of the UAV body was 4.46 m. The gas monitor was attached at 4.39 m above ground, from which the measuring points were extended to varying distances vertically below, above, and horizontally beside the UAV. The gas added to the chamber was primarily inert N₂, which was mixed with 1000 ppm of NO. The NO mixture was diluted into the ambient air inside the 211 m³ building. Over time, the NO reacted with the oxygen in the ambient chamber air to create NO₂. The gas in the chamber reached maximum NO_x concentrations that were less than 100 ppb, which is the EPA's 1-hour exposure limit for NO₂ (the EPA does not set an exposure limit for NO) [98]. Even though the concentration in the chamber was always at safe levels according to the EPA, people entering the chamber were still required to wear a NO_x-filtering respirator and to limit their time within the chamber to a minimum. As an even further level of safety, no person was inside of the chamber for more than a maximum total time of 30 minutes per 1-hour period.

Three configurations were studied, shown in Figure 4.5. The first had the gas monitor measuring points extended vertically below the UAV. Distance was measured as distance below the base of the UAV body. The constant measuring point was used as a point of reference. The constant vertical distance was 2.0 m based on the results from Section 3, which measured the least turbulence at a range of 1.87-2.16 m beneath the UAV. The second configuration extended the measuring points horizontally by attaching

the air pumps to a wooden dowel rod. The dowel was attached to two of the UAV stand's legs at a height level with the gas sensor and parallel to the UAV body. Measuring point distance was measured as horizontal distance from the propeller tip. The constant horizontal measuring point was 0.4 m as the midpoint. The third configuration placed one sensor directly on top of the UAV body; the second sensor was placed at 0.4 m horizontally for one test and 2.0 m vertically for two tests.

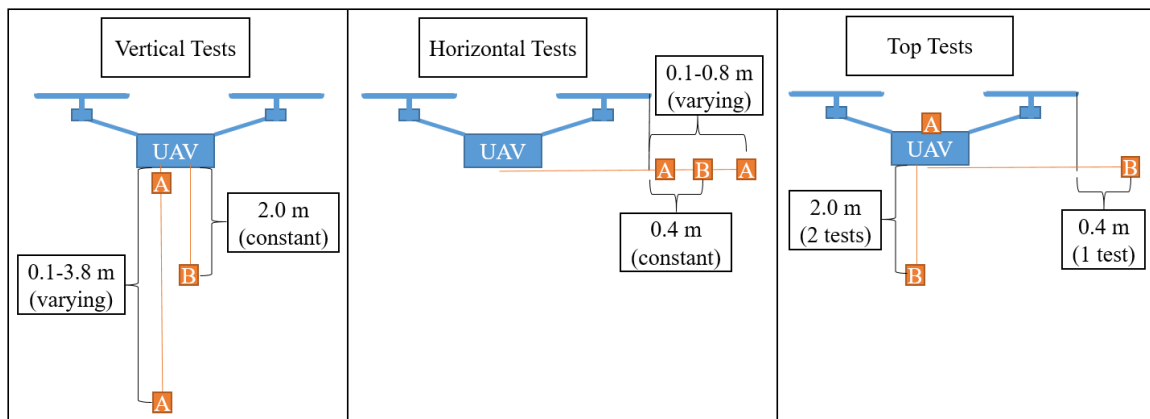


Figure 4.5. Test Configurations (Orange Boxes Are Sensor A and Sensor B Measuring Points)

Table 4.1 shows the number of tests and exact distances from the UAV at which concentration was measured for each series. Two series of vertical tests and four series of horizontal tests were performed. Three top tests were performed with the control sensor below the UAV for two tests and extended horizontally for one test. The number of tests in each series was related to the distance range and interval. The shorter horizontal range was based on prior literature review that showed downwash extends vertically downwards much further than the downwash that extends horizontally

[50,72,49,120,121,70,71]. The Top series has the fewest number of tests because only one distance was evaluated.

Table 4.1. Test Series Information

Series	Number of Tests	Min Distance (m)	Max Distance (m)	Constant Distance (m)	Distance Interval (m)
Vertical 1	12	0.5	3.8	2.0	0.3
Vertical 2	35	0.1	3.5	2.0	0.1
Horizontal 1-3	8	0.1	0.8	0.4	0.1
Horizontal 4	4 ^a	0.2	0.7	0.4	0.1 ^a
Top	3	0.0	0.0	-	-

^a Eight tests were planned from 0.1 to 0.8 m, but constraints did not allow full completion.

Via email correspondence, the gas sensor manufacturer recommends a minimum sample rate of 0.1 s to reduce noise [135]. The data logger was capable of sampling once per 1.6 ms [133], therefore, instantaneous samples were collected every 0.1008 s which is the fastest sample rate above 0.1 s that is a factor of 1.6 ms.

The procedure for vertical and horizontal tests was similar. The horizontal tests were performed in a randomized order of distances, but procedural constraints required the vertical tests to be performed sequentially. After adding the NO mixture and using fans to mix the NO_x throughout the chamber, a period of 60 s was given to allow the airflow in the chamber to cease. Gas monitor data was recorded with the rotors off for a period of at least 120 s, the rotors were turned on and given 30 s to reach stable hovering rotor speeds, and then gas monitor data was recorded for at least 180 s with the rotors on. Next, the UAV was turned off and given 30 seconds for airflow to cease. Finally, data was recorded for another period of at least 120 s to obtain concentration measurements

before and after applying downwash. This process was repeated for every test. Note that Section 3 concludes samples should not be collected for 6 seconds after UAV motion has ceased, but 30 seconds was used for this project simply as an additional safety factor.

Between tests, researchers entered the chamber to change the measuring point location. After every third test, additional NO was added into the chamber to account for NO_x that was lost as the researchers opened the chamber door. Additional NO was injected until total NO_x concentration reached 90-100 ppb. After three tests, the measured NO_x concentration typically dropped to 20-30 ppb. Whenever additional gas was injected into the chamber, the fan was turned on for 3-5 min to circulate the gas throughout the chamber.

4.2.2. Data Processing. A time delay was present as the gas moved from the measuring point through the tubes to the gas sensors. Adjusting to account for the delay allowed for a real-time comparison of events between the two measuring points. The recorded time was adjusted according to Equation (5), where t_1 is the adjusted time, t_0 is the measured time, l is the tube length, D is the tube inner diameter, and Q is the air pump flow rate.

$$t_1 = t_0 - (l)(\pi) \left(\frac{D}{2}\right)^2 \left(\frac{1}{Q}\right) \quad (5)$$

Equations (6) and (7) were used to convert the sensor output voltages into concentrations. The equations were provided by the manufacturer [136], where C is concentration, s is the calibrated sensor sensitivity, WE is the working electrode voltage, and AE is the auxiliary electrode voltage. n_T and k'_T are both temperature corrections that are dependent on the equation used, type of gas measured, and air temperature at the sampling time. The WE and AE subscripts are defined as follows: e is the calibrated

constant offset voltage due to natural electronic interference, 0 is the sensor's calibrated zero voltage, and u is the raw measured voltage value. WE_u and AE_u are the only variables in both equations [136]. The sensor calibration constants are given in Table 4.2.

$$C_{NO} = [(WE_u - WE_e) - (WE_0 - AE_0) - k'_T(AE_u - AE_e)] \left(\frac{1}{S}\right) \quad (6)$$

$$C_{NO_2} = [(WE_u - WE_e) - n_T(AE_u - AE_e)] \left(\frac{1}{S}\right) \quad (7)$$

Table 4.2. Sensor Calibration Constants

Constant	Sensor A		Sensor B	
	NO	NO2	NO	NO2
WEe (V)	0.266	0.303	0.275	0.307
WEo (V)	-0.005	0.478	0.008	0.478
AEe (V)	0.280	0.294	0.273	0.307
AEo (V)	0.018	0.448	0.026	0.398
Sensitivity (mV/ppb)	-0.351	0.286	-0.404	0.299
nT (30 C)	-	1.9	-	1.9
k'T (30 C)	1.2	-	1.2	-

In addition to the 0.1 ms minimum sample time, the gas sensor manufacturer also recommended using an exponential moving average technique where the number of samples per average is approximately equal to 10 divided by the sample rate in seconds [135]. The sample rate was one sample per 0.1008 s, so the number of samples per average was 100.

4.2.3. Variables. Several variables were held constant during all tests. Rotor speeds remained constant with 95% statistical confidence. Temperature in the chamber

did not vary significantly, so the temperature-based calibration constants were relevant for all tests. Fan pump batteries were replaced frequently to maintain flowrate. The fixed location sensor was in a constant position. NO_x is heavier than ambient atmosphere, so to mitigate the potential for stratification, fans were turned on to circulate air throughout the chamber in between tests and whenever additional NO was added to the chamber.

Four significant variables could not be held constant. The first and only intentional variable was the varying sensor location. Three known variables could not be individually defined, but the sum result of these errors was defined. The first undefined variable was the natural decay of NO as it interacts with O₂ to produce NO₂. The reaction was expected to cause a decrease in NO and an increase in NO₂ over time. The second variable was that, although most of the chamber was sealed, the door was not perfectly sealed to grant researchers access to move the measuring point between each test; the imperfectly sealed chamber may have allowed for mixing with ambient air or NO_x-laden air to escape the chamber. As the NO_x escaped or was mixed with ambient air, a decrease in NO_x over time was expected. The third variable was potential gas stratification over time due to differences in gas density. Specific gravities for NO, NO₂, and ambient air are approximately 1.2, 1.9, and 1.0, respectively. Without these three sources of concentration variation, the NO and NO₂ concentrations were expected to remain relatively linear. The linear slope of the results was adjusted using linear de-trending. Equation (8) was used, where C_n is the adjusted instantaneous concentration (ppb), C_o is the original instantaneous concentration (ppb), t_n is the time at which C_o was measured (s), t_{mid} is the midpoint time for the entire test (s), and s is the slope of the test results (ppb/s). This adjustment rotated the trend line around the midpoint time, producing a line

with no slope at the overall average concentration. This rotation produced less accurate concentration values (C_n), but it allowed for unbiased evaluation of standard deviation changes. Therefore, this adjustment was only used when comparing standard deviations between tests.

$$C_n = C_o - (t_n - t_{mid})(s) \quad (8)$$

Equation (8) applies to the data section where the UAV is turned on, but does not apply for the two sections where the UAV is turned off because the three sections have differing slopes. Equation (9) was used for the “UAV Off” regions, where t_a is the midpoint of the adjustment period relevant to the time n , s_{on} is the slope of the “UAV On” region, and s_{off} is the slope of the “UAV Off” region relevant to the time n .

$$C_n = C_o - (t_a - t_{mid})(s_{on}) - (t_n - t_a)(s_{off}) \quad (9)$$

4.3. RESULTS

The primary objective was to evaluate changes to measured gas concentration caused by downwash. If downwash significantly altered concentration measurements, then a secondary objective was to determine if such changes could be mitigated by varying the measuring point location within the downwash region. The overall results are shown in Table 4.3, which combines all vertical test results from all vertical series, and which likewise combines all horizontal test results from all horizontal series. The average concentrations are the weighted average of average measured concentrations from all individual tests, weighted according to the number of samples in each test. Likewise, the average standard deviation is the weighted average of the individual test deviations. Note

that these concentration values include normalizing for uncontrolled variables as discussed in Section 3.3. See Section 4.3.1 for the results averaged by test series.

Table 4.3. Measured Concentration Results, Average of All Tests

Gas	Sensor Extension	UAV Rotors	Sensor	Average Concentration (ppb)	Average Std. Dev. (ppb)
NO	Vertical	Off	A	38.28	0.44
			B	38.30	0.55
		On	A	36.97	0.33
			B	36.90	0.29
	Horizontal	Off	A	36.79	0.33
			B	36.78	0.33
		On	A	35.78	0.25
			B	35.77	0.40
NO₂	Vertical	Off	A	16.40	0.30
			B	16.43	0.27
		On	A	16.19	0.36
			B	16.24	0.28
	Horizontal	Off	A	15.75	0.17
			B	15.80	0.33
		On	A	15.60	0.21
			B	15.56	0.36
NO_x	Vertical	Off	A	52.88	0.51
			B	52.91	0.59
		On	A	51.51	0.39
			B	51.48	0.38
	Horizontal	Off	A	52.54	0.37
			B	52.59	0.45
		On	A	51.38	0.34
			B	51.34	0.49

Note that concentration values should not be directly compared unless they are taken from the same test. The variables discussed in Section 4.2.3 makes concentration comparisons between separate tests meaningless. However, comparisons between concentrations measured by sensors A and B within the same test are relevant and are a deciding factor in whether or not the varying location within the downwash region has affected concentration measurements. Additionally, standard deviation can be used to evaluate consistency of a dataset, so comparisons between standard deviation are applicable in all cases.

Table 4.4 shows the number of tests performed in each series and the total number of samples measured across all tests within the series. “UAV Off (Before)” refers to the samples collected prior to turning on the UAV, and “UAV Off (After)” refers to the samples collected after powering off the UAV.

Table 4.4. Number of Tests and Samples Collected in Each Test Series

Series	Number of Tests	Total Number of Samples		
		UAV Off (Before)	UAV On	UAV Off (After)
Vertical 1	12	27,382	31,002	No Data
Vertical 2	35	43,166	70,389	43,153
Horizontal 1	8	16,866	18,151	No Data
Horizontal 2	8	11,707	19,343	9,671
Horizontal 3	8	11,510	17,560	11,112
Horizontal 4	4	5,356	9,673	4,910
Top	3	3,576	5,257	3,572
Total	78	119,563	171,375	72,418

4.3.1. Measured Concentration Results. Table 4.5 through Table 4.11 contain the average concentration measurements for all tests in each test series. All of the data in this section is summarized in Table 4.3 (Section 4.3). The results are separated by the UAV rotor condition (on or off) and by individual sensors. Note that measurements with the UAV off were not taken after measurements with the UAV on for the series Vertical 1 and Horizontal 1.

Table 4.5. Measured Concentration Results, Average of Vertical 1 Tests

Gas	UAV Rotors	Sensor	Average Concentration (ppb)	Average Std. Dev. (ppb)
NO	Off (before)	A	23.27	0.60
		B	23.32	0.53
	On	A	22.99	0.37
		B	22.87	0.33
NO ₂	Off (before)	A	12.51	0.23
		B	12.60	0.23
	On	A	12.54	0.35
		B	12.71	0.37
NO _x	Off (before)	A	35.78	0.68
		B	35.91	0.59
	On	A	35.53	0.40
		B	35.57	0.42

Table 4.6. Measured Concentration Results, Average of Vertical 2 Tests

Gas	UAV Rotors	Sensor	Average Concentration (ppb)	Average Std. Dev. (ppb)
NO	Off (before)	A	43.03	0.48
		B	43.03	0.80
	On	A	43.14	0.31

Table 4.6. Measured Concentration Results, Average of Vertical 2 Tests (Cont.)

NO	On	B	43.08	0.27
	Off (after)	A	43.04	0.31
		B	43.09	0.30
NO₂	Off (before)	A	17.66	0.36
		B	17.67	0.34
	On	A	17.80	0.37
		B	17.80	0.24
	Off (after)	A	17.61	0.30
		B	17.62	0.21
NO_x	Off (before)	A	58.44	0.56
		B	58.45	0.82
	On	A	58.56	0.38
		B	58.49	0.36
	Off (after)	A	58.17	0.35
		B	58.17	0.37

Table 4.7. Measured Concentration Results, Average of Horizontal 1 Tests

Gas	UAV Rotors	Sensor	Average Concentration (ppb)	Average Std. Dev. (ppb)
NO	Off (before)	A	30.69	0.52
		B	30.51	0.38
	On	A	27.31	0.26
		B	27.39	0.62
NO₂	Off (before)	A	12.50	0.19
		B	12.63	0.39
	On	A	12.51	0.26
		B	12.49	0.46
NO_x	Off (before)	A	31.60	0.58
		B	31.16	0.43
	On	A	31.51	0.23
		B	31.09	0.73

Table 4.8. Measured Concentration Results, Average of Horizontal 2 Tests

Gas	UAV Rotors	Sensor	Average Concentration (ppb)	Average Std. Dev. (ppb)
NO	Off (before)	A	42.31	0.34
		B	42.50	0.41
	On	A	41.16	0.28
		B	40.96	0.32
	Off (after)	A	41.23	0.21
		B	41.21	0.25
NO ₂	Off (before)	A	17.52	0.14
		B	17.65	0.43
	On	A	17.65	0.14
		B	17.51	0.33
	Off (after)	A	17.66	0.09
		B	17.65	0.26
NO _x	Off (before)	A	59.83	0.35
		B	60.15	0.50
	On	A	58.82	0.36
		B	58.46	0.45
	Off (after)	A	58.89	0.24
		B	58.87	0.37

Table 4.9. Measured Concentration Results, Average of Horizontal 3 Tests

Gas	UAV Rotors	Sensor	Average Concentration (ppb)	Average Std. Dev. (ppb)
NO	Off (before)	A	32.25	0.27
		B	32.16	0.33
	On	A	30.23	0.21
		B	30.40	0.28
	Off (after)	A	30.29	0.20
		B	30.34	0.23
NO ₂	Off (before)	A	15.04	0.16
		B	15.13	0.24
	On	A	14.61	0.27

Table 4.9. Measured Concentration Results, Average of Horizontal 3 Tests (Cont.)

NO₂	On	B	14.60	0.29
	Off (after)	A	14.82	0.19
		B	14.84	0.22
NO_x	Off (before)	A	47.28	0.32
		B	47.40	0.46
	On	A	44.84	0.34
		B	45.00	0.38
	Off (after)	A	45.13	0.28
		B	45.18	0.32

Table 4.10. Measured Concentration Results, Average of Horizontal 4 Tests

Gas	UAV Rotors	Sensor	Average Concentration (ppb)	Average Std. Dev. (ppb)
NO	Off (before)	A	47.30	0.38
		B	47.46	0.38
	On	A	50.95	0.23
		B	50.89	0.38
	Off (after)	A	49.70	0.22
		B	49.66	0.25
NO₂	Off (before)	A	19.18	0.33
		B	18.71	0.51
	On	A	19.11	0.12
		B	19.17	0.35
	Off (after)	A	19.02	0.07
		B	19.13	0.22
NO_x	Off (before)	A	66.49	0.47
		B	66.17	0.46
	On	A	70.06	0.24
		B	70.06	0.46
	Off (after)	A	68.72	0.23
		B	68.82	0.36

Table 4.11. Measured Concentration Results, Average of Top Tests

Gas	UAV Rotors	Sensor	Average Concentration (ppb)	Average Std. Dev. (ppb)
NO	Off (before)	A	37.48	0.78
		B	37.44	0.63
	On	A	37.53	0.25
		B	37.47	0.28
	Off (after)	A	37.44	0.22
		B	37.81	0.24
NO ₂	Off (before)	A	19.73	0.34
		B	19.51	0.31
	On	A	19.37	0.15
		B	19.28	0.29
	Off (after)	A	19.76	0.08
		B	19.44	0.23
NO _x	Off (before)	A	57.22	0.97
		B	56.95	0.84
	On	A	56.90	0.32
		B	56.75	0.41
	Off (after)	A	57.20	0.23
		B	57.25	0.29

4.3.2. Accounting for Uncontrolled Variables. As discussed in Section 4.2.3, uncontrolled variables such as changes in ambient air and NO-to-NO₂ conversion were accounted for using linear de-trending. Normalization data are shown in Table 4.12, where the average linear slope and average standard deviation take the weighted average of all test results. Note that NO_x error is not included as NO_x results are simply a summation of NO and NO₂ measurements rather than a direct NO_x measurement. For both gases, the relatively high standard deviations may have been caused by inconsistencies in the addition of ambient air, escape of NO_x from the chamber, and

mixture within the chamber. The deviations could also be caused by the inherent sensor error. The inherent sensor errors were ± 0.43 ppb for NO and ± 0.27 ppb for NO₂ for Sensor A and ± 0.38 ppb for NO and ± 0.25 ppb for NO₂ for Sensor B. Propagating the error yields a total NO_x error of ± 0.51 ppb for Sensor A and ± 0.45 ppb for Sensor B. Both gases experienced a lower slope while the UAV was on, which was probably caused by the rotors creating a greater influx of ambient air and escape of NO_x.

Table 4.12. Averages of the Linear Slopes Used to Adjust for Undefined Error

Gas	UAV Rotors	Average Linear Slope (ppb/min)	Average Std. Dev. (ppb/min)
NO	Off	-0.22	0.46
	On	-0.84	0.40
NO₂	Off	0.14	0.31
	On	0.11	0.20

Table 4.12 shows that measurements taken while the UAV was turned on depict a considerable decrease in NO concentration and little effect on NO₂ concentration. The author believes that increased air circulation may have expedited the NO-to-NO₂ conversion rate. An increase in NO₂ concentration over time would thereby be expected, although it appears this increase was counteracted by the leakage of NO_x over time. NO_x and ambient air stratification was not evaluated during the 120 s recording intervals in which the UAV was off. If stratification did occur, its effects would vary based on measuring point elevation; measuring points at higher elevations would see a decrease in NO_x over time while measuring points at lower elevations would see an increase.

4.3.3. Effects of Downwash Presence. This experiment aimed to determine if UAV downwash can affect concentration measurements by altering the pressure within the downwash region. The effects were evaluated by comparing recorded concentrations with and without the presence of downwash. Any statistically significant difference in the results would imply a pressure difference great enough to alter the concentration measurements. If no statistically significant difference is seen, then the presence or absence of downwash did not affect measured concentration values.

Figure 4.6, Figure 4.7, Figure 4.8, and Table 4.13 show percent differences between NO_x concentrations measured while the UAV is on and while the UAV is off while the measuring points were extended vertically beneath the UAV. Positive percentages refer to instances when the average “UAV on” concentration was greater than the average “UAV off” concentration, and negative percentages are the inverse. Sensor B was fixed at 2.0 m below the UAV, which was the distance determined to have the lowest turbulence in Section 3, so the horizontal axis refers to the location of Sensor A as distance from the bottom of the UAV.

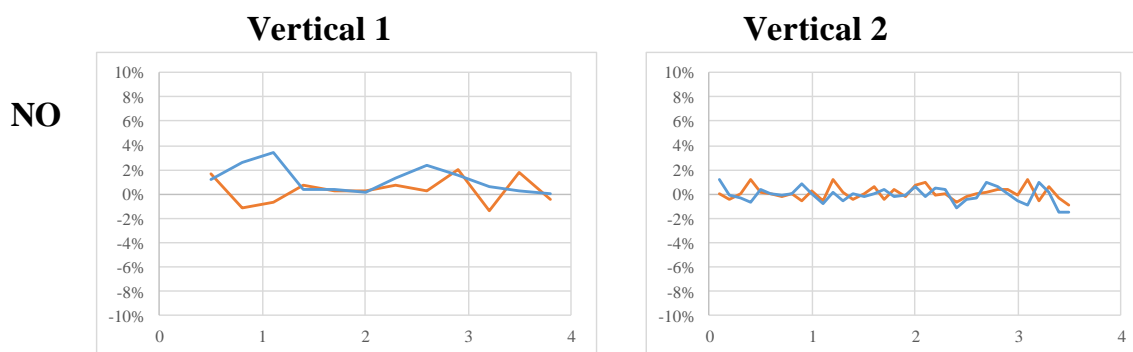


Figure 4.6. Results for Percent Difference between “UAV On” and “UAV Off”, with Relation to Vertical Distance beneath the UAV

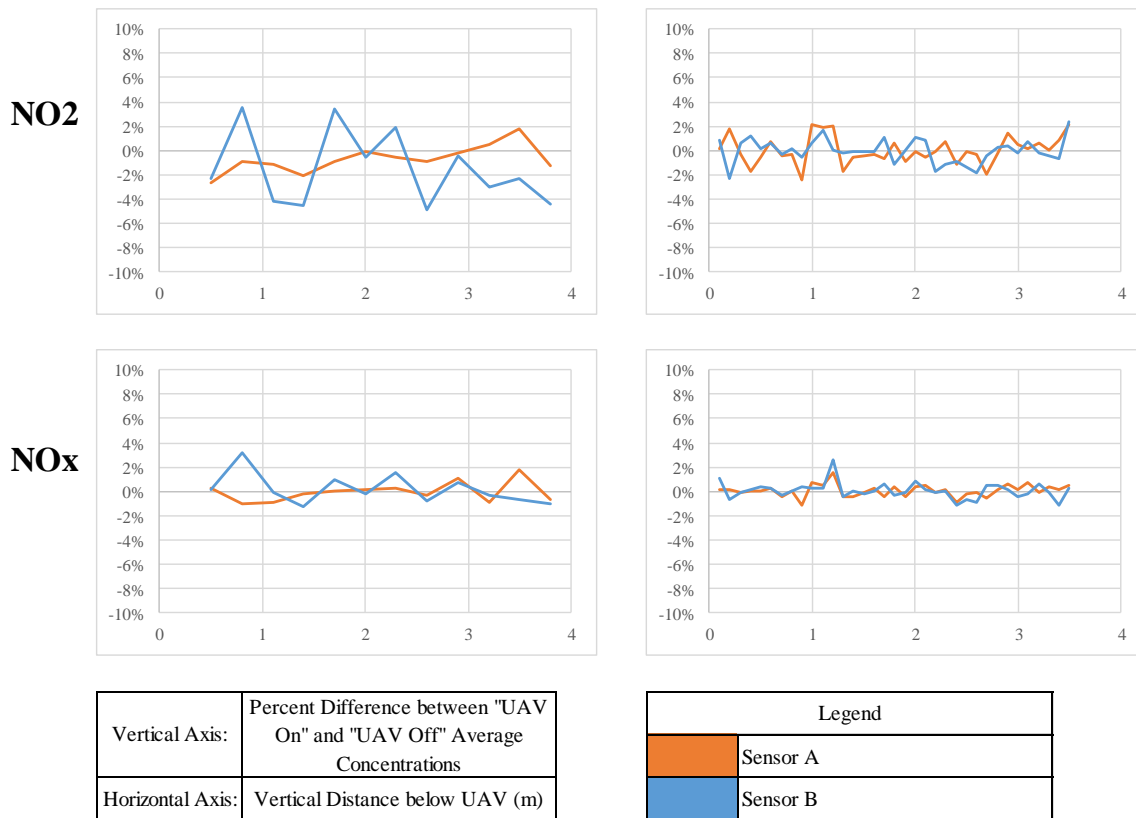


Figure 4.6. Results for Percent Difference between “UAV On” and “UAV Off”, with Relation to Vertical Distance beneath the UAV (Cont.)

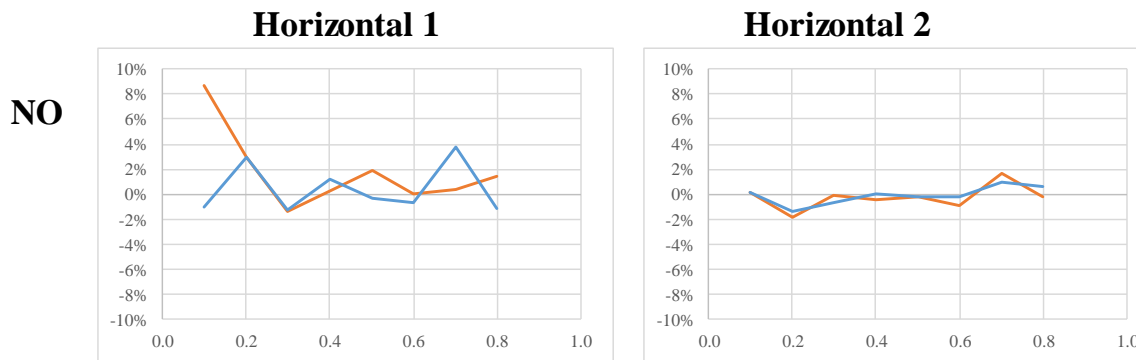


Figure 4.7. Results for Percent Difference between “UAV On” and “UAV Off”, with Relation to Horizontal Distance beside the UAV, Series Horizontal 1 and Horizontal 2

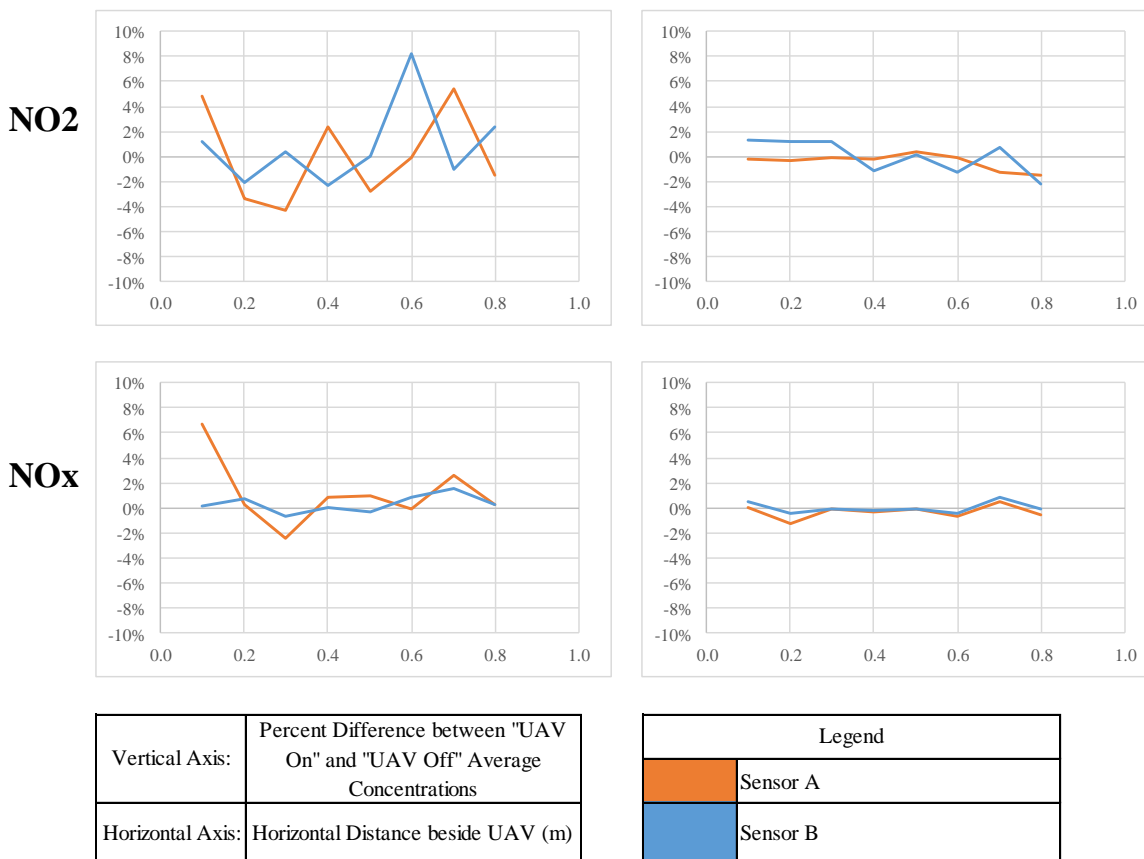


Figure 4.7. Results for Percent Difference between “UAV On” and “UAV Off”, with Relation to Horizontal Distance beside the UAV, Series Horizontal 1 and Horizontal 2 (Cont.)

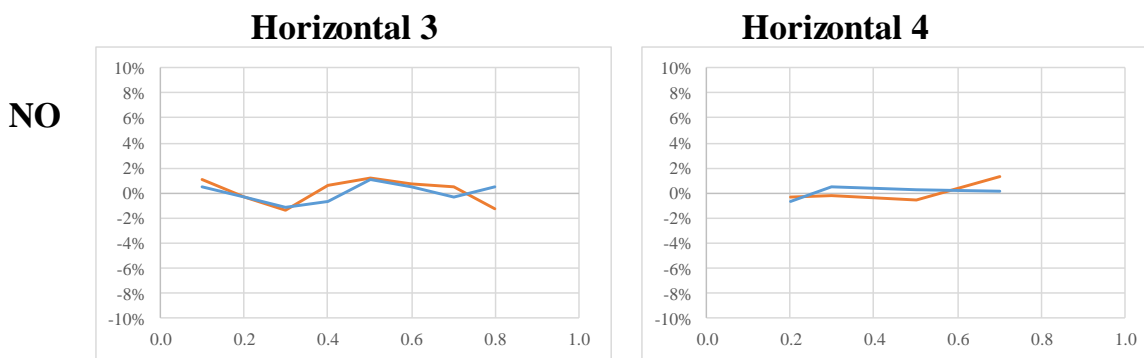


Figure 4.8. Results for Percent Difference between “UAV On” and “UAV Off”, with Relation to Horizontal Distance beside the UAV, Series Horizontal 3 and Horizontal 4

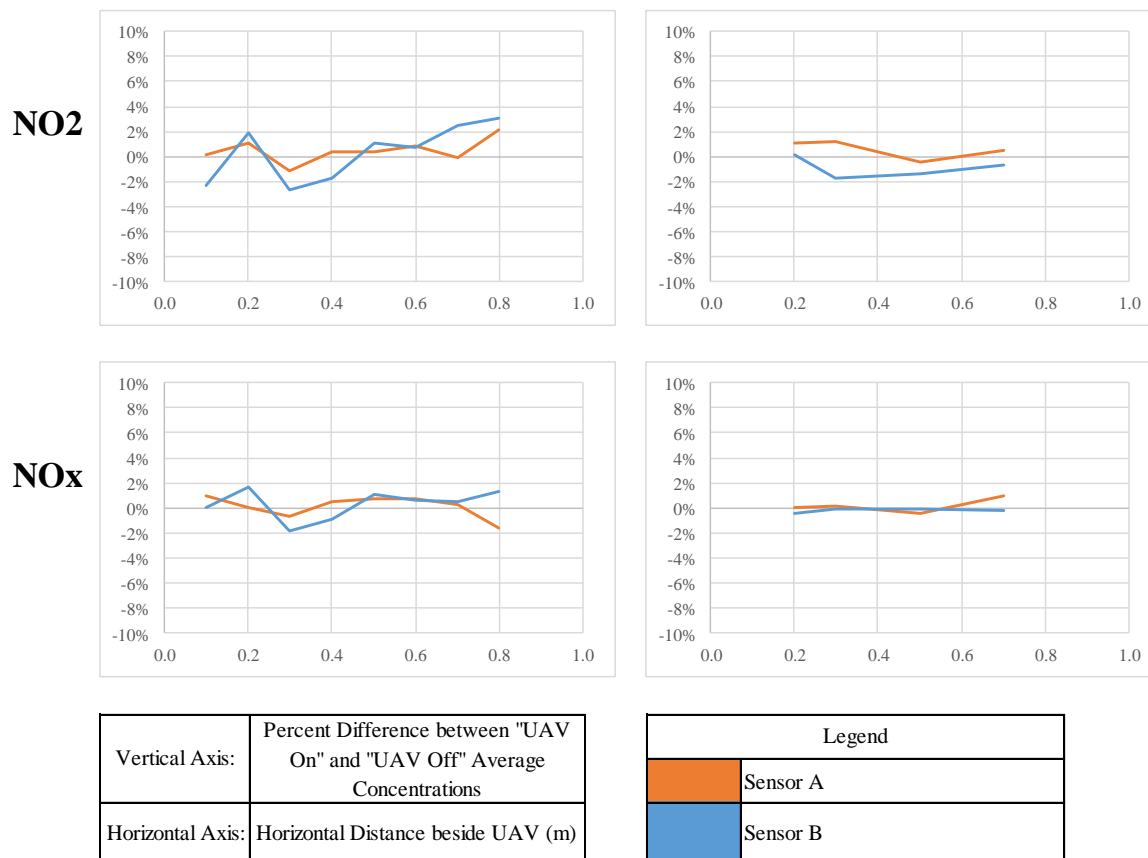


Figure 4.8. Results for Percent Difference between “UAV On” and “UAV Off”, with Relation to Horizontal Distance beside the UAV, Series Horizontal 3 and Horizontal 4 (Cont.)

Table 4.13. Results for Percent Difference between “UAV On” and “UAV Off”, with Comparison of Measurements on Top of the UAV to Vertical Distance beneath the UAV and Horizontal Distance beside the UAV

		Percent Difference (On vs Off)		
Sensor B Location:		0.4 m beside the UAV	2.0 m beneath the UAV	
Gas	UAV	Test 1	Test 2	Test 3
NO	Sensor A	1.1%	-0.2%	-0.7%
	Sensor B	-0.7%	-0.6%	0.1%
NO ₂	Sensor A	0.4%	-0.6%	-0.1%
	Sensor B	0.2%	-0.5%	0.8%
NO _x	Sensor A	0.8%	-0.3%	-0.4%
	Sensor B	-0.4%	-0.6%	0.4%

Statistical difference was calculated for each test using a t-test where a difference was confirmed with a p-value less than 0.05. Of the 49 vertical tests, 26 horizontal tests, and 3 top tests, zero NO, NO₂, or NO_x tests saw statistically different results between “UAV On” and “UAV Off”. The complete lack of statistical difference strongly indicates that UAV downwash had no effect on measured concentration values at the evaluated measuring point locations. These results imply that even in the most turbulent locations in the downwash region, the turbulent pressure variations are not varied enough from ambient pressure to significantly alter the density of the gas. Therefore, the gas can be assumed to be incompressible within the downwash region, and the presence of downwash does not induce measurement error.

4.3.4. Effects of Varying Measuring Point Location. This experiment also aimed to determine if changes in concentration measurements could be mitigated by changing the measuring point location within the downwash region. The effects were evaluated by comparing a sensor of varying locations to a sensor with fixed location, and any statistically significant difference between the two sensor concentration results would imply a pressure difference between those distances caused by downwash turbulence. If no statistically significant difference is seen, then location within the downwash region did not affect measured concentration values.

Figure 4.9, Figure 4.10, Figure 4.11, and Table 4.14 show percent differences between concentrations measured from Sensor A (variable distance from the UAV) and concentrations measured from Sensor B (fixed distance from the UAV) while the measuring points were extended vertically beneath the UAV. Positive percentages refer to instances when the average Sensor A concentration was greater than the average

Sensor B concentration, and negative percentages are the inverse. Sensor B was fixed at 2.0 m below the UAV, which was the distance determined to have the lowest turbulence in Section 3, so the horizontal axis refers to the location of Sensor A as distance from the bottom of the UAV.

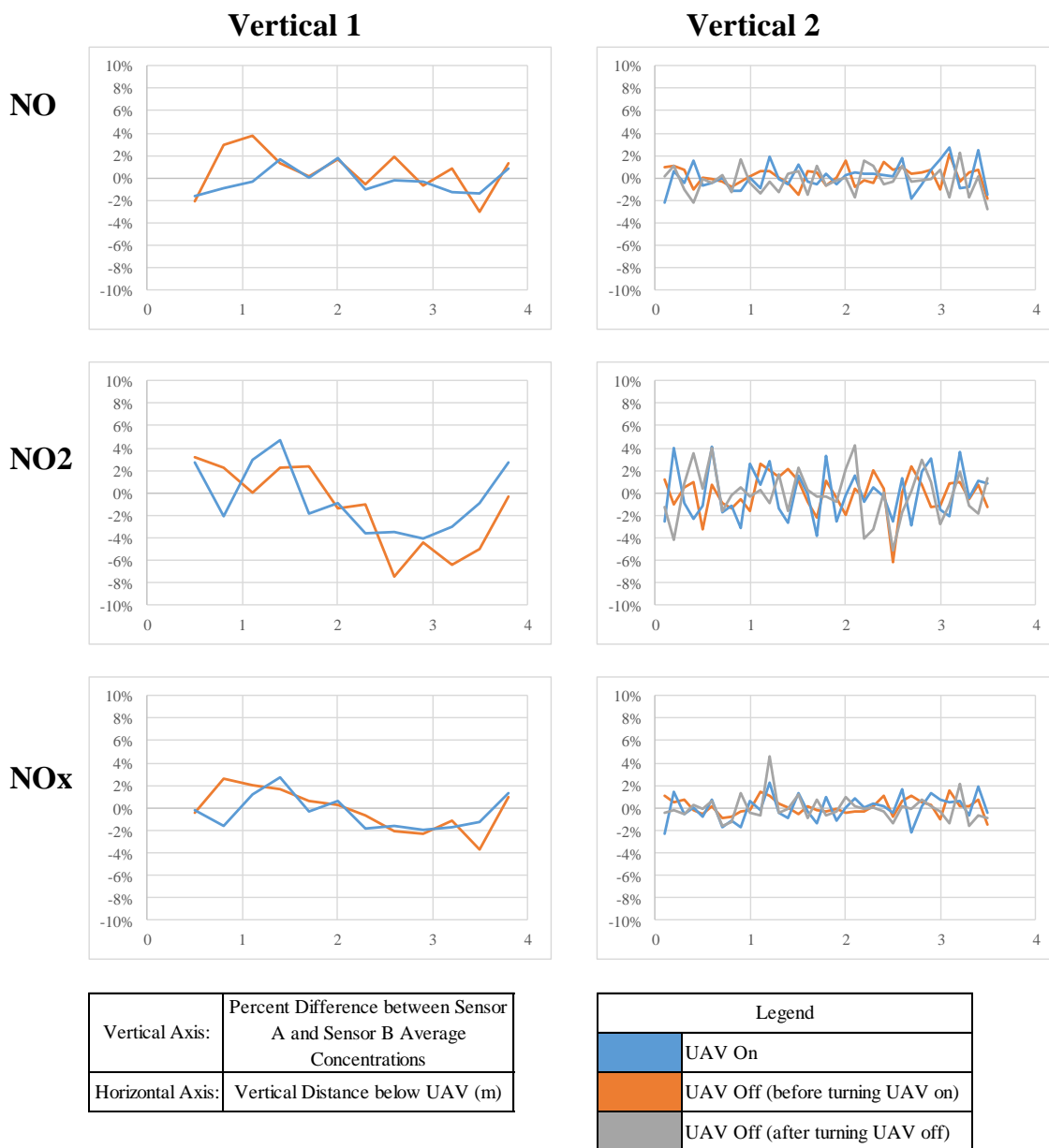


Figure 4.9. Results for Percent Difference between Sensor A and Sensor B, with Relation to Vertical Distance beneath the UAV

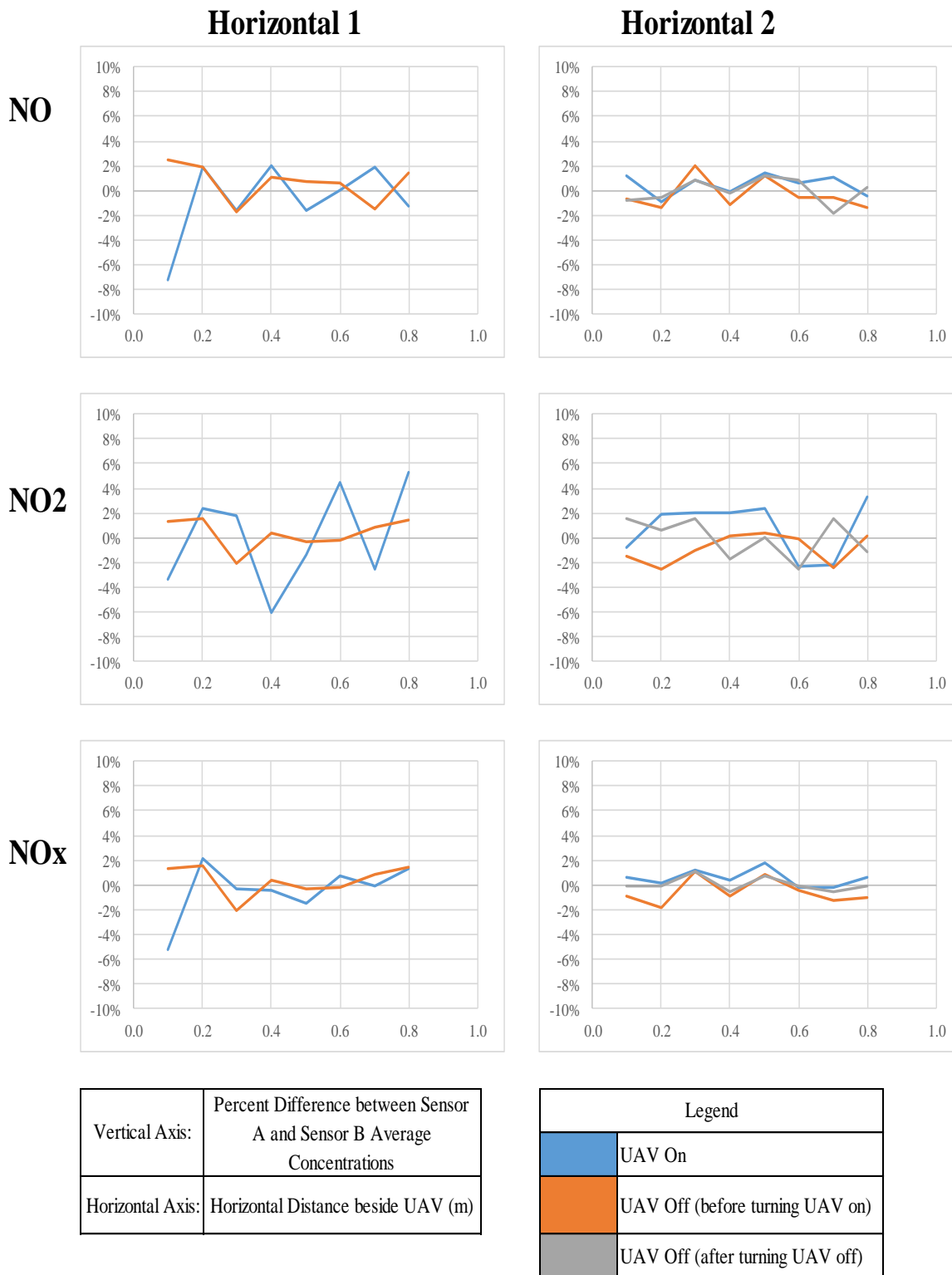


Figure 4.10. Results for Percent Difference between Sensor A and Sensor B, with Relation to Horizontal Distance beside the UAV, Series Horizontal 1 and Horizontal 2

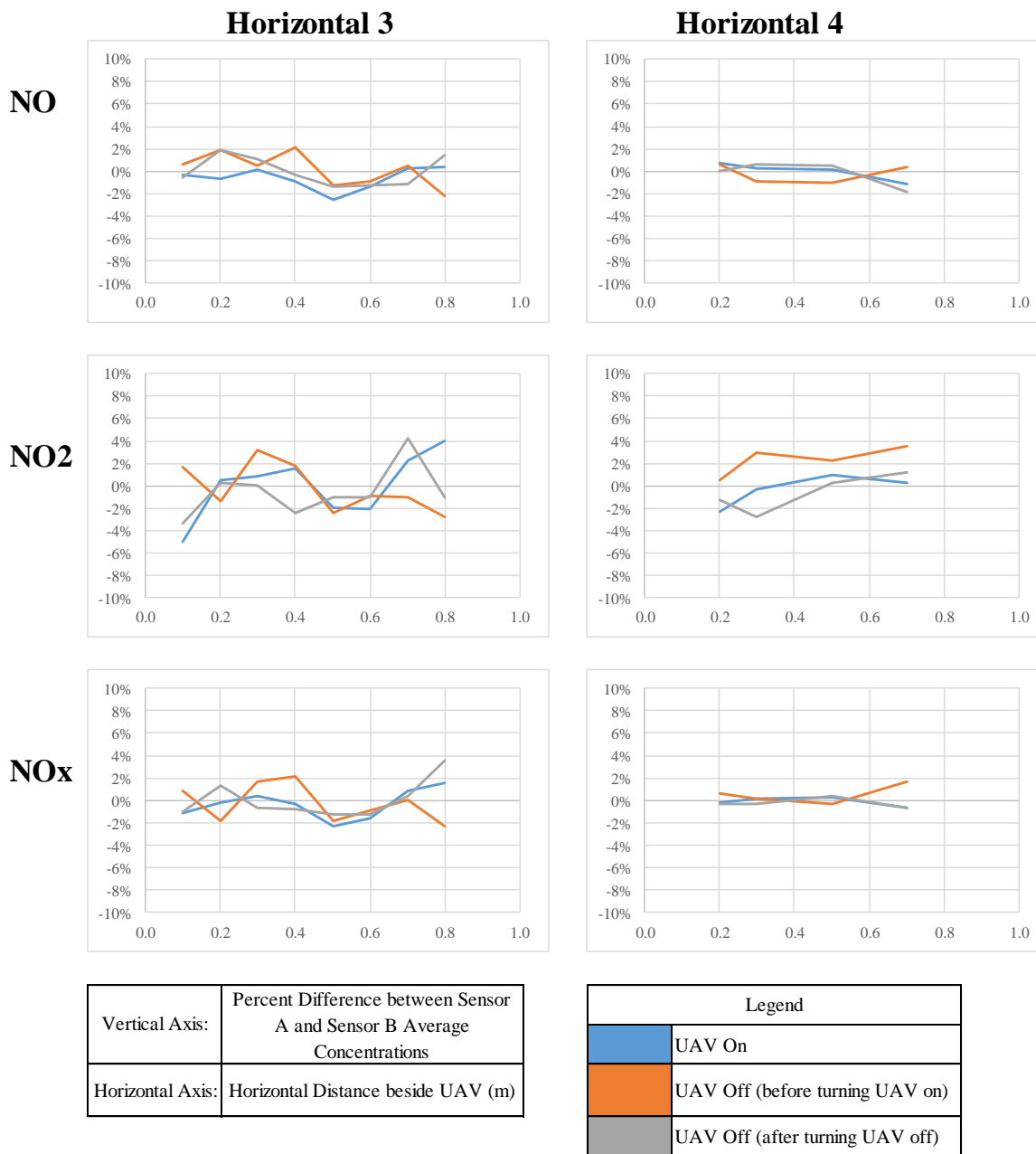


Figure 4.11. Results for Percent Difference between Sensor A and Sensor B, with Relation to Horizontal Distance beside the UAV, Series Horizontal 3 and Horizontal 4

Statistical difference was calculated for each test using a t-test where a difference was confirmed with a p-value less than 0.05. Of the 49 vertical tests and 3 top tests, zero NO, NO₂, or NO_x tests saw statistically different results between Sensors A and B. Of the

Table 4.14. Results for Percent Difference between Sensor A and Sensor B, with Comparison of Measurements on Top of the UAV to Vertical Distance beneath the UAV and Horizontal Distance beside the UAV

Sensor B Location:		Percent Difference (Sensor A vs Sensor B)		
		0.4 m beside the UAV	2.0 m beneath the UAV	
Gas	UAV	Test 1	Test 2	Test 3
NO	Off (before)	1.4%	-1.9%	-2.2%
	On	0.0%	0.3%	-0.8%
	Off (after)	-1.2%	1.6%	-0.2%
NO ₂	Off (before)	0.0%	1.8%	-0.4%
	On	2.9%	-0.6%	3.1%
	Off (after)	0.5%	0.5%	2.3%
NO _x	Off (before)	0.9%	-0.5%	-1.5%
	On	0.8%	0.0%	0.3%
	Off (after)	-0.6%	1.2%	1.0%

26 horizontal tests, 0 NO, 1 NO₂, and 1 NO_x tests saw statistical differences between Sensors A and B. However, neither of the two significant differences were present in the same test, test series, or any other tests at the same sensor location. Statistical analysis confirms both of the significantly different measurements were outliers with 95% confidence. Therefore, measurement location within the UAV downwash region had no effect on observed concentration values when the measuring point was positioned 0.1-3.5 m below the UAV, 0.1-0.8 m beside the UAV, or directly on top of the UAV. These results verify the conclusions from Section 4.3.3 that the presence of downwash does not induce measurement error regardless of measuring point location.

4.3.5. Relation to Turbulence. Standard deviations were compared to evaluate relative stability. The majority of standard deviation values were lower than the inherent sensor error, which strongly suggests that the deviation was caused by inherent error and

not influenced by downwash. Standard deviation in excess of inherent error for all gases and test series are shown in Figure 4.12, Figure 4.13, Figure 4.14, and Table 4.15.

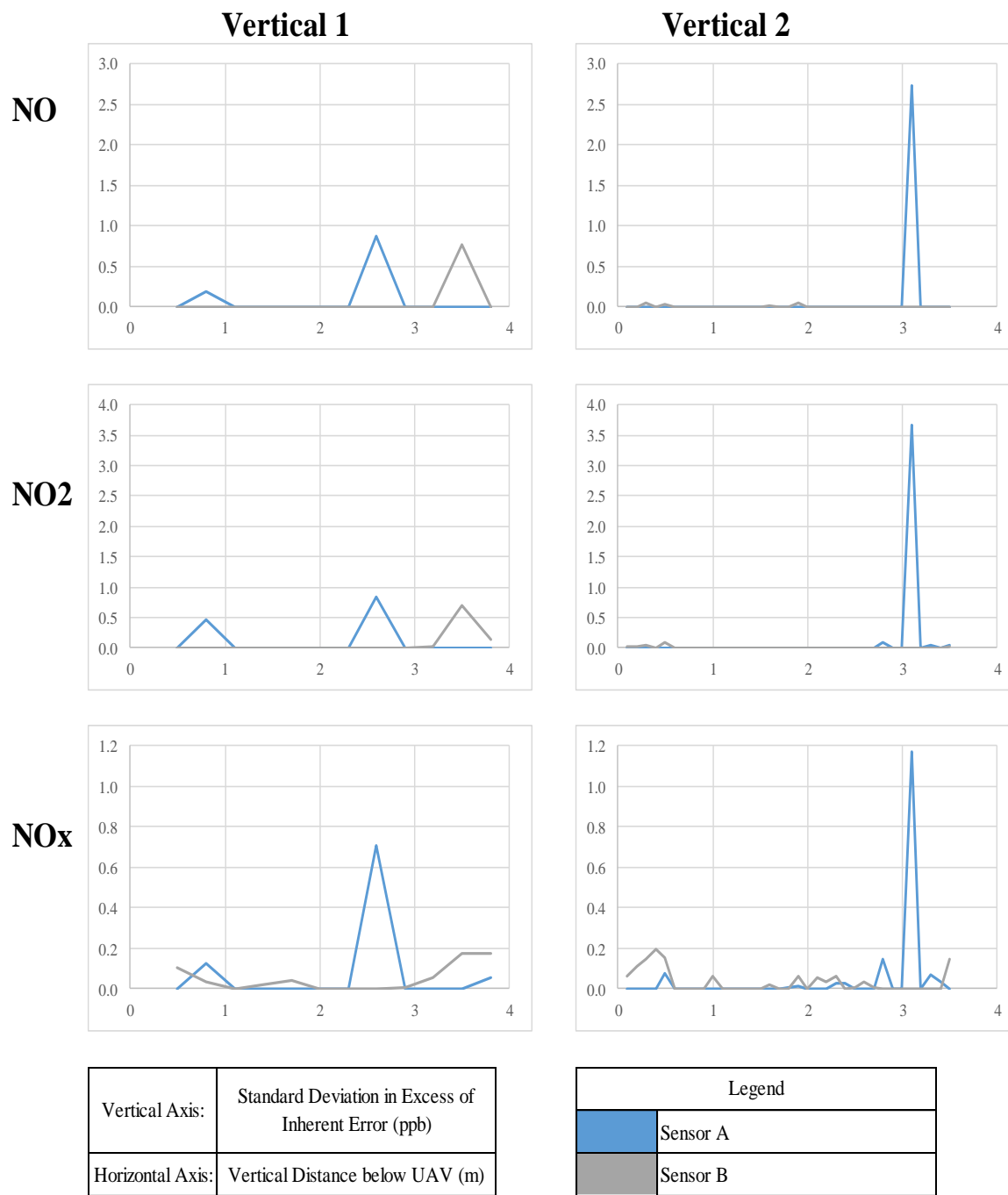


Figure 4.12. Standard Deviation in Excess of Inherent Error, with Relation to Vertical Distance beneath the UAV

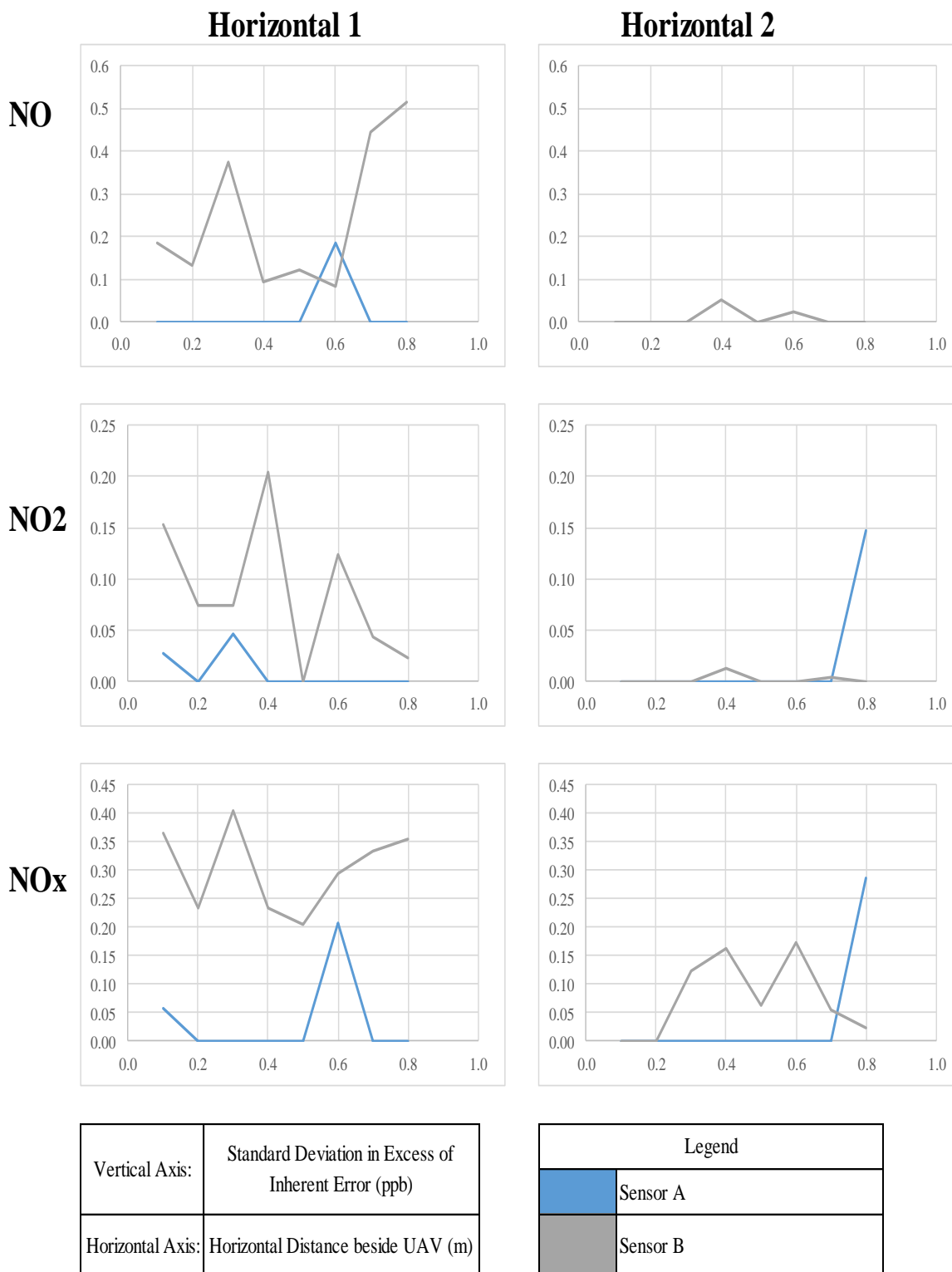


Figure 4.13. Standard Deviation in Excess of Inherent Error, with Relation to Horizontal Distance beside the UAV, Series Horizontal 1 and Horizontal 2

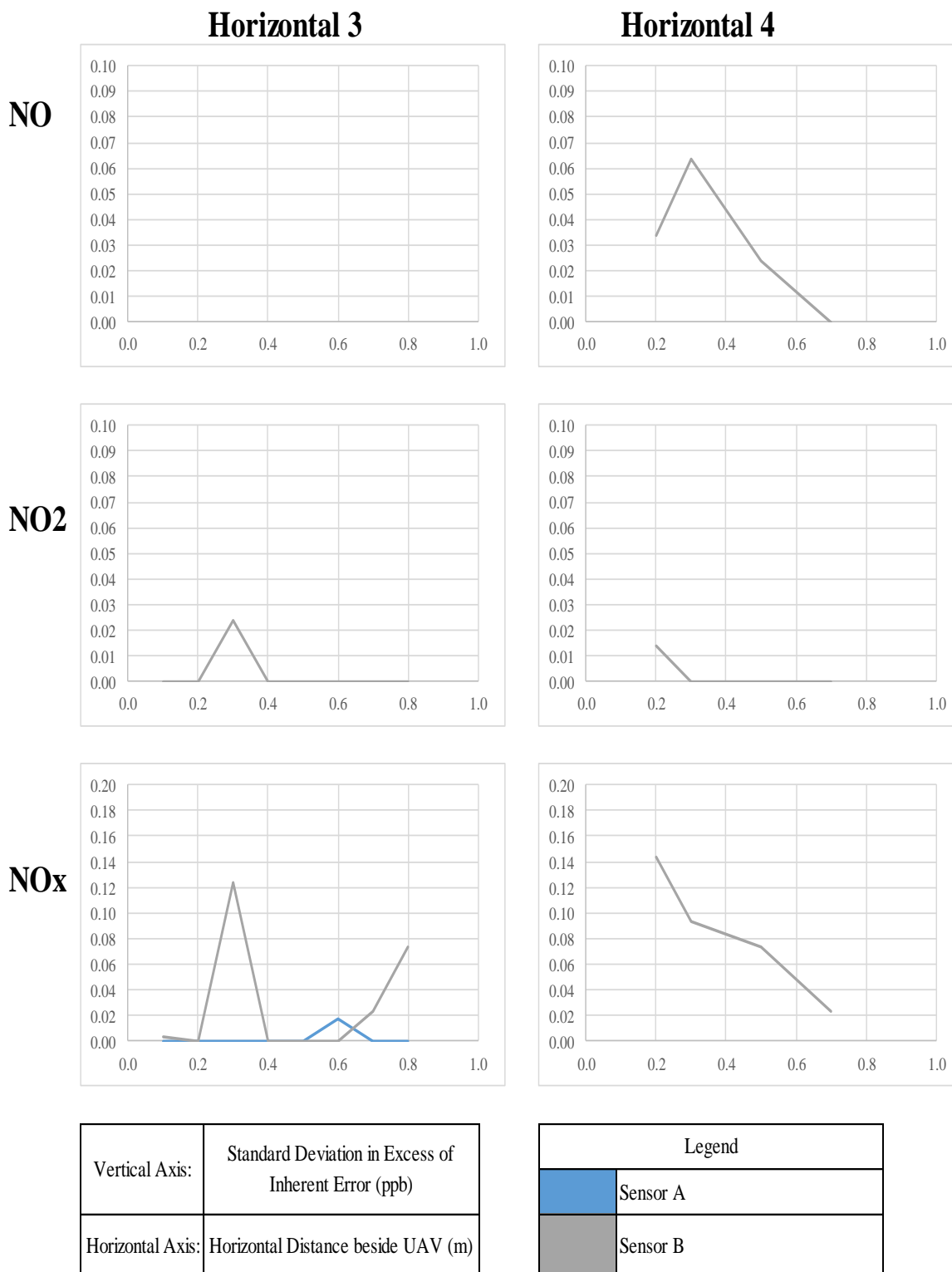


Figure 4.14. Standard Deviation in Excess of Inherent Error, with Relation to Horizontal Distance beside the UAV, Series Horizontal 3 and Horizontal 4

Table 4.15. Standard Deviation in Excess of Inherent Error, with Comparison of Measurements on Top of the UAV to Vertical Distance beneath the UAV and Horizontal Distance beside the UAV

		Standard Deviation in Excess of Inherent Error (ppb)		
Sensor B Location:		0.4 m beside the UAV	2.0 m beneath the UAV	
Gas	UAV	Test 1	Test 2	Test 3
NO	Off (before)	0.83	0.40	0.00
	On	0.00	0.00	0.00
	Off (after)	0.00	0.00	0.00
NO₂	Off (before)	0.00	0.21	0.00
	On	0.00	0.00	0.00
	Off (after)	0.00	0.00	0.00
NO_x	Off (before)	0.95	0.69	0.00
	On	0.00	0.04	0.05
	Off (after)	0.00	0.00	0.00

Standard deviation data was compared using the t-test for measurements taken while the UAV was off and on. The t-test results are shown in Table 4.16, where a p-value less than 0.05 (highlighted in the table) indicates a statistically significant change in standard deviation while the UAV was either on or off. Only standard deviations in excess of the inherent error were considered. The “vertical” results have a higher percentage of results with statistical difference, and all “vertical” results contained at least one individual test with deviations higher than the inherent error. Turbulence was the most likely cause for observed concentration changes in excess of inherent error, so these results imply that the downwash region vertically beneath the UAV has greater turbulence than the regions beside and above the UAV. Regardless of turbulence, the difference in deviation does not cause a significant difference in measured concentration values.

Table 4.16. p-values when Comparing Standard Deviation between Measurements Taken with the UAV On and Off (Dash “-“ Refers to a Series where All Tests Have Std. Dev. Lower than Sensor Error)

Series	p value					
	UAV On Compared to UAV Off (before)					
	NO		NO2		NOx	
	Sensor A	Sensor B	Sensor A	Sensor B	Sensor A	Sensor B
Vertical 1	22.4%	24.8%	43.8%	24.1%	4.8%	4.9%
Vertical 2	33.7%	0.2%	63.1%	2.3%	3.7%	0.3%
Horizontal 1	11.3%	1.3%	18.8%	15.4%	10.6%	9.9%
Horizontal 2	35.1%	7.4%	35.1%	11.4%	47.7%	41.0%
Horizontal 3	35.1%	21.7%	100.0%	62.1%	43.2%	9.6%
Horizontal 4	10.0%	81.3%	25.0%	40.1%	39.1%	95.5%
Top	42.3%	35.3%	42.3%	42.3%	41.0%	38.8%
Series	p value					
	UAV On Compared to UAV Off (after)					
	NO		NO2		NOx	
	Sensor A	Sensor B	Sensor A	Sensor B	Sensor A	Sensor B
Vertical 1	-	-	-	-	-	-
Vertical 2	97.3%	20.9%	88.5%	36.9%	83.1%	29.7%
Horizontal 1	-	-	-	-	-	-
Horizontal 2	100.0%	20.6%	35.1%	24.3%	45.1%	3.9%
Horizontal 3	100.0%	100.0%	100.0%	35.1%	59.8%	15.2%
Horizontal 4	100.0%	9.6%	100.0%	39.1%	100.0%	10.5%
Top	100.0%	100.0%	100.0%	100.0%	42.3%	42.3%

The research discussed in Section 3 measured turbulence for this experimental setup in the vertical direction beneath the UAV. Figure 4.15 compares that measured turbulence with the standard deviation in excess of error. The highest turbulence region

results in a moderately increased standard deviation of less than 0.5 ppb, while the highest deviations were seen in a relatively low turbulent region. While the results of this study indicate the possibility of turbulence affecting standard deviation, the relationship does not appear to be direct.

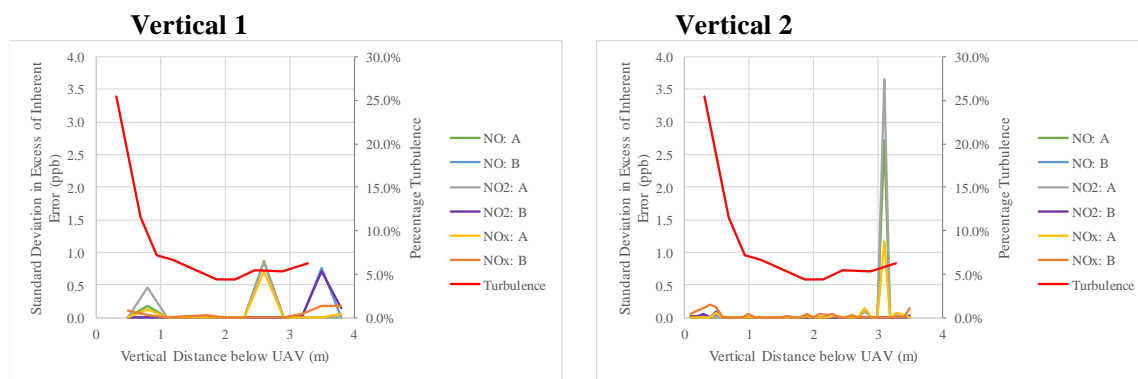


Figure 4.15. Comparison of Turbulence (red) to Standard Deviation in Excess of Inherent Error

4.3.6. Applicability of Results to Other UAVs. This experimentation only collected results for a single UAV model. However, the turbulent pressures active on the gas measuring point varied drastically throughout this study with no significant difference on measured gas concentration measurements. Therefore, the results are applicable to all locations within the downwash regions for the UAV used. Previous studies have simulated air pressures for a variety of UAV models with widely varying propeller shapes, number of rotors, and rotor configurations. Air pressure changes due to downwash were relatively similar across all studies [49,70,72]. By calculating the change in pressure with relation to ambient pressure, the results imply that density-based gas concentrations would only be altered by a maximum of $\pm 0.10\%$. Therefore, the author

hypothesizes that pressure changes caused by the downwash region are unlikely to affect measured gas concentrations, regardless of the UAV model, propeller shape, and rotor configuration used.

4.4. DISCUSSION

Airflow effects on measured gas concentration were studied for a UAV-mounted gas monitor. The UAV was “hovering” stationary in a chamber that contained constant NO_x concentration to avoid effects of mixture with ambient air. There was 95% statistical confidence that the presence of UAV downwash caused no significant changes to measured concentration values. Additionally, there was 95% statistical confidence that changing the measuring point location within the downwash region, including directly attached to the UAV, does not cause significant changes to measured concentration values. These conclusions apply to distances 0.1-3.5 m vertically below the UAV, 0.1-0.8 m horizontally from the UAV propeller tip, and directly on top of the UAV body. Turbulence was expected to be the most probable source of observed concentration fluctuation, yet the measured concentration values showed no correlation to the turbulent regions discovered in Section 3. Because no significant concentration changes were observed and concentration measurements had no correlation with turbulence, it was improbable that the presence of rotor downwash or the measuring point location within the downwash region had any effect on recorded concentration values.

Standard deviation in the concentration measurements implies the presence of turbulence. The standard deviation experienced few significant changes due to downwash. In most of the measured datasets, the deviation was less than the inherent

system errors, which implies turbulence has minimal effect on standard deviation. Evidence shows the region beneath the UAV has higher turbulence than the regions beside or above the UAV, although the difference in standard deviation was minor relative to the recorded concentration value. Most importantly, the deviations still made no statistically significant impact on the concentration measurements, which were not affected by downwash. Comparison with pressure data from prior research suggests that these conclusions may be applicable to a variety of the UAV models, propeller shapes, and rotor configurations used.

Based on this experiment, UAV-mounted gas monitors may be used to evaluate gas concentrations without concern for downwash effects, assuming the UAV and measuring point are entirely contained within the gas cloud. In open-air scenarios such as surface mine blasting, there is potential for mixing with ambient air, and the effects of that mixing were not evaluated. The region beneath the UAV experienced greater turbulence, so even though measured concentration values were not affected by downwash at any measuring point position, future field studies that wish to limit standard deviation should place the measuring point above or beside the UAV.

4.5. SUMMARY

Airflow effects on measured gas concentration were studied for a UAV-mounted gas monitor. The UAV operated in a stationary hovering configuration inside a chamber that contained constant NO_x concentration to avoid the effects of mixture with ambient air. All variables were either controlled or corrected for so that the only experimental

variable was the potential for downwash pressures to alter density-based gas concentration measurements. Conclusions from this experimentation included:

- UAV downwash caused no significant changes to measured concentration values (95% statistical confidence).
- Changing the measuring point location within the downwash region, including directly attaching the measuring point to the UAV, caused no significant changes to measured concentration values (95% statistical confidence).
- Measured concentration values showed no correlation to the turbulent regions discovered in Section 3.
- Turbulence has minimal effect on standard deviation. The region beneath the UAV has higher turbulence than the regions beside or above the UAV, although the difference in standard deviation was minor relative to the recorded concentration value.

5. CONCLUSIONS

This research grants confidence in gas concentrations measured by a UAV-mounted gas monitor. Experimental results provide substantial evidence to support the assumption that measurement error due to downwash pressures is statistically negligible because the pressure changes induced by downwash are not significant enough to cause compressible flow. Three objectives were completed:

- *Objective 1: Establish the time required for the downwash region to stabilize after UAV rotor thrust variations cease.* The time required for the downwash region to stabilize once the UAV stopped applying thrust and returned to an unvarying thrust configuration was 6 seconds. This objective allowed gas collection experiments to isolate the presence of downwash as the sole potential source of measurement error.
- *Objective 2: Quantify the effects of downwash on gas concentration measurements.* Rotary-wing UAV downwash was determined to have no statistically significant effect on measured gas concentrations. This source of error was previously undefined, and this conclusion provides an essential advancement towards validating UAS as a means of gas sample collection.
- *Objective 3: Develop a system for correcting measured concentration according to location within the downwash region.* Results from Objective 2 provided substantial evidence that a stabilized downwash region does not create statistical differences in measured concentration, and developing a

correction factor was not necessary. This conclusion applied to all test scenarios irrespective of measurement location within the downwash region.

Based on this experiment, UAV-mounted gas monitors can be used to evaluate gas concentrations without concern for downwash effects, assuming the UAV and measuring point are entirely contained within the gas cloud. In open-air scenarios such as surface mine blasting, there is potential for mixing with ambient air, and the effects of that mixing were not evaluated. The region beneath the UAV experienced greater turbulence, so even though measured concentration values were not affected by downwash at any measuring point position, future field studies that wish to limit standard deviation should place the measuring point above or beside the UAV. Comparisons with results from previous studies imply these conclusions are applicable to a wide variety of UAV models, propeller shapes, and rotor configurations. These conclusions are valid for:

- distances 0.1-3.5 m vertically below the UAV,
- distances 0.1-0.8 m horizontally from the UAV propeller tip,
- distances 0.0 m on top of the UAV body,
- situations in which both the UAV and the measuring point are located entirely within the gas cloud, and
- samples collected after the UAV has ceased altering motion and the downwash region is allowed to stabilize.

5.1. DOWNWASH REGION STABILIZATION TIME

Downwash region stabilization times were determined after movement was simulated using a 6-rotor UAV. Data was collected by mounting the UAV to a stand,

placing the stand in a controlled indoor environment with no external sources of airflow, and placing anemometers at ten locations beneath the UAV. Turbulence results were collected that were specific to the test setup for this research. Conclusions from this experimentation included:

- Turbulence stabilized up to 6 seconds after the UAV returned to an unvarying thrust configuration. The 6-second maximum period was observed after altering both vertical and rotational movement, and preliminary evidence suggests that altering horizontal motion would also yield similar results. Therefore, the author recommends all future research refrain from recording gas samples until at least 6 seconds after UAV rotor thrust alterations have ceased.
- Turbulence was greatest when vertical thrust was applied, and it was significantly less prevalent when altering rotational motion. Based on UAV rotor speeds, altering horizontal motion is likely to create similar or less turbulence than rotational motion.
- The presence of outside wind is unlikely to alter UAV rotor speeds significantly enough to cause greater downwash disturbance than any applied UAV motion.

5.2. EFFECTS OF DOWNWASH ON GAS CONCENTRATIONS

Airflow effects on measured gas concentration were studied for a UAV-mounted gas monitor. The UAV operated in a stationary hovering configuration inside a chamber that contained constant NO_x concentration to avoid effects of mixture with ambient air.

All variables were either controlled or corrected for so that the only experimental variable was the potential for downwash pressures to alter density-based gas concentration measurements. Conclusions from this experimentation included:

- UAV downwash caused no significant changes to measured concentration values (95% statistical confidence).
- Changing the measuring point location within the downwash region, including directly attaching the measuring point to the UAV, caused no significant changes to measured concentration values (95% statistical confidence).
- Measured concentration values showed no correlation to the turbulent regions discovered in Section 3.
- Turbulence has minimal effect on standard deviation. The region beneath the UAV has higher turbulence than the regions beside or above the UAV, although the difference in standard deviation was minor relative to the recorded concentration value.
- Comparisons with downwash air pressures from previous studies imply these conclusions are applicable to a wide variety of UAV models, propeller shapes, and rotor configurations.

6. FUTURE WORK

Previous research implies UAVs will primarily be used for gas evaluation in open-air scenarios, which has the additional complication of an unrestrained gas release. If the topmost portion of the downwash region is not contained entirely within the gas cloud, it may be possible for the rotors to pull ambient air into the cloud, thereby artificially reducing the measured gas concentration. Future studies should evaluate the effects and likelihood of ambient air mixture in an open-air gas cloud, specifically a determination of the size of cloud needed to prevent ambient air mixture and the distance the UAV must travel into the cloud before ambient air mixture ceases to occur.

One potential use of UAV-mounted gas monitors is health risk assessment of immediate gas releases, such as those seen in surface mine blasting. Before performing such assessment, the effects of ambient air mixture must be quantified, and then a method must then be developed for calculating the total quantity of gas released based on measurements collected by a UAV-mounted gas monitor. The authors theorize this can be calculated using a variation of puff cloud dispersion equations, which theoretically only require a single sample collected at a single point within the cloud. If the gas sensor can collect a sample every 0.1 s like the sensors used in this experiment, a single blast event can provide hundreds of data points with which to obtain an average quantity of gas released. The benefits of using multiple UAVs in tandem for even greater number of samples at varying locations in the gas cloud should also be evaluated. However, surface mine blasting uses multiple blastholes, thereby necessitating an investigation into whether puff cloud dispersion equations must be varied to include multiple point sources

of gas release or if the blast site can be treated as a single gas source. Finally, other puff cloud dispersion equations for downwind human exposure can be used to determine quantified health risk to those downwind from a gas release.

The conclusion regarding a 6-second maximum time for post-movement downwash region stabilization does not have comparable data from previous research. Further research is required to ensure this conclusion is applicable to a wide variety of UAV models, propeller shapes, and rotor configurations. Future studies should evaluate the effect of altering thrust on downwash pressures to determine whether the downwash region stabilization period is essential or if the changes to measured gas concentration remain statistically negligible while UAV motion is altered. At a minimum, these studies should focus on altering vertical thrust, which experienced the greatest downwash air speeds and turbulence. Tests with the UAV carrying its maximum payload should also be conducted as additional vertical thrust would be necessary to offset the additional weight.

This dissertation did not evaluate whether the gas monitor used compromised the chemical integrity of the NO_x to any degree. NO₂ is a relatively robust gas molecule, and therefore an integrity compromise is not anticipated to have occurred during this testing, but this effect should be evaluated for future gas sampling research, especially when monitoring more reactive gases. Additionally, if particulate matter is airborne within the gas cloud, the matter may disrupt the functionality of the gas monitor itself, and the potential for this effect must be evaluated.

BIBLIOGRAPHY

- [1] Richard J Mainiero, Marcia L Harris, and James H Rowland III, "Dangers of Toxic Fumes from Blasting," National Institute for Occupational Safety and Health, Jan 2007.
- [2] I Onederra, V Bailey, G Cavanough, and A Torrance, "Understanding Main Causes of Nitrogen Oxide Fumes in Surface Blasting," *Mining Technology*, vol. 121, no. 3, 2012.
- [3] C R Barnhart, "Understanding the 'Orange Smoke' Problem in Cast Blasting," in *Proceedings of the Annual Conference on Explosives and Blasting Technique*, International Society of Explosives Engineers, 2003.
- [4] C R Barnhart, "Analytical Measurements in Cast Blasting to Identify the Cause and Cure for 'Orange Smoke' Formation," in *Proceedings of the Annual Conference on Explosives and Blasting Technique*, International Society of Explosives Engineers, 2004.
- [5] ISMR (Indiana Society of Mining & Reclamation), "ANFO & Emulsion Characteristics," in *ISMR Technology Transfer Seminar*, N.D.
- [6] Paul N Worsey, "Lecture 5.1: Blasting Vibration and Fumes," in *Missouri University of Science and Technology*, 2016, pp. EXP ENG 5622 - Blasting Design and Technology.
- [7] NRC (National Research Council), "Appendix E: Acute Toxicity of Nitrogen Dioxide," in *Assessment of Exposure-Response Functions for Rocket-Emission Toxicants*, NRC Subcommittee on Rocket-Emission Toxicants, Ed. Washington, DC: National Academies Press, 1998.
- [8] ATSDR (Agency for Toxic Substances and Disease Registry), "Medical Management Guidelines for Nitrogen Oxides (NO, NO₂, and Others)," ATSDR, Centers for Disease Control and Prevention, Oct 21, 2014.
- [9] EPA (Environmental Protection Agency), "Air Quality Criteria for Oxides of Nitrogen," Environmental Criteria and Assessment Office, Office of Health and Environmental Assessment, and Office of Research and Development; EPA, Aug 1993.
- [10] Vahid Mohsenin, "Human Exposure to Oxides of Nitrogen at Ambient and Supra-Ambient Concentrations," *Toxicology*, vol. 89, no. 3, May 20, 1994.

- [11] G. R. Jones, A. T. Proudfoot, and J. I. Hall, "Pumonary Effects of Acute Exposure to Nitrous Fumes," *Thorax*, vol. 28, 1973.
- [12] Maria A Mayorga, "Overview of Nitrogen Dioxide Effects on the Lung with Emphasis on Military Relevance," *Toxicology*, vol. 89, no. 3, May 20, 1994.
- [13] David C Dugdale and Michael A Chen, "Pulmonary Edema," in *MedlinePlus Medical Encyclopedia*.: MedlinePlus, US National Library of Medicine, Jun 4, 2012.
- [14] Joseph P Lynch et al., "Obliterative (Constrictive) Bronchiolitis," *Seminars in Respiratory and Critical Care Medicine*, vol. 33, no. 5, Oct 2012.
- [15] NIH (National Institutes of Health), "Respiratory Failure," National Heart, Lung, and Blood Institute, NIH, US Department of Health & Human Services, Health Topics N.D.
- [16] NRC (National Research Council), *Acute Exposure Guideline Levels for Selected Airborne Chemicals, Vol. 11*, Committee on Toxicology, Board on Environmental Studies on Toxicology, and Division on Earth and Life Studies Committee on Acute Exposure Levels, Ed. Washington, DC: The National Academies Press, 2012.
- [17] WHO (World Health Organization), "Environmental Health Criteria 188: Nitrogen Oxides, Ed. 2," International Program on Chemical Safety, WHO, Internal Labour Organisation, United Nations Environment Programme, 1997.
- [18] S M Brooks, M A Weiss, and I L Bernstein, "Reactive Airways Dysfunction Syndrome (RADS): Persistent Asthma Syndrome after High Level Irritant Exposures," *Chest*, vol. 88, no. 3, Sep 1985.
- [19] K V Woolnough and K M Ross, "Cough: Bronchospasm or Not?," *Canadian Family Physician*, vol. 31, Mar 1985.
- [20] EPA (Environmental Protection Agency), "Compilation of Air Pollutant Emission Factors," *AP-42*, pp. 11.3-1 to 11.3-5, 1980.
- [21] A Lashgari, Catherine E Johnson, Vlad Kecojevic, Braden Lusk, and J M Hoffman, "NOx Emission of Equipment and Blasting Agents in Surface Coal Mining," *Mining Engineering*, vol. 65, no. 10, Oct 2013.
- [22] James H Rowland III and Richard J Mainiero, "Factors Affecting ANFO Fumes Production," in *Proceedings of the Annual Conference on Explosives and Blasting Technique*, International Society of Explosives Engineers, 2000.

- [23] James H Rowland III, Richard J Mainiero, and Donald A Hurd, Jr., "Factors Affecting Fumes Production of an Emulsion and ANFO/Emulsion Blends," in *Proceedings of the Annual Conference on Explosives and Blasting Technique*, International Society of Explosives Engineers, 2001.
- [24] R Turcotte, R Yang, M C Lee, B Short, and R Shomaker, "Factors Affecting Fume Production in Surface Coal Blasting Operations," in *Proceedings of the Annual Conference on Explosives and Blasting Technique*, International Society of Explosives Engineers, 2002.
- [25] Lee Schettler and Stuart Brashear, "Effect of Water on ANFO/Emulsion Blends in Surface Mine Blasting," in *Proceedings of the Annual Conference on Explosives and Blasting Technique*, International Society of Explosives Engineers, 1996.
- [26] Michael Sapko, James H Rowland III, Richard J Mainiero, and Isaac Zlochower, "Chemical and Physical Factors that Influence NO_x Production during Blasting," in *Proceedings of the Annual Conference on Explosives and Blasting Technique*, International Society of Explosives Engineers, 2002.
- [27] R F Chaiken, E B Cook, and T C Ruhe, "Toxic Fumes from Explosives: Ammonium Nitrate-Fuel Oil Mixtures," Bureau of Mines, US Department of the Interior, Pittsburgh Mining and Safety Research Center; Pittsburgh, PA, 1974.
- [28] E M De Souza and P D Katsabanis, "On the Prediction of Blasting Toxic Fumes and Dilution Ventilation," *Mining Science and Technology*, vol. 13, 1991.
- [29] Richard J Mainiero, "A Technique for Measuring Toxic Gases Produced by Blasting Agents," in *Proceedings of the Annual Conference on Explosives and Blasting Technique*, International Society of Explosives Engineers, 1997.
- [30] DNRM (Department of Natural Resources and Mines), "Explosives Safety Alert No. 28 - Post Blast Gases," DNRM, Queensland, Australia, Jul 9, 2009.
- [31] Cole Latimer, "Blasting on Hold at BMA Coal Mines," *Australian Mining*, Mar 15, 2011.
- [32] Cole Latimer, "Blast Fumes Injure Miners," *Australian Mining*, Apr 5, 2011.
- [33] Vern Madden, "Prevention and Management of Blast Fumes," Department of Natural Resources and Mines, Queensland, Australia, Explosives Safety Alert No. 44 Mar 15, 2011.
- [34] 25 Pennsylvania Code § 211.152. Control of gases, including carbon monoxide and oxides of nitrogen, 2018.

- [35] Ohio Administrative Code 1501:13-9-06. Use of explosives in coal mining and coal exploration operations, 2018.
- [36] Ohio Administrative Code 1501:13-9-10. Training, examination, and certification of blasters, 2018.
- [37] PA DEP (Pennsylvania Department of Environmental Protection), "DEP Regulatory Update: Feb 24, 2023," Environmental Quality Board, PA DEP, Feb 24, 2023.
- [38] OSMRE (Office of Surface Mining Reclamation and Enforcement), "FR Doc. 2019-16125: Closure of Petition for Rulemaking; Use of Explosives on Surface Coal Mining Operations," OSMRE, Department of the Interior, Jul 29, 2019.
- [39] Robert Brendan McCray, "Utilization of a Small Unmanned Aircraft System for Direct Sampling of Nitrogen Oxides Produced by Full-scale Surface Mine Blasting," Mining Engineering, University of Kentucky, Theses and Dissertations 2016.
- [40] Miguel Alvarado, Felipe Gonzalez, Peter Erskine, David Cliff, and Darlene Heuff, "A Methodology to Monitor Airborne PM10 Dust Particles Using a Small Unmanned Aerial Vehicle," *Sensors*, vol. 17, Feb 14, 2017.
- [41] Johanna Aurell et al., "Field Determination of Multipollutant, Open Area Combustion Source Emission Factors with a Hexacopter Unmanned Aerial Vehicle," *Atmospheric Environment*, vol. 166, Jul 28, 2017.
- [42] Susan Smith Nash, "Drones and UAVs for Methane Emissions Detection, Monitoring, and Regulatory Compliance," *Journal of Biological Science*, vol. 3, no. 1, Jan 2017.
- [43] Siwen Liu, "Development of a UAV-based System to Monitor Air Quality over an Oil Field," 2018.
- [44] Martin Willett, "Remote Gas Sensing Using UAVs," 2019/0128862 A1, May 2, 2019.
- [45] Adil Shah et al., "Testing the Near-field Gaussian Plume Inversion Flux Quantification Technique Using Unmanned Aerial Vehicle Sampling," *Atmospheric Measurement Techniques*, vol. 13, Mar 30, 2020.
- [46] Levi M Golston et al., "Natural Gas Fugitive Leak Detection Using an Unmanned Aerial Vehicle: Localization and Quantification of Emission Rate," *Atmosphere*, vol. 9, no. 333, Aug 23, 2018.

- [47] Scott Simmie, "What's That Smell? This Gas-sniffing Drone Sensor Can Tell," DroneDJ, Aug 18, 2020.
- [48] Patrick P Neumann, "Gas Source Localization and Gas Distribution Mapping with a Micro-Drone," Jun 6, 2013.
- [49] Patrick Haas et al., "Development of an Unmanned Aerial Vehicle UAV for Air Quality Measurements in Urban Areas," *Proceedings of the 32nd American Institute of Aeronautics and Astronautics (AIAA) Applied Aerodynamics Conference*, Jun 2014.
- [50] Tommaso Francesco Villa, Farhad Salimi, Kye Morton, Lidia Morawska, and L Filipe Gonzalez, "Development and Validation of a UAV Based System for Air Pollution Measurements," *Sensors*, vol. 16, no. 2202, Dec 21, 2016.
- [51] Oscar Alvear, Nicola Roberto Zema, Enrico Natalizio, and Carlos T. Calafate, "Using UAV-based Systems to Monitor Air Pollution in Areas with Poor Accessibility," *Journal of Advanced Transportation*, vol. 2017, Aug 7, 2017.
- [52] Henok Ali, Momen Odeh, Ahmed Odeh, Ali Abou El-Nour, and Mohammed Tarique, "Unmanned Aerial Vehicular System for Greenhouse Gas Measurement and Automatic Landing," *Network Protocols and Algorithms*, vol. 9, Dec 21, 2017.
- [53] Mohamed Aboubakr, Ahmed Balkis, Ali-Abou ElNour, and Mohammed Tarique, "Environmental Monitoring System by Using Unmanned Aerial Vehicle," *Network Protocols and Algorithms*, vol. 9, Dec 31, 2017.
- [54] Oscar Alvear et al., "A Discretized Approach to Air Pollution Monitoring Using UAV-based Sensing," *Mobile Networks and Applications*, vol. 23, May 28, 2018.
- [55] Gian Marco Bolla et al., "ARIA: Air Pollutants Monitoring Using UAVs," in *Proceedings from the 2018 5th IEEE International Workshop on Metrology for Aerospace*, IEEE, 2018.
- [56] Qijun Gu, Drew R. Michanowicz, and Chunrong Jia, "Developing a Modular Unmanned Aerial Vehicle (UAV) Platform for Air Pollution Profiling," *Sensors*, vol. 18, 2018.
- [57] Fan Liu, Xiaohong Zheng, and Hua Qian, "Comparison of Particle Concentration Vertical Profiles between Downtown and Urban Forest Park in Nanjing (China)," *Atmospheric Pollution Research*, vol. 9, 2018.

- [58] Yao Yao, Shanlin Wei, Honghui Zhang, and Qiong Li, "Application of UAV in Monitoring Chemical Pollutant Gases," *Chemical Engineering Transactions*, vol. 67, 2018.
- [59] A. Ahlawat et al., "Performance Evaluation of Light Weight Gas Sensor System Suitable for Airborne Applications against Co-location Gas Analysers over Delhi," *Science of the Total Environment*, vol. 697, Aug 20, 2019.
- [60] Chaoqun Li et al., "An Unmanned Aerial Vehicle-Based Gas Sampling System for Analyzing CO₂ and Atmospheric Particulate Matter in Laboratory," *Sensors*, vol. 1051, Feb 15, 2020.
- [61] Sławomir Pochwała, Arkadiusz Gardecki, Piotr Lewandowski, Viola Somogyi, and Stanisław Anweiler, "Developing of Low-Cost Air Pollution Sensor - Measurements with the Unmanned Aerial Vehicles in Poland," *Sensors*, vol. 20, no. 3582, Jun 24, 2020.
- [62] Tommaso Francesco Villa, E Rohan Jayaratne, L Filipe Gonzalez, and Lidia Morawska, "Determination of the Vertical Profile of Particle Number Concentration Adjacent to a Motorway Using an Unmanned Aerial Vehicle," *Environmental Pollution*, vol. 230, Nov 2017.
- [63] Raphael Mawrence, Sandra Munniks, and João Valente, "Calibration of Electrochemical Sensors for Nitrogen Dioxide Gas Detection Using Unmanned Aerial Vehicles," *Sensors*, vol. 20, no. 7332, Dec 20, 2020.
- [64] Chih-Chung Chang, Jia-Lin Wang, Chih-Yuan Chang, Mao-Chang Liang, and Ming-Ren Lin, "Development of a Multicopter-carried Whole Air Sampling Apparatus and Its Applications in Environmental Studies," *Chemosphere*, vol. 144, 2016.
- [65] Chih-Chung Chang et al., "A Study of Atmospheric Mixing of Trace Gases by Aerial Sampling with a Multi-rotor Drone," *Chemosphere*, vol. 144, 2018.
- [66] Tommaso Francesco Villa et al., "Characterization of the Particle Emission from a Ship Operating at Sea Using an Unmanned Aerial Vehicle," *Atmospheric Measurement Techniques*, vol. 12, no. 1, Jan 31, 2019.
- [67] Fan Zhou, Jing Gu, Wei Chen, and Xunpeng Ni, "Measurement of SO₂ and NO₂ in Ship Plumes Using Rotary Unmanned Aerial System," *Atmosphere*, vol. 10, Oct 29, 2019.

- [68] Juan Jesus Roldan, Guillaume Joossen, David Sanz, Jaime del Cerro, and Antonio Barrientos, "Mini-UAV Based Sensory System for Measuring Environmental Variables in Greenhouses," *Sensors*, vol. 15, Feb 2, 2015.
- [69] Qing Tang et al., "Droplets Movement and Deposition of an Eight-rotor Agricultural UAV in Downwash Flow Field," *International Journal of Agricultural and Biological Engineering*, vol. 10, no. 3, May 2017.
- [70] Fengbo Yang, Xinyu Xue, Ling Zhang, and Zhu Sun, "Numerical Simulation and Experimental Verification on Downwash Air Flow of Six-rotor Agricultural Unmanned Aerial Vehicle in Hover," *International Journal of Agricultural and Biological Engineering*, vol. 10, no. 4, Jul 2017.
- [71] Fengbo Yang, Xinyu Xue, Chen Cai, Zhu Sun, and Qingqing Zhou, "Numerical Simulation and Analysis on Spray Drift Movement of Multirotor Plant Protection Unmanned Aerial Vehicle," *Energies*, vol. 11, Sep 11, 2018.
- [72] Yongjun Zheng et al., "The Computational Fluid Dynamic Modeling of Downwash Flow Field for a Six-rotor UAV," *Frontiers of Agricultural Science Engineering*, Apr 23, 2018.
- [73] Feng Tan, Qi Lian, Chang-Liang Liu, and Bing-Kun Jin, "Measurement of Downwash Velocity Generated by Rotors of Agriculture Drones," *INMATEH - Agricultural Engineering*, vol. 55, no. 2, 2018.
- [74] Vaclav Smidl and Radek Hofman, "Tracking of Atmospheric Release of Pollution Using Unmanned Aerial Vehicles," *Atmospheric Environment*, vol. 67, 2013.
- [75] Daniele Facinelli, Matteo Larcher, Davide Brunelli, and Daniele Fontanelli, "Cooperative UAVs Gas Monitoring Using Distributed Consensus," in *Proceedings from the 43rd Annual Computer Software and Applications Conference (COMPSAC)*, IEEE, 2019.
- [76] Miron Kaliszewski et al., "The Multi-Gas Sensor for Remote UAV and UGV Missions - Development and Tests," *Sensors*, vol. 21, no. 7608, Nov 16, 2021.
- [77] James M. Brady, M. Dale Stokes, Jim Bonnardel, and Timothy H. Bertram, "Characterization of a Quadrotor Unmanned Aircraft System for Aerosol-Particle-Concentration Measurements," *Environmental Science & Technology*, vol. 50, Jan 5, 2016.

- [78] Xiaochi Zhou, Johanna Aurell, William Mitchell, Dennis Tabor, and Brian Gullett, "A Small, Lightweight Multipollutant Sensor System for Ground-mobile and Aerial Emission Sampling from Open Area Sources," *Atmospheric Environment*, vol. 154, 2017.
- [79] Javier Burgues, Maria Deseada Esclapez, Silvia Doñate, Laura Pastor, and Santiago Marco, "Aerial Mapping of Odorous Gases in a Wastewater Treatment Plant Using a Small Drone," *Remote Sensing*, vol. 13, no. 1757, Apr 30, 2021.
- [80] Claudio Crazzolaro et al., "A New Multicopter-based Unmanned Aerial System for Pollen and Spores Collection in the Atmospheric Boundary Layer," *Atmospheric Measurement Techniques*, vol. 12, Mar 12, 2019.
- [81] Dale Crane, *Dictionary of Aeronautical Terms, 3rd Ed.* Newcastle, WA: Aviation Supplies and Academics, 1997, p. 172.
- [82] OSHA (Occupational Safety and Health Administration), "Chemical Sampling Information: Nitrogen Dioxide," OSHA, US Department of Labor, N.D.
- [83] Centers for Disease Control and Prevention (CDC), "Appendix B: Air Concentration Calculations for Comparison to OSHA Standards," in *NIOSH Manual of Analytical Methods*: CDC, National Institute for Occupational Safety and Health (NIOSH), Aug 15, 1994.
- [84] Lloyd M English and Yi Luo, "Mountaintop Mining/Valley Fill Technical Studies: Study of Fugitive Dust and Fumes," Department of Mining Engineering, College of Engineering and Mineral Resources, West Virginia University, 2001.
- [85] Per-Anders Persson, Kay Brower, George Harker, Ricky Vance, and George Griffith, "Reaction Kinetics in the 1-10 GPa Pressure Regime; A Tool for Controlling the Generation of Fumes from Mining Explosives," National Science Foundation, Feb 10, 1995.
- [86] Battelle, "West Virginia Air Quality Assessment Near a Surface Coal Mine Blasting Operation," West Virginia Department of Environmental Protection, Aug 10, 2012.
- [87] Bruce A Kunkel, "AFTOX 4.0 - The Air Force Toxic Chemical Dispersion Model - A User's Guide," Phillips Laboratory, Directorate of Geophysics, Air Force Systems Command, Hanscom Air Force Base, MA, Environmental Research Papers, No. 1083 May 8, 1991.
- [88] Karl B Schnelle, "Atmospheric Diffusion Modeling," in *Encyclopedia of Physical Science and Technology*, Ed. 3. San Diego, CA: Academic Press, 2002, pp. 679-705.

- [89] Michael J Pilat, "Atmospheric Air Pollutant Dispersion," Air Pollution Control, University of Washington, 2009.
- [90] Xiaoying Cao, Gilles Roy, William J Hurley, and William S Andrews, "Dispersion Coefficients for Gaussian Puff Models," *Boundary-Layer Meteorol*, vol. 139, 2011.
- [91] John Stockie, "Mathematics of Atmospheric Dispersion Modelling," *SIAM Review*, vol. 53, no. 2, 2011.
- [92] Frank Gronwald and Shoou-Yuh Chang, "Evaluation of the Precision and Accuracy of Multiple Air Dispersion Models," *Journal of Atmospheric Pollution*, vol. 6, no. 1, 2018.
- [93] A J C Berkhout, J B Bergwerff, D P J Swart, M Haaima, and H Volten, "The miniDOAS: Low Cost, High Performance Contactless Ammonia Measurements," National Institute for Public Health and the Environment, Spectroscopy - Application Notebook Feb 1, 2013.
- [94] Maria McCutchen, "The 10 Most Expensive Drones You Can Actually Buy," *Electronics*, 2017.
- [95] Laurent Spinelle, Michel Gerboles, Gertjan Kok, Stefan Persijn, and Tilman Sauerwald, "Review of Portable and Low-cost Sensors for the Ambient Air Monitoring of Benzene and Other Volatile Organic Compounds," *Sensors*, vol. 17, Jun 28, 2017.
- [96] Tyler Kersnovski, L. Felipe Gonzalez, and Kye Morton, "A UAV System for Autonomous Target Detection and Gas Sensing," *Proceedings from the 2017 IEEE Aerospace Conference*, Mar 2017.
- [97] Jacqueline Akhavan, *The Chemistry of Explosives*, 3rd ed. Cambridge, UK: Royal Society of Chemistry, 2011.
- [98] EPA (Environmental Protection Agency), "NAAQS Table," Dec 20, 2016.
- [99] NIOSH (National Institute for Occupational Safety and Health), "Immediately Dangerous to Life or Health Concentrations (IDLH): Nitrogen Dioxide," NIOSH, Centers for Disease Control and Prevention, Dec 4, 2014.
- [100] NIOSH (National Institute for Occupational Safety and Health), "NIOSH Pocket Guide to Chemical Hazards: Nitrogen Dioxide," NIOSH, Centers for Disease Control and Prevention, Apr 11, 2016.

- [101] EPA (Environmental Protection Agency), "Technical Assistance Document for the Reporting of Daily Air Quality - The Air Quality Index," EPA, May 2016.
- [102] 30 CFR § 816.67(a) Use of explosives: Control of adverse effects: General Requirements.
- [103] AEISG (Australian Explosives Industry and Safety Group, Inc.), "Code of Practice: Prevention and Management of Blast Generated NO_x Gases in Surface Blasting, 2nd Ed.," AEISG, Aug 2011.
- [104] Jeremy Nichols, "Petition for Rulemaking under the Surface Mining Control and Reclamation Act, 30 USC § 1211(g)," WildEarth Guardians, Apr 14, 2014.
- [105] Edward M. Green, "Clinet Alert: OSM Announces Plans to Regulate Gases Released During Surface Mine Blasting," Mar 9, 2015.
- [106] Moetaz I Attalla, Stuart J Day, Tony Lange, William Lilley, and Scott Morgan, "NO_x Emissions from Blasting Operations in Open-Cut Coal Mining," *Atmospheric Environment*, vol. 42, 2008.
- [107] William Alan Harrison, David J Lary, Brian J Nathan, and Alec G Moore, "The Neighborhood Scale Variability of Airborne Particles," *Journal of Environmental Protection*, vol. 6, May 11, 2015.
- [108] M Johansson et al., "Mobile mini-DOAS Measurement of the Outflow of NO₂ and HCHO from Mexico City," *Atmospheric Chemistry and Physics*, vol. 9, no. 15, Aug 10, 2009.
- [109] Claudia Rivera et al., "Tula Industrial Complex (Mexico) Emissions of SO₂ and NO₂ during the MCMA 2006 Field Campaign Using a Mobile mini-DOAS System," *Atmospheric Chemistry and Physics*, vol. 9, Sep 2, 2009.
- [110] Claudia Rivera et al., "NO₂ Fluxes from Tijuana Using a Mobile mini-DOAS during Cal-Mex 2010," *Atmospheric Environment*, vol. 70, May 2013.
- [111] Jorg Sintermann et al., "A miniDOAS Instrument Optimized for Ammonia Field Measurements," *Atmospheric Measurement Techniques*, vol. 9, no. 6, Jun 29, 2016.
- [112] William Alan Harrison, David J Lary, Brian J Nathan, and Alec G Moore, "Using Remote Control Aerial Vehicles to Study Variability of Airborne Particles," *Air, Soil, and Water Research*, vol. 8, 2015.

- [113] David H Slade, *Meteorology and Atomic Energy*. Division of Reactor Development Technology, US Atomic Energy Commission; Springfield, VA: Clearinghouse for Federal Scientific and Technical Information, National Bureau of Standards, US Department of Commerce, Jul 1968.
- [114] R Bhattacharya, "Atmospheric Dispersion," Asian Nuclear Safety Network, International Atomic Energy Agency, N.D.
- [115] James Benson, "Boundary-layer Response to a Change in Surface Roughness," Department of Meteorology, The University of Reading, Aug 15, 2005.
- [116] Guiliano Augusti, Alessandro Baratta, and Fabio Casciati, *Probabalistic Methods in Structural Engineering*. London, UK: Chapman and Hall, Jul 19, 1984, p. 85.
- [117] Stephen Burt, *The Weather Observer's Handbook*. New York, USA: Cambridge University Press, Jun 29, 2012, p. 213.
- [118] Fred W Thomas, S B Carpenter, and W C Colbaugh, "Plume Rise Estimates for Electric Generating Stations," *Journal of the Air Pollution Control Association*, vol. 20, no. 3, 1970.
- [119] Kayvon Sharghi, "Exploring Drone Aerodynamics with Computers," Aeronautics, National Aeronautics and Space Administration (NASA), Jan 11, 2017.
- [120] Derrick Yeo, Elena Shrestha, Derek A Paley, and Ella Atkins, "An Empirical Model of Rotorcraft UAV Downwash Model for Disturbance Localization and Avoidance," in *Proceedings of the AIAA Atmospheric Flight Mechanics Conference*, American Institute of Aeronautics and Astronautics, Inc., Jan 2015.
- [121] Jun Ni et al., "Development of an Unmanned Aerial Vehicle-borne Crop-growth Monitoring System," *Sensors*, vol. 17, Mar 3, 2017.
- [122] Qiang Shi et al., "The Airflow Field Characteristics of UAV Flight in a Greenhouse," *Atmosphere*, vol. 11, no. 634, Jul 7, 2021.
- [123] Pietro Tosato et al., "An Autonomous Swarm of Drones for Industrial Gas Sensing Applications," in *Proceedings from the 20th International Symposium on "A World of Wireless, Mobile, and Multimedia Networks" (WoWMoM)*, IEEE, 2019.
- [124] Thomas E. Barchyn, Chris H. Hugenholtz, Stephen Myshak, and Jim Bauer, "A UAV-based System for Detecting Natural Gas Leaks," *Journal of Unmanned Vehicle Systems*, vol. 6, no. 1, 2018.

- [125] Peng-Xiang Bao et al., "Multi-UAV Gas Concentration Map Fusion Using the Image Repair Algorithm Based on Clustered Directed Diffusion Model," *Proceedings from the 2019 IEEE International Symposium on Olfaction and Electronic Noise (ISOEN)*, May 2019.
- [126] Jacob Lane Brinkman, Brent Davis, and Catherine Emily Johnson, "Post-Movement Stabilization Time for the Downwash Region of a 6-rotor UAV for Remote Gas Monitoring," *Heliyon*, vol. 6, no. 9, Sep 2020.
- [127] DJI (Dà-Jiāng Innovations Science and Technology Co., Ltd). (2018) Matrice 600 Pro: Specs.
- [128] Jacob Lane Brinkman and Catherine Emily Johnson, "Effects of Downwash from a 6-rotor Unmanned Aerial Vehicle (UAV) on Gas Monitor Concentrations," *Mining, Metallurgy, and Exploration*, vol. 38, May 20, 2021.
- [129] Alphasense, "Technical Specification: NO-A4 Nitric Oxide Sensor," Feb 2016.
- [130] Alphasense, "Technical Specification: NO2-A43F Nitrogen Dioxide Sensor," Dec 2018.
- [131] Alphasense. (2013) FAQs.
- [132] Andrew Lindemann, Personal Interview, Jan 2018, Geotech Environmental Equipment, Inc.
- [133] National Instruments, "Specifications: USB-6008," Sep 1, 2017.
- [134] Alphasense, "Alphasense User Manual: A4 Analogue Front End (AFE) Circuit Board Family," Jul 3, 2014.
- [135] Wah On Ho, "Email correspondence," Jun 13, 2019.
- [136] Alphasense, "Alphasense Application Note 803-05: Correcting for Background Currents in Four Electrode Toxic Gas Sensors," Mar 2019.

VITA

Jacob “Jake” Lane Brinkman was raised across the United States and abroad as the son of an Air Force pilot. He spent the majority of his childhood in Wichita Falls, TX, where he met his future wife.

Jake had a keen interest and ability in mathematics, and after discovering a love for physics in high school, he was called to combine the two interests and study engineering. He completed a Bachelor of Science in Mining Engineering in May 2015 at the University of Kentucky. He was then invited by Dr. Catherine Johnson to attend the Missouri University of Science and Technology to pursue a PhD in Explosives Engineering, where he earned a Master of Science in Explosives Engineering in December 2017 and joined the Energetics Research Team.

Jake began graduate school studying explosives engineering primarily to specialize in one of the wide variety of fields that mining engineering teaches. However, his explosives engineering studies and his work as part of the Energetics Research Team exposed him to fundamental detonation mechanics and research studies funded by the Department of Defense, through which he developed an interest in the mechanics of high explosives as used for US military weapons. In 2019, he took a Core Engineering Specialist position in the Focused Experiments group at the Pantex Plant, where he works to manage research and development projects related to high explosives.

While working at the Pantex Plant and raising a growing family, Jake earned his PhD in Explosives Engineering from the Missouri University of Science and Technology in May 2023.